GL01035

AN ELECTRICAL RESISTIVITY SURVEY OF THE COLADO HOT SPRINGS PROSPECT, PERSHING COUNTY, NEVADA

VOLUME I

SUBMITTED TO

GETTY OIL COMPANY

BY

ELECTRODYNE SURVEYS

SPARKS, NEVADA

APRIL, 1978

FINAL REVISION

ABSTRACT

Electrical resistivity, gravity, and magnetic reconnaissance surveys followed by electrical resistivity detailing surveys were performed to find anomalous areas that may be coincident with geothermal zones or cells at depth in the Colado Hot Springs Prospect. The reconnaissance electrical resistivity methods used were scalar AMT-MT soundings, roving vector telluric soundings, and end-on-end telluric profiles. The detailing electrical resistivity methods used were dc electrical resistivity soundings and profiles and time domain electric field and magnetic field soundings. The areal extent surveyed in the prospect was approximately 100 square miles.

Six anomalous areas were found in the prospect that have the structural and resistivity parameter indications that link them to probable geothermal zones at depth. These areas are indicated on Plates V and VI. They vary in areal extent from 2 to 4 square miles.

Area 2 is a fault controlled feature. All other areas are out in the valley floor and the tops of the anomalous zones appear to be located between 4,000 feet and 6,000 feet of depth in the geologic section. The thickness of the zones is interpreted to range from 1,500 feet to 3,000 feet. The electrical resistivity survey data gives a strong indication that the anomalous areas are interconnected by a geothermal plumbing system at depth in the section.

A recommended temperature gradient test hole program is described starting with Areas 1 and 2, Plate VI. Continuation of the program into the other geothermal areas is dependent on the results of the tests in Areas 1 and 2.

TABLE OF CONTENTS

LIST OF PLATES

VOLUME II

TABLE OF CONTENTS

INTRODUCTION

An electrical resistivity survey was conducted in the Colado Hot Springs Prospect, Pershing County, Nevada, during the months of July, October, and November, 1977 for the Getty Oil Company of Bakersfield, California by Electrodyne Surveys of Sparks, Nevada. This survey and an associated gravity and magnetics survey covered approximately 100 square miles in an area centered about Colado, Nevada, which is located 7 miles northeast of Lovelock, Nevada. Plates I, II, and III show the areal coverage performed by the reconnaissance and detailed electrical resistivity surveys and by the gravity and magnetic survey of the prospect.

The prospect surveys were performed in two parts. One part was a reconnaissance survey which included the use of scalar magnetotelluric (MT) and audio magnetotelluric (AMT) measurements, roving vector telluric measurements, and telluric profiling (Plate I) and associated gravity and magnetic surveys (Plate III) to discover the following:

(1) The structural control in the prospect that could indicate the possible location of geothermal cells or zones at depth in the geologic section.

(2) Anomalous low apparent resistivity value zones that could indicate the possibility of geothermal reservoirs, especially those associated with the determined structural control. and

(3) Areas indicating large apparent resistivity value contrasts which might correspond with structural features and which might also delineate the lateral extent of the geothermal cells.

The electrical resistivity reconnaissance surveys included 31 MT-AMT soundings, 17 roving vector telluric soundings (associated with 4 vector telluric base stations) and a total of 231

end-on-end telluric measurements made along telluric profiles. Description of the field operation, data reduction and analysis of these reconnaissance techniques and the data for this survey are given in Volume II of this report. The composite results and interpretation for the 14 Hz Schumann Band frequency and the 0.03-0.05 Hz telluric frequency band are given on Plates VII and VIII respectively.

In conjunction with the reconnaissance electrical resistivity survey, Lanton Survey Company of Vallejo, California performed data acquisition of 423 locations along profiles in the gravity and magnetic measurements at locations along profiles in the prospect as shown in Plate III. Electrodyne Surveys performed second derivative reduction from these data, and the interpretation of the structural aspects of this prospect as shown by these data is given on Plate XIII. This interpretation is combined with the electrical resistivity interpretation on Plate V. The survey data acquired by the Lanton Survey Company have been forwarded to the Getty Oil company under separate cover.

The reconnaissance electrical resistivity survey was followed by detailed electrical resistivity surveys located as shown on Plate II. The detailing surveys were performed to give a better quantitative measure of the electrical resistivity distribution as a function of depth and similarly to give a better quantitative determination of lateral limits of anomalous areas than those presented by the reconnaissance surveys. The electrical resistivity detailing surveys included 11 (dc) galvanic electrical resistivity (ER) soundings, 156 dc electrical-field measurements along profiles parallel to dc sources, 7 time-domain electromagnetic (TDEM) electric field soundings, and 8 combined electric field and magnetic field TDEM soundings.(See Plate II). The interpretative results of the detailed surveys are given in Plates IX, X, and XI. These results are incorporated in the composite interpretations given in Plates IV and V. Description of the field operation, data reduction and analysis of the detailing techniques and the data for this survey are given in Volume II of this report.

GEOLOGY

To the best of our knowledge there has been no surface geologic mapping of the Colado Hot Springs Prospect area published. We highly recommend that such survey mapping be performed by Getty and others that have a continuing interest in the prospect area.

The western two-thirds of the prospect area is a valley covered by eolian deposits which probably thin out to reveal Lake Lahontan silt and sand deposits, which in turn thin out to reveal fanglomerates along the Humboldt Range foothills in the eastern one-third of the prospect. The approximate location of the valley-foothills contact is indicated on Plate VI.

There is evidence of extensive hydrothermal alteration and mineralization in the foothills in Sections 25, 26, 35, and 36 T28N,R32E and Sections 2, 11, and 12 T27N,R32E. There are probably other areas that are not as clearly visible as the above mentioned areas. There appears to be evidence of both basic and acidic intrusives, as well as almost every type of sedimentary deposit exposed in the foothills, at least in the part traversed by Electrodyne's field crews. Also, evidence of folding, faulting, and metamorphism was found throughout the foothills in the prospect.

Structurally, several northeast trending faults (the predominant structural trend) cut the Humboldt Range in the prospect. At almost 90 degrees to this predominant trend, there is evidence in the foothills of cross faults trending to the northwest. Tufa deposits found in the valley floor trend in these two predominant directions.

Aside from the tufa found in the valley and the alteration and mineralization seen in the foothills, the anomalous temperature gradients found in the Section 26, T 28N,R32E attest to the fact that anomalous heat exists in the upper crust section of the prospect area.

MAJOR FINDINGS OF THE SURVEYS

There are a number of subsurface geophysical findings that suggest many areas of the Colado Hot Springs Prospect show promise of geothermal possibilities. The major findings are as follows:

1. The major northeast and northwest fault trends seen in the Humboldt Range are also evident in the subsurface geophysical measurements. (See Plate IV). Such a cross-faulted subsurface picture indicates a very positive suggestion that geothermal cells or zones may exist in the geologic section.

2. Many areas within the prospect indicate anomalously low apparent resistivity values (less than 3 ohm-meters) at depth within the geologic section. (See Plates X and XI).

3. There is good correspondence between anomalous low apparent resistivity value areas and areas showing cross faults.

4. The thickness of the apparent low resistivity value zones is interpreted to vary between 1,500 and 2,500 feet in the valley west of the foothills.

5. The depth to the possible geothermal zones is interpreted to vary from 4,000 to 7,000 feet. (See Plate V).

6. The gravity high areas (Plate XIII) and the resistivity high areas (Plates VII and VIII) in the northern and northeastern parts of the prospect qualitatively coincide. These areas may be areas of anomalous heat sources.

7. The fault area (Area 2 on Plate V) in the Humboldt Range foothills shows considerable promise based upon the electrical resistivity measurements.

8. We have chosen six areas to be tested for confirmation as to good geothermal prospects by thermal gradient measurements. These areas are outlined on Plate V. There is a strong suggestion in the geophysical results that indicates that these six areas are interconnected in the subsurface.

RECOMMENDED THERMAL GRADIENT TEST HOLE PROGRAM

Six areas are recommended for thermal gradient (T.G.) test holes to confirm or reject the geophysical survey findings. (See Plate V). We strongly urge that both Areas 1 and 2 be tested before a negative conclusion is reached. If a positive conclusion is reached for Area 1, we recommend continuation of testing to include tests in Areas 3, 4, 5, and 6. Finally, we recommend re-evaluation of the geophysical survey interpretation after the T.G. tests are complete and before deep drill tests are performed.

The recommended plan for T.G. holes for testing Areas 1 and 3-6 are as shown on Plate VI for Area 1. In Area 1, three initial holes are located near the expected conductive-resistive contact (at depth) on the conductive side (within the anomalous area) of the contact. The initial hole locations should give the maximum T.G. response without worry of drilling out of the anomalous area at depth (that is, into the resistive side of the contact).

Given positive results from one or more of these initial T.G. test holes, a step-out test hole to the A location from each successful initial hole should be done to better quantify the geothermal zone contact.

For initial T.G. test holes that prove unsuccessful or questionable, a step-out test-hole to the B location should be done to establish the validity, or lack thereof, of the geophysical anomaly.

Any additional T.G. holes should be added on the basis that preceding T.G. hole findings dictate.

Area 2 requires a different T.G. hole program than above. Three initial holes are located in sub-areas of Area 2 where we believe the maximum areal extent of the anomaly falls in Getty's

proposed or possible land aquisition. We believe that the results of T.G. test holes in Section 36, T28N,R32E, Section 12, T27N,R32E, and Section 18, T27N,R33E will be positive. We believe there is a probability of positive results from T.G. test holes in Sections 2 and 14, T27N,R32E and Section 6, T27N,R33E if the initial test holes prove to have positive results.

Additional T.G. test holes after these should be added to establish the breadth of the geothermal anomaly. It is quite difficult to define the lateral limits of an electrical resistivity anomaly of this type. The "state of the art" in electrical geophysical methods today only locates fracture dominated systems; they do not necessarily give a quantitative outline of the feature causing the anomaly.

As we have discussed, the best T.G. program will evolve with a geologist on site at the time of the drilling and at the time of the T.G. measurements so that the decision as to the best plan to be followed evolves as the drilling and testing proceeds.

Further, as has been discussed, Getty's maximum test hole depth will be limited to 500 feet. A possible cap rock problem (that is, insufficient drilling depth for testing) might be expected in Areas 3 and 5. Also, one should investigate the shape of the temperature gradient logs as a function of depth to prevent overestimating geothermal possibilities from such shallow tests.

Revised

DETAILED FINDINGS OF THE SURVEY

There are a number of subsurface geophysical findings which suggest that many areas of the Colado Hot Springs Prospect show promise of geothermal possibilities. These findings are as follows:

1. The two major fault trends, that is the northeast trends and northwest trends, are indicated to be predominant in the valley as well as seen exposed in the Humboldt Range foothills. (See Plate IV). These trends are evidenced by all geophysical surveys in areas of a high spatial density of measurements. (Compare Plates IV, VII, VIII, IX, and XIII).

2. The northeast trending apparent fault features (shown by closely spaced contour areas) appear to be normal fault features with dip toward the basin or graben center. (Compare Plates VII and VIII). Penetration into the geologic section is much deeper in measurements shown on Plate VIII than on Plate VII.

3. The northwest trending apparent fault features appear to be strike-slip and/or rotating block-type faulting. This is best shown on Plate IX. This type of faulting is expected in a spreading graben development.

4. There are areas showing coincidence of subsurface apparent density highs and subsurface apparent resistivity value highs. Compare Plate IV to Plates VII, VIII, and IX. The areas showing coincidence could indicate locations of buried intrusives, therefore possibly areas of anomalous heat.

Revised

5. There are areas showing coincidence of subsurface apparent density lows and subsurface apparent resistivity value lows. Compare Plate IV to Plates VII, VIII, and IX. The areas showing coincidence indicate possible locations of geothermal zones at depth in the geologic section.

6. The simple Bouguer gravity map suggests that the maximum depth to dense basement is about 7,000 feet in the central part of the basin. (See Plate XII). Such a depth estimate forecasts reasonable depth of drilling to geothermal targets.

7. The electric field TDEM depth estimates to the top of the low resistivity zone at depth (Plate XI) are increased by a 50 percent factor and shown on Plate V for the anomalous areas. This is the overburden thickness. (The depth estimates from TDEM soundings are more correct than estimates from TDEM magnetic field measurements or from MT measurements; but they are always equal to or less than true depths). The overburden thickness is estimated to vary from 4,000 feet near the foothills to 7,000 feet near the valley center.

8. The dc electrical resistivity sounding estimates of depth to electrical basement varies from 5,500 feet near the foothills to 10,000 feet at the valley center. These estimates forecast an apparent geothermal zone that varies from 1,500 feet near the foothills to 3,000 feet in the valley center.

9. The apparent resistivity values at depths of the probable geothermal zones in the southern parts of the prospect are equal to or less than 3 ohm-meters. These are certainly very low apparent resistivity values for such depths. (See Plates V, IX, X, and XI).

10. The depths and lateral limits of possible geothermal

Revised

zones in the northern part of the prospect are more difficult to predict on the basis of the electrical resistivity surveys. One reason for this is that the upper section apparent resistivities are higher in this area. (See Plate X). (The uniform magnetic intensity values in this area, Plate XIV, may reflect extensive recent near-surface flows over the area). The surface expression of the Humboldt River and the gravity and electrical resistivity surveys in this area indicate a higher degree of complexity in the northern and western parts of the prospect than in the southern and western parts of the prospect. (Plate V).

11. The evidence of gravity, resistivity value, and magnetic field highs and lows to the north of the prospect indicate a very good probability of anomalous heat source in that area.

12. The promising anomalous Areas 4 and 6 (Plate V) in the southwestern part of the prospect are not closed to the south and west. Additional geophysical investigations should be considered if initial temperature gradient tests indicate a promising area.

DISCUSSION OF THE PLATES

Because the interpretation of a number of electrical geophysical method surveys, Plates VII-XI, and the gravity and magnetic surveys, Plates XII-XIV, are integrated into two composite interpretation maps; one for interpretation of geologic structure and one for interpretation of geometric and resistivity parameter description of anomalous zones at depth; a brief description of each Plate is provided.

Plate I -- Scalar MT-AMT, Vector Telluric and Telluric Profile Location Map.

The most effective reconnaissance electrical resistivity surveys are obtained from continuous profile coverage across the prospect. The profiles are normally directed perpendicular to the regional trend of the geologic structure in the area. The interpretation objective of the reconnaissance surveys is qualitative delineation of areas that show large contrasts in resistivity value, both at depth below and laterally along and across the profiles. The areas showing very low resistivity values, about 1.0 to 3.0 ohm-meters, are the areas of primary interest. The areas showing large contrasts only, are also of interest. These are of interest because the depth of penetration of P_c magnetotelluric (and telluric) electromagnetic reconnaissance data may extend deep into the electrical basement and the apparent resistivity values determined will tend to reflect resistivity values of the basement rock rather than resistivity values of the conductive section above basement.

The cultural features (such as 60 Hz power lines) at and near the highway and Humboldt River; plus the limited access

Added to Revision

in the area (BLM and privately owned land) prevented the continuous profile approach to be utilized in the central part of the prospect. Similarly, land access (BLM lands) and the highly variable topography in the Humboldt Range foothills prevented the continuous profile approach in the eastern part of the prospect.

As shown on Plate I, continuous profiles were made across areas of unlimited access. Continuity of information across areas of limited access was provided by scalar MT-AMT and vector telluric measurements. Additional measurements of all types, chosen on the most applicable method basis as features of interest were detected during progress of the reconnaissance survey. The vector telluric and/or scalar MT-AMT measurements were also used to intertie telluric profiles.

Plate II -- DC Electrical Resistivity Sounding and Profiling Location and Time Domain Electromagnetic Sounding Location Map.

The areas of interest shown by the reconnaissance surveys (Plates VII, VIII, XIII, and XIV) were as follows:

a) One to two miles on either side of the Coal Canyon road, in the Humboldt Range foothills.
b) Several Sections south and southwest of Sections 26 and 27, T28N,R32E, in the area bounded by the foothills to the East and the Humboldt River to the West. The survey did not reach the southern boundary of anomalous areas.
c) The Sections bounded by the Humboldt River on the West and Sections 24, 25, and 26, T28N,R32E on the East.
d) The area about 4 miles NNE of Lovelock and west of the Humboldt River.

(See the preliminary Electrodyne Surveys report for detail of the reconnaissance survey indications).

The various detailing electrical geophysical methods are discussed in the Appendices, Volume II. The purpose of the

detailing surveys are to quantify the geometric limits and the resistivity parameter definition of anomalous conductive zones in the prospect and to mute consideration of areas that were indicated promising by the reconnaissance, but found questionable by the detailing surveys.

Plate III -- Gravity and Magnetic Survey Station Location Map

The location of gravity and magnetic stations was faced by the same access problems that the location of electrical survey sites was faced with. Further, location of gravity and magnetic stations in many areas was limited because of access washout problems by heavy rain storms during much of this survey phase.

Plate IV -- Structural Interpretation Map

Reference in other parts of the text are made to the close correlation between apparent structural trends and possible faults as interpreted by the 2^{nd} derivative gravity map, Plate XIII and the electrical resistivity maps, Plates VIII, IX, X, and XI. At first consideration of Plate IV, this may not be evident. Therefore, the statement is qualified as follows:

1) The depth of penetration by the various electrical resistivity methods, as well as any one method type survey over a prospect is highly variable. Therefore, coincidence of interpreted features should not necessarily be expected.
2) The resistivity parameter and density parameter definition are not necessarily expected to interpret coincidence of features. Most of the electrical resistivity surveys penetrate to depth above basement where large parameter contrasts are not well established or lateral changes detected may be related to lithofacie contrasts rather than structural contrasts. The gravity survey variations detected are thought to reflect variations in structure of the basement surface.

Added to Revision

The P_c scalar MT data reflects penetration well into the basement as well as indicating features above basement. Therefore, these measurements present a composite indication of the above survey indications.

3) Not all of the lines from the gravity map, Plate XIII, suggesting faults are expected to indicate fault locations. Many of these reflect anomalous character and trends of structure rather than giving conclusive evidence that structure exists at the locations or is as extensive as indicated.

In summary, Plate IV is interpreted to show that the very complex structural picture shown by the 2nd derivative gravity map reduces to two major structural trends, NE and NW in direction. Further, we suggest that if drilling tests should find anomalous geothermal character in the geologic section, that one could assume (therefore continue testing) on the basis that extention of anomalies will be in the SW-NE and/or SE-NW directions.

Plate V -- Anomalous Low Resistivity Value Areas Map

Self-Explanatory

Plate VI -- Proposed Temperature Gradient Drill Test Program Map

The drill location sites are chosen to test the interpreted boundaries of the anomalous low resistivity anomalies. If the drill tests indicate that the resistivity anomalies are associated with geothermal occurrences, the true lateral boundaries of the zones should provide the shallowest drilling locations for the highest water temperatures (steam?).

Plate VII -- 14 Hz Normalized Apparent Resistivity Reconnaissance Map

Added to Revision

This map is used to discover areas of large contrasts in resistivity alone. These contrasts would be located within the first 1,000 feet of the geologic sections in most of the prospect. The normalized values are meaningless other than on a relative basis.

The relative coincidence of locations of anomalous features (compare Plate VII and VIII)indicate that fairly shallow thermal gradient tests over conductive anomalies should be informative. This,though,is borne out by the follow-up detailed survey indications.

Plate VIII -- 0.03-0.05 Hz Apparent Resistivity Reconnaissance Map

The anomalous conductive areas indicated on this plate, in our judgment, led to productive detailing surveys. The north-south trending anomalies south of Colado and Coal Canyon are bifurcated into NE and/or NW trending anomalies by the detailed survey interpretations.

The apparent relatively high-resistivity value ridge trending SW from Colado, as interpreted from the detailed survey interpretation, is thought to be caused by a mistie in the telluric profile intertie information. Similarly the broad conductive area, Sections 20 and 21, T28N,R32E, is caused by a probable mistie in the telluric profile intertie information. Both of these misties are caused by interties based on vector telluric or MT-AMT data taken in areas of large lateral resistivity contrasts. This condition cannot always be forecast at the decision time to stop reconnaissance and to commence detailed surveys.

As a general statement, this reconnaissance map suggests that the low resistivity areas at depth are extensive and interconnected. This was borne out by the follow-up dc resistivity. Values much less than 1.0 ohm-meters do correlate with anomaly boundaries as expected in the final interpretation of anomalies (Plate V).

Added to Revision

Plate IX -- Parallel E-Field DC Electrical Resistivity Profile Map

These data show variable depth of penetration both along and between the various profiles. This can be seen by comparison of Profiles 9.3 and 10.3. Quite logically, some of the variation seen on these two profiles can be attributed to current flow away from different source locations.

In any case, these data are not contoured, but used to discover relationships between anomalous conductive and resistive areas. It was this data that led us to an interpretation of only two major fault or structural trends in the prospect.

After this decision, the interpretation of the complexity of the 2nd derivative map, Plate XIII, became considerably reduced and the composite interpretation of all geophysical surveys became more logical and manageable. This last capability map possibly be attributed to our need for simple solutions that we can understand and/or conceive as possible.

The profile indications showing extensive areas of resistivity values equal to or less than 6.0 ohm-meters are greater than 1.0 ohm-meter. At least those south and southwest of Colado and Coal Canyon, indicate broad, interconnected anomalous zones at depth. This is borne out by the dc sounding interpretations shown on Plate X.

Plate X -- DC Electrical Resistivity Sounding Map

The dc soundings performed south and southwest of Colado and Coal Canyon do not show much expression of "geological noise" for intermediate-to-great depths of penetration. This indicates that anomalous conductive sections at depth are interconnected.

The lateral resistivity control shown on interpretations of sounding array expansions to the East into the Humboldt Range foothills and Coal Canyon indicate that the anomalous areas are fault-fracture controlled. This was expected.

Added to Revision

The soundings to the north of Colado indicate a more complicated geologic Section in this direction. The higher resistivity values in this direction (also shown on Plate IX) indicate that deeper thermal gradient test holes will be required to test for geothermal occurrences. Further, the anomalous features are expected to be smaller in lateral extent and probably are not interconnected.

The unit thickness and/or depth to basement estimates from these soundings are expected to be somewhat greater than the true thickness or depth because of probable vertical anisotropy in the geoelectric section. Similarly, the thickness of the overburden (combined First and Second Layer interpretations) are probably underestimated because of interconnection at depth of anomalous areas. True depths lie between the maxima and minima shown by interpretations on Plates X and XI.

Plate XI -- Time Domain EM Soundings Map

All EM soundings in the foothills of the Humboldt Range are indicated to be fault and/or fracture controlled. The resistivity values as interpreted by a vertical sounding approach are much less than the true resistivity values. Therefore, the depth of penetration estimates are meaningless in true value. However, areas of minimum resistivity and depth should locate the areas where the shallowest depth of drilling will be required to test for geothermal occurrences in the general areas.

As a note of caution, all temperature gradient drill samples and deep drill test samples should be observed for sulphide mineralization. Such occurrences may indicate a part of the cause for conductive anomalies; may lead to a means for subsurface mapping of fracture and/or fault systems; and could possibly provide discovery of a viable mineral deposit. Such has occurred in the past. The high 60 Hz noise experienced in the foothills (which prevented the H_z sounding to be made at these locations)

Added to Revision

is often an expression of such mineralization.

Many sounding locations out in the valley have interpretations that indicate fault-like control on the soundings. Such control suggests that the geoelectric section is not so simple as indicated by the dc soundings and profiles. Those locations showing a large residual coductance, S_R , (greater than 300 mhos) could be considered promising, either on a basis of a more conductive area extending to depth or localized concentrations of geothermal fluids at depth at or near these locations.

When one removes the apparent vertical anisotropy from the interpreted resistivity values at good vertical sounding locations, one finds that the resistivity values at depth are most promising.

Discussions as to the reliability of depth to basement and overburden thickness in the valley from the EM sounding interpretations is covered in the discussion of Plate IX given above.

Plate XII -- Simple Bouguer Gravity Map

The regional interpretation of this map is as follows:

1) The interpretation suggests a graben valley with maximum depth to basement about one mile west of the Humboldt River. The interpretation suggests enechelon normal faults along the graben flanks which dip basinward.

2) The regional trend appears NE-SW.

3) A density high to the north of the prospect area appears promising for a possible heat source at depth because the magnetic data in the same area do not show anomalous character. There are many other interpretations possible.

Plate XIII -- Second Derivative Gravity Map

As can be seen, this plate shows a hodge podge of secondary anomalies. As in the discussion on Plate IV above, this very complex secondary look is interpreted as being anomalous signatures

of two basic trends. These are considered to be normal fault trends which strike NE-SW and strike slip and/or rotating block fault trends which strike NW-SE. Some of the density highs may reflect intrusives above basement floor along the fault features.

Plate XIV -- Magnetic Field Variation Map

The main interpretation features of this map are:

1) Most of the valley area is relatively featureless.

2) The magnetic field amplitudes in the valley are of a larger amplitude than the magnetic field amplitudes over exposed basement areas in the foothills in the east part of the prospect.

Our conclusion of the meaning of the interpretation features is that the valley is probably extensively covered by basic type flows and/or deposits at shallow-to-intermediate depth in the geologic section.

We are unsure as to whether or not the anomalous character shown in the southwestern part of the prospect is due to features in the geologic section or due to features related to cultural noise.

Added to Revision

AN ELECTRICAL RESISTIVITY SURVEY OF THE COLADO HOT SPRINGS PROSPECT, PERSHING COUNTY, NEVADA

VOLUME II

Survey Method Description;
Data Acquisition, Reduction,
and Analysis Description;
Apparent Resistivity Values;
and Interpreted Depth Sounding Curves

SUBMITTED TO

GETTY OIL COMPANY

BY

ELECTRODYNE SURVEYS

SPARKS, NEVADA

APRIL, 1978

VOLUME II

TABLE OF CONTENTS

APPENDIX I

Glossary of Terms

Glossary of Terms

Apparent Depth of Penetration, D_a: The apparent depth of penetration is normally defined as the depth of penetration into the earth (which is not completely uniform), that would be computed based upon considerations of the electrical resistivity method used, the geometry of the source-receiver array and the assumption that the earth is a homogeneous half-space.

Apparent Resistivity, ρ_a: The apparent resistivity is normally defined as the resistivity of the earth, which is not completely uniform, that would be computed based upon considerations of the electrical resistivity method used, the geometry of the array and the assumption that the earth resistivity is homogeneous to the depth of penetration achieved. (MKS: ohm-meters) The apparent resistivity parameter may be viewed as the weighted average of the true resistivities from the surface to the depth of penetration.

Array: Any geometric combination of a source-receiver pair used in making electrical resistivity measurements.

Audio-Magnetotelluric Soundings, AMT: Vertical resistivity soundings of the earth utilizing the plane-wave response of naturally and culturally induced electromagnetic fields for the frequency band, 2.0 Hz to 1,000 Hz.

Coefficient of Anisotropy, λ: The coefficient of anisotropy is defined as the square root of the ratio of the resistivities measured in the two principal directions, that is, resistivity across the bedding planes, ρ_t, and the resistivity along the

bedding plane, ρ_1, (non-dimensional). $\lambda = \rho_t / \rho_1$

Conductance, S: The measure of the ratio of the thickness of a conductive material between two insulating plates to the resistivity of the conductive material. An earth crust example is the conducting sedimentary section between the free-air half-space and electrical basement (generally granitic and/or Pre-Cambrian rocks).

Conductivity, σ: The relative ability of materials to conduct electricity when a voltage is applied across the material (MKS: mhos/meter). Conductivity is the reciprocal of resistivity.

Early Time: The portion of the transient response in a TDEM sounding related to the plane-wave (farfield) response of an FDEM sounding.

Effective Apparent Resistivity, ρ_{aE}: The logrithmic average of the apparent resistivities of orthogonal components of a vector apparent resistivity. $\rho_{aE} = (\rho_{ax} \cdot \rho_{ay})^{\frac{1}{2}}$

Effective Apparent Separation, r_E: The array separation that is calculated for source-receiver bipole arrays to equate the array to a source-receiver dipole array. The only bipole array where r_E is correctly calculated as a dipole array separation, r, is an equatorial bipole array.

Electrical Basement: Any thick sequence of rocks or thick layer at depth such as crystalline rocks, which presents a resistivity contrast of 10:1 or greater to the rock sequences or layers above it. Usually the total resistance, T, (a multiplication of resistivity times the sequence thickness) of the electrical basement is so large that it screens out any resolution of conductive rock sequences or layers below it.

Electro Sonde Log, ESL: A pseudo-electrical log of resistivity as a function of depth as determined from data obtained by a five-component surface-based electromagnetic receiver of both naturally induced and a surface-based controlled source(s) induced electromagnetic fields. The five-component receiver measures two orthogonal horizontal components of the electric field and three orthogonal components of the magnetic field. The total ESL system will perform measurements of the frequency spectrum from 0.001 Hz to 1,000 Hz. The frequency range measurements are sub-divided by sources as 0.001 Hz to 0.1 Hz, MT sources; 0.08 Hz to 20 Hz, controlled source; and 8.0 Hz to 1,000 Hz, AMT sources.

Electro Sonde Profiles, ESP: Measurements similar to ESL measurements are made along a continuous profile. One horizontal electric field component, inline with the profile, and a horizontal magnetic field component, perpendicular to the profile, and a vertical magnetic field component are measured at the receiver. The controlled source is a grounded bipole source aligned parallel to the profile with the source-receiver array separation at least twice the depth of penetration in the controlled source minimum frequency. The source field and frequency bands are identical to those for the ESL measurements.

Far Field: See Plane-Wave Field.

Formation Factor of Rocks: The ratio of the resistivity of a rock to the resistivity of the water filling the pore space for a given porosity.

Frequency Domain Electromagnetic Soundings, FDEM: Controlled source electromagnetic soundings generated by a frequency sweep source.

Galvanic Resistivity Sounding, VES: Nomenclature interchangeable with dc Electrical Resistivity sounding in the literature. Vertical electrical resistivity sounding of resistivity as a function of depth. A grounded electrical source generating a static electric field and grounded electrical receivers measuring potential drop between electrodes are utilized. Increase in the depth of penetration is effected by increasing the source-receiver separation of the array.

Geoelectric Section: The geoelectric section differs from the geologic section in that the boundaries between layers or features of contrast change at boundaries determined by resistivity contrasts rather than by the combination of factors used by the geologists in establishing these boundaries. The electrical resistivity of most rocks is determined primarily by the rock porosity, water content and water temperature. The boundaries in a geoelectric section coincide with the boundaries in a geologic section most often when there is a pronounced change in one of the above parameters.

Geometric Factor, K: The geometric factor accounts for the source-type and configuration, the receiver type and configuration, and the separation between the source and receiver geometry in the determination of apparent resistivity.

J-Factor: The ratio of apparent conductance at two locations determined from telluric current measurements at a specified frequency. For end-on-end or in-line telluric profiles, J is the ratio of the simultaneous potential drops measured at two locations. For vector telluric measurements, J is the ratio of the average ellipse areas simultaneously scribed by the two component telluric measurements at two locations.

Late Time: The portion of the transient response in a TDEM sounding between the early time response and the static field response.

The late time response for TDEM is directly related by the Fourier Transform to the quasistatic response of FDEM.

Longitudinal Conductance, S_l: The conductance from the ratio of the total thickness to the parallel or bedding layers of an anisotropic geoelectric unit. $S_l = H/\rho_l$

Longitudinal Resistivity, ρ_e: The resistivity determined by the parallel summation of resistivity values of parallel or bedding layers of an anisotropic geoelectric unit.

Magnetotelluric Sounding, MT: Vertical resistivity sounding of the earth utilizing the plane-wave response of naturally induced electromagnetic fields for the frequency band, 0.001 Hz to 1.0 Hz.

Near Field: Electromagnetic fields for frequencies such that the electromagnetic components are not orthogonal in the propogating source wave. The near field response includes both the quasistatic response and static response portions of FDEM soundings.

P_c Frequency Band: Frequency band from 0.001 Hz to 0.1 Hz.

Plane-Wave Response: The frequency domain response where the electric field and magnetic fields are orthogonal to one another in electromagnetic propagation frequency spectrum.

Quasistatic Response: The frequency domain response between the plane-wave response and static response of an electromagnetic propagation frequency spectrum.

Residual Conductance, S_R: The difference between the total dc electrical resistivity conductance and the total TDEM resistivity conductance. $S_R = S_{dc} - S_{EM}$.

Resistivity, ρ: Specific resistance offered by a material to current flow when a voltage is applied across the material (MKS: ohm-meters). Resistivity is the reciprocal of conductivity.

Scalar MT Analysis: Resistivity values are determined from data reduction and interpretation of ratio of the power spectrum of an electric field component to the power spectrum of an magnetic field component orthogonal to the electric field component.

Schumann Band Frequencies: The frequencies in the frequency range, 8 Hz to 44 Hz, caused by electromagnetic fields generated by lightning strokes that propagate in the earth-ionosphere wave guide.

Sonde: Equivalent to sounding.

Static Response: Frequency Domain EM response near zero frequency. The static electric field response is used to calculate the apparent dc electrical resistivity value. The static magnetic field response is independent of the resistivity parameter; therefore, it has no interpretation value in the determination of the geoelectric section.

Telluric Currents: Currents caused to flow in the earth by natural electromagnetic source wave induction.

Tensor MT Analysis: A highly sophisticated analysis of magnetotelluric data which attempts to analyze only assured plane-wave energy fields (based upon coherence tests) and can give two and three-dimensional interpretation capability.

Thickness, H: The thickness of any rock sequence that appears macroscopically homogeneous in resistivity to the interpretation of a particular electrical method (MKS: meters).

Tipper Analysis: Analysis leading to data for interpretation of lateral resistivity variation about an MT recording site. The data reflects the wave-tilt from vertical propagation of the electromagnetic wave propagating in the earth.

Total-field Apparent Conductance, ST: The conductance of the nonuniform overburden and sedimentary column that rests upon an electrical insulator at a finite depth, which is not completely uniform, and which is underlain at finite depth by an electrical insulator, which is based upon the assumption of cylindrical current spreading from each source electrode in a completely uniform earth (MKS: mhos).

Total-field Apparent Resistivity, RT: The observed resistivity of the earth, which is not completely uniform, that would be computed based upon the geometric factor due to a finite length source with spherical current spreading from each source-electrode in a completely uniform earth (MKS: ohm-meters).

Transmittance (Transverse Resistance), T: The product of the thickness and the series summation of the resistivity values of parallel or bedding layers of an anisotropic geoelectric unit.

Transverse Resistivity, ρ_t: The resistivity determined by the series summation of resistivity values of parallel or bedding layers of an anisotropic geoelectric unit.

Type A Geoelectric Section: Resistivity distribution of a three layer sequence. $\rho_1 < \rho_2 < \rho_3$

Type H Geoelectric Section: Resistivity distribution of a three layer sequence. $\rho_1 > \rho_2 < \rho_3$

Type K Geoelectric Section: Resistivity distribution of a three layer sequence. $\rho_1 < \rho_2 > \rho_3$

Type Q Geoelectric Section: Resistivity distribution of a three layer sequence. $\rho_1 > \rho_2 > \rho_3$

APPENDIX II

SCALAR AMT-MT SOUNDINGS

Contents:

General Description of AMT-MT Sources and Wave Progation

In the magenetotelluric (MT)sounding method and the telluric current methods, naturally occuring electromagnetic fields are used as source fields. Electromagnetic waves impinging on the earth's surface are generally refracted vertically into the earth medium below. This happens because of the resistivity contrast at the free air - earth interface. The incoming electromagnetic wave (in free space) essentially has only one component, a magnetic field component, because the free space has a nearly infinite resistivity value, therefore current will not flow. Once the electromagnetic wave has been refracted into the relatively conductive earth space, the magnetic field induces an electric field component.

There are two criteria for the electromagnetic wave propagation that must be met before the "state of the art" MT interpretation can be performed. These criteria are:

1. The electromagnetic waves must propogate vertically into the earth at the free space-earth interface. (An example of where the criteria is not met is on Greenland and its ice cap).
2. The electromagnetic wave must be a plane-wave, that is, the magnetic field component and its induced electric field component must be orthogonal to one another. If one assumes a point source, such as a lightning stroke (spheric), the source location must be at least one free-space wave-length away from the point of measurement.

Criteria 1 above is met adequately over most of the surface of the earth, excluding the polar regions where there is an ice cover.

Criteria 2 above is met by much of the energy classified as P_c frequencies (1.0×10^{-5} Hz to 2.0 Hz) and the Audio MT frequencies (2.0 Hz to 1000 Hz) energy. See Figure 1 below.

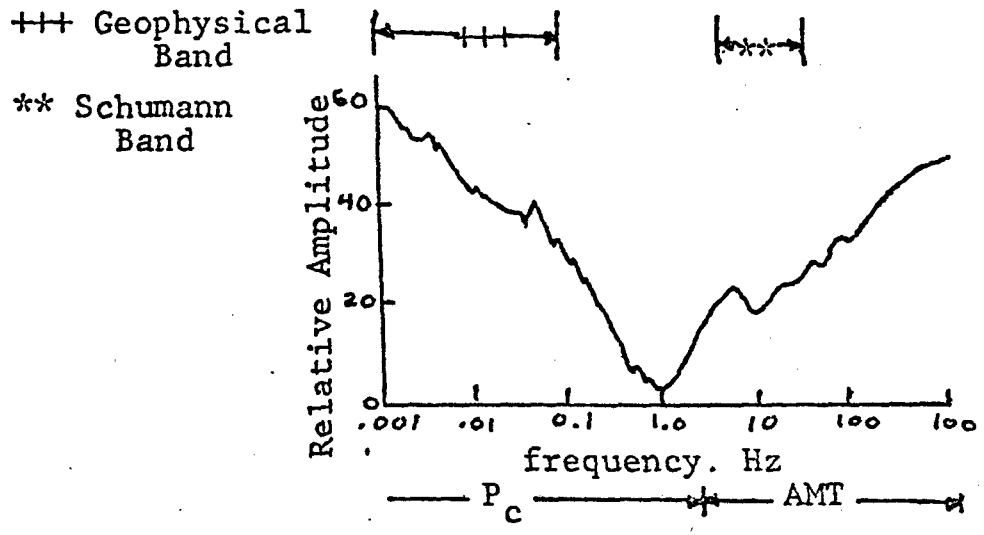

Figure 1. Typical distribution of electromagnetic change vs. freq.

In the 2.0 Hz to 1000 Hz (AMT) spectrum, the electromagnetic waves propagate in the earth-ionosphere wave-guide and/or along the earth's surface. The major source type found in this spectrum is the spheric source which generates frequencies in the Schumann Band (8.0 Hz to 44.0 Hz). Spheric source energy from the three major storm cell areas of the earth (Central Africa, Brazil, and Pacific Ocean storm areas) provide plane-wave energy over most of the earth. One cannot use this energy if a measuring site is within 1000 kilometers of the edges of any one of the storm cells. Further, local thunder storms are usually too close to provide plane-wave energy (far field energy).

In the 1.0×10^{-5} Hz (approximate diurnal variation frequency) to the 2.0 Hz spectrum, pseudo-electromagnetic waves are generated by large ring currents and standing waves established by the interaction of the solar winds and the earth's magnetic field and its ionosphere. The effective very large pseudo-wave fronts generate plane-wave electromagnetic waves in the earth. These wave-fronts impinge nearly vertical on the earth.

Geophysicists generally limit their use of these waves to the to the 0.001 Hz to the 2.0 Hz frequency band.

Magnetotelluric Receivers & Data Acquisition Requirements

Magnetotelluric recevers, thereby the type of interpretation one wishes to make; qualitative or quantitative. This interpretation criteria specifies the data reduction technique to be used. The data reduction techniques all face the decision as to what signals in a given time window are plane-wave in character and propagating in a vertical sense just below the earth-free space interface and as to what signals are not. The later signals are noise to be overcome.

The above decision, for qualitative interpretation, is generally made on the basis of repeatability of power spectra ratios, J-Factor ratios or individual signal signature ratios which give statistical repeatability of the intrinsic impedance, $\bar{Z}$,

$$\bar{Z}(k)_{f_i} = \frac{\bar{E}(k)}{\bar{H}(k)} \quad f_i$$

where $\bar{E}(k)$ is the electric field for a sampling of k units,
$\bar{H}(k)$ is the magnetic field for a sampling of k units,
at some frequency, f_i. (Impedance is used in the calculation of apparent resistivity because it eliminates the need to know the source strength as would be necessary for apparent resistivity calculations from either the electric field or magnetic field components alone). Repeatable intrinsic impedance, no matter how derived, is what is termed Scalar MT Analysis.

There are two specific frequency ranges where the qualitative data reduction provides a high degree of precision or correctness of the determination of apparent resistivity. These ranges are the 0.01 Hz to 0.1 Hz range and the 8.0 Hz to 36 Hz range (within the Schumann Band. Figure 1 above of the narural field spectrum shows

that these ranges have a relative high energy level and shows high energy peaks at discrete frequencies within each of the ranges.

The qualitative data reduction approach is not reliable in the 0.1 Hz to 5.0 Hz frequency range (tha frequency range showing minimum energy, Figure 1). Therefore, scalar data reduction doesn't provide a continuous spectrum for interpreting soundings.

If one wishes to determine an MT sounding utilizing the full MT-AMT spectrum, one must resort to tensor analysis for data reduction. This approach which provides data for quantitative interpretation, and goes beyond the the reduction for qualitative interpretation by the use of various schemes of the autopower spectrum and cross power spectrum analysis of the electromagnetic components on a number of selected time windows of the MT signal.

Electrodyne does not perform tensor MT soundings. Pritchard and others at the Colorado School of Mines and the USGS reached the conclusion, during the IGY and ISQY Programs, 1957 thru 1965, along with many others on a world wide basis, that there are some basic drawbacks to deriving adequate interpretation of the electrical resistivity distribution of the earth crust by MT soundings alone. The above group of investigators have found that an approach of supplementing the 0.1 Hz to 5.0 Hz spectrum "hole" by controlled source electromagnetic measurements is a wiser course of action to acheive reliable data for interpretation. This "hole" frequency band is the the frequency band that most often gives interpretation--quantitative interpretation at the depth of maximum interest in the geologic section. Therefore, this band for interpretation has to be retrieved with as much accuracy as possible.

Pritchard and many other investigators have found that scalar data acquisition and reduction of data in the two high energy frequency bands mentioned above provide a useful and cost effective

for reconniassance surveys. These reconnaissance surveys help to locate areas with zones of high contrast in the resistivity parameter (both shallow and at depth) in the geologic section. Also, these measurements will often locate the major and/or regional structural trends in Basin and Range type geoelectric sections.

Electrodyne Scalar AMT-MT Data Acquisition

Scalar AMT-MT data in the Schumann Band frequencies (8 Hz to 32 Hz) and the P_c band frequencies (0.02 Hz to 0.06 Hz) are obtained by simultaneous recording of orthogonal horizontal components of the naturally occuring telluric and magnetic fields. The telluric field is generally measured using delta potential dipoles 190 meters in length and the magnetic field is measured by a two-axis fluxgate magnetometer with a 0.5 gamma sensitivity. For most Basin and Range Province surveys, the Y-telluric component is oriented along an azimuth of N20E, if possible, and the X-telluric component is orthognal to the Y-component or oriented along an azimuth of N110E (see Plate I of the text). The typical scalar AMT-MT site used is shown in Figure 2.

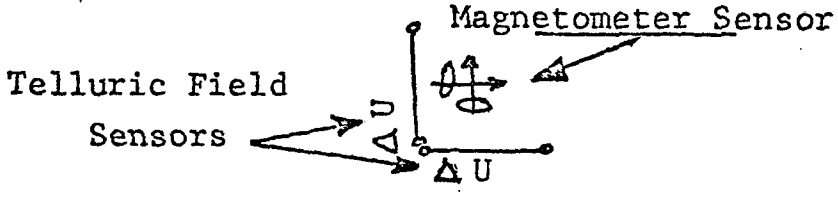

Figure 2. Scalar Magnetotelluric Site Layout.

The data or incoming signal is passed through a signal conditioner (filters and amplifiers) and recorded on a 4-channel analog tape. The peak amplitude resolution of these tape recordings is 45 db. In addition to the tape recordings, graphic recordings of the incoming signal are made for quality control of the tape recordings and as a back up measurement in case of failure of the tape recorders.

The fluxgate magnetometer mentioned above, with a 0.5 gamma sensitivity used in 1977 by Electrodyne, did not always give

adequate signal recovery of the magnetic field in the Schumann Band frequiencies. For this reason, normalized scalar apparent resistivity values were determined for these frequencies by considering the telluric signal strength alone.

It was discovered during the IGY and IQSY programs, and possibily before, that the telluric field strength of spheric source signals from the world storm centers only vary by ± 50 percent in amplitude on any given day. This was found to be true by Pritchard among others, and Electrodyne has retested this variation criteria on numerous occassions during 1977 and found that the criteria still holds. The most recent reference to this criteria was made by Telford, 1977, where he states the variation is only ± 30 percent in his findings. There are numerous references to this variation in the Journal of Geophysical Research (AGU) during the period of 1957 to 1966.

Because of this important criteria, one can make use of the Schumann Band frequencies for qualitative investigations, even in the event that the signal is to small to be measured by a magnetometer at any given time. Investigators in their surveys use the qualitative reconniassance tellurics and AMT-MT measurements to to discover areas that show gross anomalous change in resistivity over an area. The gross changes in resistivity looked for are of the order of 2 to 10 or even greater. The correspnding changes in amplitude are from 200 to 1,000 percent or even greater. So it is seen that the small percent change over any given day of recording is small and insignificant in light of the spatial variations looked for in reconnaissance surveys.

Electrodyne has upgraded its scalar magnetic field detection capability by incorporating an active fluxcollector, fluxgate mag-

Telford, W. M., 1977, Characteristics of audio and sub-audio telluric signals, Geophysical Prospecting, v. 25, 321-333.

netometer whose internal noise level (peak to peak) is about 20 milligammas. Presently, Electrodyne is continuing support of the R & D effort on the magnetometer to reduce the internal noise level to a 5 milligamma threshhold in the Schumann Band frequencies.

Electrodyne Scalar AMT-MT Data Reduction

Electrodyne normally performs scalar AMT-MT data reduction by amplitude spectral analysis of visually inspected windows of recording time. The analysis procedure stacks, thereby averages, a number of spectral amplitude versus frequency curves to get a good statistical average of a data segment. The stacking of the amplitude spectra for various wide band frequency recordings is as follows:

1. stacking of spectrums from 4 to 8 time-windows in the P_c range, and
2. stacking of spectrums from 16 to 64 time-windows in the Schumann Band range. More than one data segment is analysed for each frequency range and the best statistical average of the compon-impedances, i. e.,

$$Z_{xy} = \frac{E_x}{H_y} \quad \text{and} \quad Z_{yx} = \frac{E_y}{H_x}$$

are used to derive the component scalar apparent resistivities.

Scalar AMT-MT Apparent Resistivity Calculation / Spectrum Frequency

$$\rho_a = 0.2\ (1/f) \left| \frac{E}{H} \right|^2$$

where

ρ_a is the scalar apparent resistivity (ohm-meters),
f is the cyclic frequency of the amplitude spectra (Hz),
E is the amplitude of the telluric field component (mv/km),
H is the amplitude of the magnetic field component (gammas).

The resulting apparent resistivity components are:

$$\rho_{a_{xy}} = 0.2\ (1/f) \left| \frac{E_x}{H_y} \right|^2$$

and

$$\rho_{a_{yx}} = 0.2\ (1/f) \left| \frac{E_y}{H_x} \right|^2$$

An Effective scalar apparent resistivity is derived from the above componet resistivities for final interpretation.

Effective Apparent Resistivity

$$\rho_{a_E} = \left| \rho_{a_{xy}} \times \rho_{a_{yx}} \right|^{\frac{1}{2}} \quad \text{(logrithmic average)}$$

The spectral analysis approach is used in the scalar data reduction to give the investigator a qualitative judgement as to the degree that the measurements are affected by two and/or three dimensional variations. Figure 3 presents an example of Electrodyne's spectral analysis fo Z_{xy} for a set of time windows over the various frequency ranges of interest.

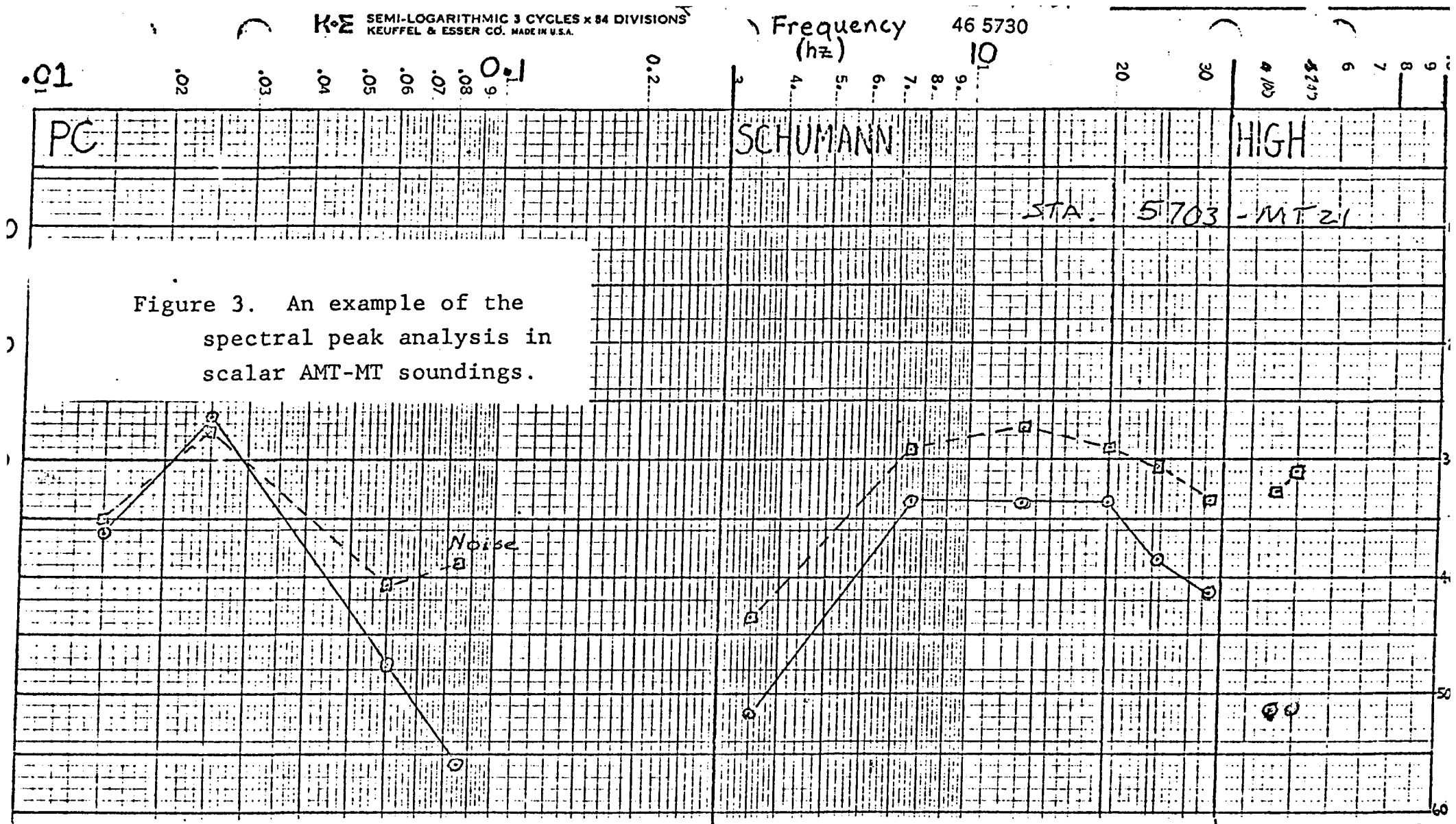

Figure 3. An example of the spectral peak analysis in scalar AMT-MT soundings.

ARRAY	REC. GAIN	P.B. ATT.	RMS	COMMENT	REC. GAIN	P.B. ATT.	RMS	COMMENT	REC. GAIN	P.B. ATT.	RMS
Ey	200 X 100	30	-59.5	4	500 X 100	30	-21.0	64	200 X 100	30	-19
	X				X				X		
	X				X				X		20
Hx	500 X 100	30	-34.6		500 X 100	30	-14.9		200 X 100	30	-15.0

Interpretation Considerations

The Schumann Band AMT frequencies, which more often than not, are limited in depth of penetration to no greater than 1,000 feet in most Basin and Range Province surveys. The general interpretation feature of this frequency band is the apparent resistivity contrasts alone in the near-surface geoelectric section. The apparent depth of penetration over the pospect varies approximately as the square root of the increase or decrease of this apparent resistivity.

For the low frequency P_c frequency band, deep penetration into the geologic section is caused, probably the penetration is well into the electrical basement section at most of the measuring sites. Therefore, one should not expect apparent resistivity values in this band to give as low a resistivity value nor an accurate dpeth estimate to conductive sections above electrical basement. But, the location of the areal location of conductive zones above electrical basement should be indicated very well by these measurements when large contrasts in resistivity are found in the survey coverage. Relatively low apparent resistivity values may indicate areas having fault-like features (two and three dimensional effects). Large areas showing relatively low apparent resistivity values may be thought to be caused by decreases in the section resistivity, ect. These considerations are true for apparent resistivity contour maps of scalar AMT-MT measurements. Because one has such a multitude of choices in interpretation to choose from, Electrodyne performs a high spatial density of measurment locations over the prospect area to provide a logical interpretation picture.

TABLE II-1

SCALAR MT-AMT APPARENT RESISTIVITY VALUES

STATION NUMBER	APPARENT RESISTIVITY (ohm-meter)	FREQUENCY (hz)		APPARENT RESISTIVITY {NORMALIZED}	FREQUENCY (hz)
1	28	0.045		0.57	14
2	19	0.04		2.8	14
3	180	0.04		3.8	14
4	160	0.04		3.2	14
5	10	0.04		5.1	14
6	500	0.04		3.7	14
7	150	0.04		9.2	14
8	1.2	0.04		1.8	14
9	35	0.04		4.3	14
10	12	0.04		1.5	14
11	0.25	0.04		2.1	14
12	1.6	0.04		1.7	14
13	56	0.035		HIGHLY SKEWED	—
14	0.36	0.04		2.3	14
15	4.1	0.035		0.46	14
16	14	0.035		1.6	14
17	16	0.03		1.8	14
18	5.5	0.03		4.0	14
19	3.1	0.035		1.4	14
20	7.2	0.03		3.9	14
21	4.5	0.035		3.2	14
22	9	0.04		5.4	14
23	5	0.04		4.4	14
24	97	0.035		2.4	14
25	71	0.03		9.8	14
26	N.V.	—		N.V.	—
27	34	0.04		5.9	14
28	7.9	0.04		3.9	14
29	9.9	0.04		6.1	14
30	5.3	0.05		2.3	14
31	3.4	0.03		1.1	14

Discussion

The vector telluric method criteria for wave-propagation, data acquisition,and reduction, and interpretation are the same as the criteria discussed for scallar AMT-MT soundings, Appendix II.

When making vector telluric measurements, one records the potential differences,on grounded dipoles for vectorial measurements, at a telluric vector base station and one or more roving vector telluric stations. See the Figure below.

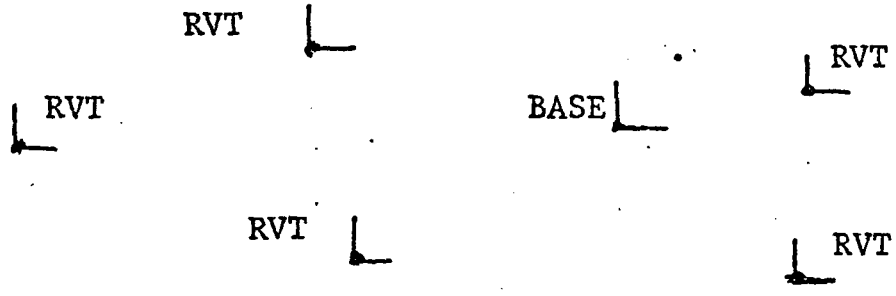

Figure 1. Typical Vector Telluric Survey Layout

The vector telluric measurements, like the telluric profile measurements discussed in Appendix IV, give normalized apparent reisitivity values when taken in ratio for two or more stations. The parameters derived from the measurements are:

Normalized Apparent Resistivity Components

$$\rho_{a_x} = Q \frac{E_x \text{ (RVT site)}}{E_x \text{ (Base)}}$$

$$\rho_{a_y} = Q \frac{E_y \text{ (RVT site)}}{E_y \text{ BASE}}$$

where

ρ_a is the normalized apparent resistivity,

E is the amplitude of the telluric field component,

and

Q is the apparent resistivity determined for the BASE Site by some other electromagnetic method, such as scalar AMT-MT measurements or controlled source measurements.

Effective Apparent Resistivity

$$\rho_{a_E} = \left| \rho_{a_x} \times \rho_{a_y} \right|^{\frac{1}{2}}$$

The vector telluric measurements were performed in this prospect for several reasons:

1. Electrodyne has been studying the cost effectiveness of several reconnaissance techniques. The results of the vector measurements study indicate that such measurements can only be cost effective for surveys of very large areas or on a long term contract basis for a vector telluric reconaissance crew.

2. Electrodyne's study indicates that one can set-up closer to cultural noise features and on days of high wind than one can in making any AMT-MT measurements. This certainly a cost effective plus for this type of measurement.

3. 1977 was an extremely quiet (low amplitude) year for magnetotellurix signals; therefore telluric measurements of low amplitude are much more reliable than low amplitude magnetic field measurements. Certainly an MT base with cryogenic magnetometer and satelite tellurin vector telluric stations are a cost effective means of obtaining multiple MT soundings.

TABLE III-1

VECTOR TELLURIC APPARENT RESISTIVITY VALUES

STATION NUMBER (VT)	APPARENT RESISTIVITY (ohm-meter)	FREQUENCY (hz)	APPARENT RESISTIVITY {NORMALIZED}	FREQUENCY (hz)	STATION NUMBER (VT BASE)
1	N.V.	0.045	N.V.	14	
2	380		6.0		B2
3	440		5.8		B2
4	230		7.9		B2
5*	40		12		B3
6	43		17		B3
7	22		26		B3
8	1.5		7.5		B3-B4
9	2.1		12		B4
10	5.3		6.0		B4
11	3.8		4.0		B4
12	9.9		6.1		B1
13	5.0		1.9		B1
14	5.5		1.0		B1
15	36.0		13		B1
16	14.	0.045	2.1	14	B1-B2

* Vector Telluric #5 = Vector Telluric Base #2

APPENDIX IV

Telluric Profile Measurements

In-line (End-On-End) Telluric Profiles

Contents:

Description and Discussion

The telluric profile method criteria for natural field electromagnetic waves, wave-propagation, data acquisition and data reduction are similar to those for scalar AMT-MT soundings, Appendix II.

The telluric profiling method layout is two or more receiver dipoles, which are contiguous to one another and are oriented in-line along the profile, that are used to make simultaneous measurements of the natural electric field (telluric field) signals in the earth. This profiling method is known as the in-line or end-on-end telluric method.

By taking the ratio of the amplitudes of correlated telluric field signatures, on the different dipoles that have been recorded simultaneously, one determines the gradient of the electric field along the survey profile.

By Ohm's Law,

$$\vec{E} = \rho \vec{J}$$

where

$\vec{E}$ is the electric field vector,

$\vec{J}$ is the current density vector,

and

ρ is the resitivity of the medium of current flow,

the gradient provides a measure of the apparent change in resistivity along the profile. This apparent change reflects both changes of resistivity as a function of depth and changes of resistivity laterally along the profile.

Figure 1 below shows a typical in-line telluric profile.

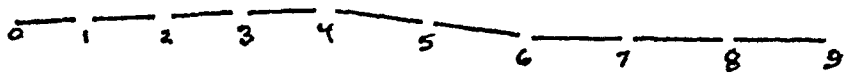

Figure 1.

Obviously, the apparent resistivity values determined from telluric profile measurements are normalized values rather than true values. The normalized values are adjusted to true apparent resistivity values by incorporation of results from scalar AMT-MT soundings, vector telluric soundings, or electromagnetic controlled source soundings performed at one or more locations along the profile.

Electrodyne does not use crossing telluric profile lines to to provide the intertie of telluric profiles because the cross over points may be controlled by a feature in the subsurface that skews telluric signals in the vicinity of the cross over points. Further, Electrodyne tries to keep its telluric profiles oriented within a solid angle of $\pm$ 45 degrees of magnetic east and west to take optimum advantage of the predominant telluric current flow direction. Telluric profile measurements along profiles oriented along lines not within the solid angle tend to cause misinterpretation of the geoelectric section because nonplane wave signal information is analysed more frequently than not. Fortunately, the Basin and Range Province regional structural trends occur in a solid angle which is generally perpendicular to the maximum current flow solid angle. Generally, the value of telluric profile interpretation is optimized when the profiles cross the predominant structural control at or near an angle of 90 degrees.

Electrodyne uses a four electric dipole receiver scheme in its in its standard field operation. The four dipoles of information are recorded on analog tape for spectral analysis similar to that

used in the scalar AMT-MT analysis. The Hewlett-packard tape recorders used by Electrodyne require all dipole receivers to have a common reference. This is acheived by the layout scheme shown in Figure 2. Location 2 in the figure is the common reference mentioned above.

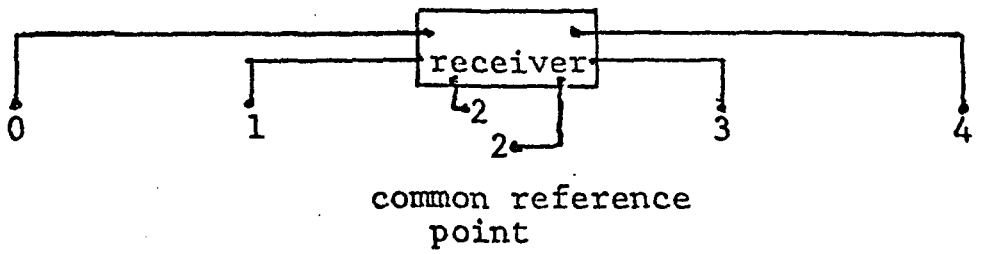

Figure 2. Electrodyne four dipole receiver layout.

The Electrodyne set-up normally uses a dipole resistivity density of 4 to 5 dipole receivers per mile.

The desired dipole potential difference measurements for data analysis are:

$$\Delta U_{0-2};\ \Delta U_{1-2};\ \Delta U_{3-2};\ \text{and}\ \Delta U_{4-3}$$

The dipole potential difference measurements that are actually measured are:

$$\Delta U_{0-2};\ \Delta U_{1-2};\ \Delta U_{3-2};\ \text{and}\ \Delta U_{4-2}$$

The desired potential difference measurements are derived after the spectral analysis of visually selected time windows of proper data. Figure 3 gives an example of the spectral analysis results of a group of time windows. Note that the amplitude spectra of arrays ΔU_{0-2} and ΔU_{4-2} are approximately 6 db larger than the normalized spectra for ΔU_{1-2} and ΔU_{3-2}. The desired normalized values for ΔU_{0-1} and ΔU_{3-2} are determined by the amplitude spectra differences as follows:

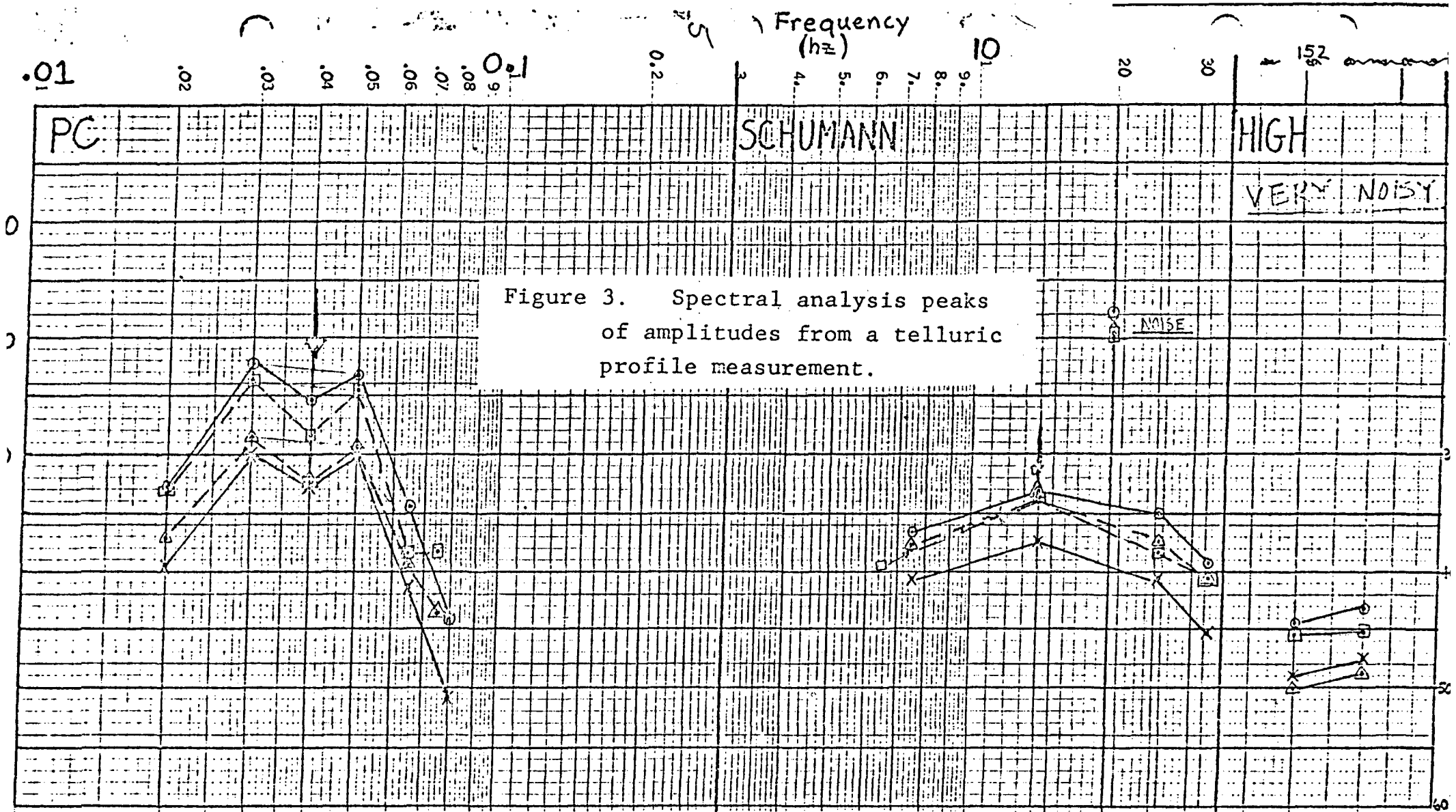

Figure 3. Spectral analysis peaks of amplitudes from a telluric profile measurement.

ARRAY	REC. GAIN	P.B. ATT.	RMS	COMMENT	REC. GAIN	P.B. ATT.	RMS	COMMENT	REC. GAIN	P.B. ATT.	RMS
O (0-2)	200 X 100	-30	-54.5	Good correlation & Pking	100 X 100	-30	-24	Noisy like TIS	100 X 10	-30	-46.
X (1-2)	200 X 100	-30	-55.5		100 X 100	-30	-23.5	Noisy just like TIS	100 X 10	-30	-47.
△ (2-3)	200 X 100	-30	-55.2		100 X 100	-30	-25.4	Noisy but [illegible]	100 X 10	-30	-45.
□ (2-4)	200 X 100	-30	-49.1	Gd correlation	100 X 100	-30	-25.4	Sch Res improving	100 X 10	-30	-42.

$$\left|\Delta U_{0-1}\right| = \left|\Delta U_{0-2}\right| - \left|\Delta U_{1-2}\right|$$

and

$$\left|\Delta U_{4-3}\right| = \left|\Delta U_{4-2}\right| - \left|\Delta U_{3-2}\right|$$

The spectral analysis approach is cost effective in data reduction (time saving) as compared to the hand picking of data from graphic records for amplitude ratio determinations. The approach is cost effective in field operation of data acquisition time because three dipoles of new data information per set-up are acquired as compared to one new dipole of information per set-up as in the standard layout approach. The wide-band recording with spectral analysis gives one considerably more confidence in the data reduction and gives a definite clue to dipole measurements that are affected by two and/or three diemnsional lateral resistivity variations such as are caused by strutural features, etc. See Figure 3.

TABLE IV-1

PROFILE 1

Telluric Profile Apparent Resistivity Values

STATION NUMBER	APPARENT RESISTIVITY (ohm-meter)	FREQUENCY (Hz)	APPARENT RESISTIVITY	FREQUENCY (Hz)	BASE NUMBER TIE
1	1.4	0.045	0.2	14	VTB-4
2	2.3	↓	0.86	↓	
3	2.3		3.3		
4	1.0		2.1		
5					
6					
7					
8					
9					
10					
11					
12					
13					
14					
15					
16					
17					
18					
19					
20					
21					
22					
23					
24					
25					
26					
27					
28					
29					
30					

TABLE IV-2

PROFILE 2

Telluric Profile Apparent Resistivity Values

STATION NUMBER	APPARENT RESISTIVITY (ohm-meter)	FREQUENCY (Hz)	APPARENT RESISTIVITY	FREQUENCY (Hz)	BASE NUMBER TIE
1	4.3	0.045	1.4	14	
2	3.1	↓	1.1	↓	
3	4.4		1.2		
4	1.9		1.3		
5	2.5		1.2		
6	1.8		1.0		
7	2.1		0.86		VT-14
8	1.6	↓	0.60	↓	
9					
10					
11					
12					
13					
14					
15					
16					
17					
18					
19					
20					
21					
22					
23					
24					
25					
26					
27					
28					
29					
30					

TABLE IV-3

PROFILE 3

Telluric Profile Apparent Resistivity Values

STATION NUMBER	APPARENT RESISTIVITY (ohm-meter)	FREQUENCY (Hz)	APPARENT RESISTIVITY	FREQUENCY (Hz)	BASE NUMBER TIE
1	3.4	0.045	0.91	14	
2	3.8		1.1		
3	4.4		1.5		
4	5.0		1.9		VT-13
5	5.7		2.9		
6	7.0		3.0		
7	5.8		7.7		
8	7.1		10		
9					
10					
11					
12					
13					
14					
15					
16					
17					
18					
19					
20					
21					
22					
23					
24					
25					
26					
27					
28					
29					
30					

TABLE IV-4

PROFILE 4

Telluric Profile Apparent Resistivity Values

STATION NUMBER	APPARENT RESISTIVITY (ohm-meter)	FREQUENCY (Hz)	APPARENT RESISTIVITY	FREQUENCY (Hz)	BASE NUMBER TIE
1	4.3	0.045	4.5	14	
2	3.5		4.7		
3	11.		5.8		
4	9.0		6.1		
5	9.9		6.1		VT-12
6	9.0		6.1		
7	10.		6.6		
8	11		7.1		
9	12		7.7		
10					
11					
12					
13					
14					
15					
16					
17					
18					
19					
20					
21					
22					
23					
24					
25					
26					
27					
28					
29					
30					

TABLE IV- 5

PROFILE 5

Telluric Profile Apparent Resistivity Values

STATION NUMBER	APPARENT RESISTIVITY (ohm-meter)	FREQUENCY (Hz)	APPARENT RESISTIVITY	FREQUENCY (Hz)	BASE NUMBER TIE
1	8.8	0.045	5.8	14	
2	9.4	↓	6.7	↓	
3	10		7.6		
4	11		8.7		
5	7.9		3.9		VTB-1
6	5.9		1.8		
7	1.7	↓	2.2	↓	
8					
9					
10					
11					
12					
13					
14					
15					
16					
17					
18					
19					
20					
21					
22					
23					
24					
25					
26					
27					
28					
29					
30					

TABLE IV-6

PROFILE 6

Telluric Profile Apparent Resistivity Values

STATION NUMBER	APPARENT RESISTIVITY (ohm-meter)	FREQUENCY (Hz)	APPARENT RESISTIVITY	FREQUENCY (Hz)	BASE NUMBER TIE
1	40	0.045	11	14	TB-2
2	40		11		
3	36		10		
4	55		9.4		
5	39		13		VT-15
6	36		6.7		
7	21		6.3		
8	21		6.3		
9	12		0.57		
10	22		1.2		
11	38		2.0		
12	54		2.0		
13					
14					
15					
16					
17					
18					
19					
20					
21					
22					
23					
24					
25					
26					
27					
28					
29					
30					

TABLE IV-7

PROFILE 7

Telluric Profile Apparent Resistivity Values

STATION NUMBER	APPARENT RESISTIVITY (ohm-meter)	FREQUENCY (Hz)	APPARENT RESISTIVITY	FREQUENCY (Hz)	BASE NUMBER TIE
1	9.6	0.045	1.1	14	
2	8.9	↓	2.1	↓	
3	8.2		2.1		VT-16
4	14		2.1		
5	9.6		2.0		
6	5.5		2.7		
7	3.1		1.5		
8	1.8	↓	2.0	↓	
9					
10					
11					
12					
13					
14					
15					
16					
17					
18					
19					
20					
21					
22					
23					
24					
25					
26					
27					
28					
29					
30					

TABLE IV- 8

PROFILE 8

Telluric Profile Apparent Resistivity Values

STATION NUMBER	APPARENT RESISTIVITY (ohm-meter)	FREQUENCY (Hz)	APPARENT RESISTIVITY	FREQUENCY (Hz)	BASE NUMBER TIE
1	<0.1	0.045	.24	14	
2	.12	↓	.58	↓	
3	.12		.26		
4	.25		.62		
5	.34		1.7		
6	.32		1.1		
7	.5	↓	3.1	↓	VTB-3
8					
9					
10					
11					
12					
13					
14					
15					
16					
17					
18					
19					
20					
21					
22					
23					
24					
25					
26					
27					
28					
29					
30					

TABLE IV- 9

PROFILE 9

Telluric Profile Apparent Resistivity Values

STATION NUMBER	APPARENT RESISTIVITY (ohm-meter)	FREQUENCY (Hz)	APPARENT RESISTIVITY	FREQUENCY (Hz)	BASE NUMBER TIE
1	43	0.045	17	14	VT-6
2	43	↓	17	↓	
3	43		17		
4	53		18		
5	41		19		
6	49		20		
7	54		23		
8	59		25		
9	66		28.		
10	63		63		
11	58		66		
12	29	↓	150	↓	
13					
14					
15					
16					
17					
18					
19					
20					
21					
22					
23					
24					
25					
26					
27					
28					
29					
30					

TABLE IV-10

PROFILE 10

Telluric Profile Apparent Resistivity Values

STATION NUMBER	APPARENT RESISTIVITY (ohm-meter)	FREQUENCY (Hz)	APPARENT RESISTIVITY	FREQUENCY (Hz)	BASE NUMBER TIE
1	17	0.045	120	14	
2	17		120		
3	28		110		
4	28		110		
5	34		91		
6	41		78		
7	49		68		
8	39		52		
9	39		52		
10	31		39		
11	11		41		
12	?		44		
13	3.9		39		
14	3.0		31		
15	2.4		31		
16	1.8		26		
17	0.41		26		
18	<0.1		6.9		
19	<0.1		1.8		
20	0.23		0.49		
21	3.2		1.4		VT-8
22	1.5		3.1		
23	2.2		7.5		
24	2.2		10		
25	2.3		3.9		VTB-4
26					
27					
28					
29					
30					

APPENDIX III

Vector Telluric Measurements

Contents:

TABLE IV-11

PROFILE 11

Telluric Profile Apparent Resistivity Values

STATION NUMBER	APPARENT RESISTIVITY (ohm-meter)	FREQUENCY (Hz)	APPARENT RESISTIVITY	FREQUENCY (Hz)	BASE NUMBER TIE
1	1.4	0.045	1.6	14	
2	5.1		1.0		
3	5.1		4.6		
4	10		3.9		MT-20
5	14		4.8		
6	20		5.8		
7	16		3.5		
8	13		3.5		
9	10		2.1		
10					
11					
12					
13					
14					
15					
16					
17					
18					
19					
20					
21					
22					
23					
24					
25					
26					
27					
28					
29					
30					

TABLE IV-12

PROFILE 12

Telluric Profile Apparent Resistivity Values

STATION NUMBER	APPARENT RESISTIVITY (ohm-meter)	FREQUENCY (Hz)	APPARENT RESISTIVITY	FREQUENCY (Hz)	BASE NUMBER TIE
1	52	0.045	26	14	
2	22	↓	26	↓	
3	22		26		VT-7
4	22		26		
5	62		29		
6	49		25		
7	27		13		
8	15		7.2		
9	8.3	↓	3.8	↓	
10					
11					
12					
13					
14					
15					
16					
17					
18					
19					
20					
21					
22					
23					
24					
25					
26					
27					
28					
29					
30					

TABLE IV-13

PROFILE 13

Telluric Profile Apparent Resistivity Values

STATION NUMBER	APPARENT RESISTIVITY (ohm-meter)	FREQUENCY (Hz)	APPARENT RESISTIVITY	FREQUENCY (Hz)	BASE NUMBER TIE
1	6.6	0.045	120	14	
2	5.9	↓	18	↓	
3	1.3		12		
4	1.7		10		
5	1.4		9.9		
6	1.1		9.9		
7	1.1		7.5		
8	0.76		12.		
9	2.1		15		VT-9
10	1.4		40		
11	9.0	↓	37	↓	
12					
13					
14					
15					
16					
17					
18					
19					
20					
21					
22					
23					
24					
25					
26					
27					
28					
29					
30					

TABLE IV-14

PROFILE 14

Telluric Profile Apparent Resistivity Values

STATION NUMBER	APPARENT RESISTIVITY (ohm-meter)	FREQUENCY (Hz)	APPARENT RESISTIVITY	FREQUENCY (Hz)	BASE NUMBER TIE
1	4.7	0.045	26	14	
2	3.6	↓	20	↓	
3	0.46		0.2		
4	3.9		8.9		VT-6
5	5.5		7.8		
6	3.6		7.8		
7	3.8		10		
8	5.3	↓	6.0	↓	MT-10
9					
10					
11					
12					
13					
14					
15					
16					
17					
18					
19					
20					
21					
22					
23					
24					
25					
26					
27					
28					
29					
30					

TABLE IV-15

PROFILE 15

Telluric Profile Apparent Resistivity Values

STATION NUMBER	APPARENT RESISTIVITY (ohm-meter)	FREQUENCY (Hz)	APPARENT RESISTIVITY	FREQUENCY (Hz)	BASE NUMBER TIE
1	5.0	0.045	9.3	14	
2	4.8		8.8		VT-8
3	3.1		8.0		
4	2.4		6.3		
5	1.7		5.3		
6	1.1		3.2		
7	1.4		2.4		
8	0.17		3.9		
9	0.14		1.3		
10	0.1		1.4		
11	<0.1		4.5		
12	0.3		12		
13	5.3		3.9		
14	4.3		8.5		
15	5.3		6.0		
16	5.0		6.0		
17	5.5		1.9		
18	3.9		1.8		
19	7.4		1.1		MT-20
20					
21					
22					
23					
24					
25					
26					
27					
28					
29					
30					

TABLE IV-16

PROFILE 16

Telluric Profile Apparent Resistivity Values

STATION NUMBER	APPARENT RESISTIVITY (ohm-meter)	FREQUENCY (Hz)	APPARENT RESISTIVITY	FREQUENCY (Hz)	BASE NUMBER TIE
1	3.6	0.045	8.5	14	
2	?		7.5		
3	3.2		3.1		
4	3.4		16		
5	2.2		0.8		
6	2.3		1.9		
7	2.2		1.5		
8	2.2		0.81		
9	2.0		1.6		
10	2.0		2.1		
11	1.9		2.1		
12	2.7		5.6		
13	1.9		6.5		
14	3.0		3.6		
15	0.73		?		VT-10
16	2.1		13		
17	4.9		8.5		
18	5.7		8.5		
19	4.6		8.5		
20	4.6		8.5		
21	4.6		15		
22	9.2		13		
23	5.1		12		
24	?		4.6		
25					
26					
27					
28					
29					
30					

TABLE IV-17

PROFILE 17

Telluric Profile Apparent Resistivity Values

STATION NUMBER	APPARENT RESISTIVITY	FREQUENCY (Hz)	APPARENT RESISTIVITY	FREQUENCY (Hz)	BASE NUMBER TIE
1	71	0.045	2.6	14	
2	69		2.5		
3	54		2.3		
4	14		1.8		
5	16		1.8		
6	12		0.83		
7	12		0.9		
8	13		1.0		
9	12		0.85		
10	11		0.85		
11	11		0.85		VT-11
12	11		0.93		
13	11		0.72		
14	12		1.3		
15	13		2.1		
16	14		3.1		
17					
18					
19					
20					
21					
22					
23					
24					
25					
26					
27					
28					
29					
30					

TABLE IV-18

PROFILE 15, 16

Telluric Profile Apparent Resistivity Values

STATION NUMBER	APPARENT RESISTIVITY (ohm-meter)	FREQUENCY (Hz)	APPARENT RESISTIVITY	FREQUENCY (Hz)	BASE NUMBER TIE
16 1 W	3.6	0.045			
1 E	3.1				
5 W	2.3				
5 E	2.4				
10 W	2.0				
10 E	1.7				
13 W	1.9				
13 E	2.7				
15 W	0.73				
15 E	<0.1				
16 W	2.1				
16 E	>6.4				
19 W	4.6				
19 E	>23				
24 W	N.R				
16 24 E	N.R				
15 1 W	N.R				
1 E	N.R				
4 W	2.4				
4 E	2.7				
7 W	1.4				
7 E	1.8				
10 W	0.1				
10 E	0.09				
13 W	5.3				
13 E	6.6				
16 W	5.0				
15 16 E	4.8				

TABLE IV-19

PROFILE 17

Telluric Profile Apparent Resistivity Values

STATION NUMBER	APPARENT RESISTIVITY (ohm-meter)	FREQUENCY (Hz)	APPARENT RESISTIVITY	FREQUENCY (Hz)	BASE NUMBER TIE
17 1 W	170	0.035			
1 E	71				
4 W	19				
4 E	14				
7 W	10				
7 E	12				
10 W	11				
10 E	17				
13 W	10				
17 13 E	11				
16					
17					
18					
19					
20					
21					
22					
23					
24					
25					
26					
27					
28					
29					
30					

APPENDIX V

Galvanic (dc) Electrical Resistivity Soundings

Contents:

Description of Methods

Qualitative interpretative Concepts

Survey Sounding Curves

Description of the Galvanic dc Resistivity Sounding and Profiling Methods

The galvanic dc resistivity sounding methods and profiling methods are:

1. Schlumberger method.
2. Monopole method,
3. Various dipole methods,
4. Modified Schlumberger method
5. Modified Polar Dipole-Bipole method,
6. Dipole-dipole method.

The choice of which method to use depends on the following:

1. Best possible sounding data with a minimum of interference from lateral resistivity variations (geologic noise).
2. Economic considerations: Monopole-shallow, Schlumberger- intermediate, and Equitorial method- deep pentration soundings.
3. Profiling methods:
   a. Modified sounding methods, Modified Schlumberger method and Modified Polar Dipole-Bipole methods for unknown depths of interest.
   b. Dipole-dipole method for known range of depths of interest.

Schlumberger Method

The Schlumberger array orientation is shown in the figure below. The two electrode pairs are in line and symmetric about the point O, with the distance AB between the source electrode

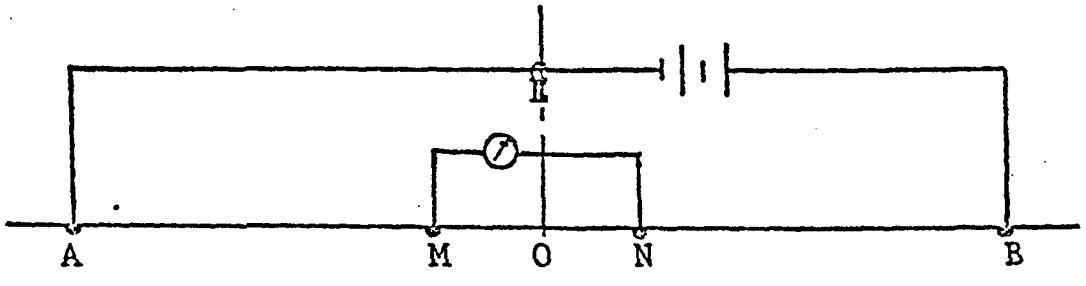

Schlumberger Array Configuration

pair being very large compared to the distance $\overline{MN}$ between the the measurement pair.

The depth of pentration is increased by increasing $\overline{AB}/2$. However, as $\overline{AB}/2$ is increased, the signal between M and N becomes too small to be detected reliably. When this occurs, the receiver seperation is increased and the measurements and $\overline{AB}/2$ expansion continues.

The apparent probing depth of the Schlumberger array in a homogeneous earth is equivalent to $\overline{AB}/2$. The location of each measurement in the geoelctric section is below the center of the array at the effective depth of penetration.

The gradient of the potential is measured between M and N because the measuring electrode pair separation is maintained small compared to the source electrode pair separation, $\overline{AB}$.

The Schlumberger array is less sensitive to lateral effects than any of the other sounding and profiling arrays, because only the source pair of electrodes is moved. These electrodes are at relatively great distances fromthe receiver pair, thus geologic noise in the vicinity of the source electrodes does not appreciably affect the gradient measurement. If geologic noise at the source electrodes is a factor in the measurements, the use of the Lee array configuration, as shown in the figure below, makes it possible to determine theselateral discontinuity effects. This is accomplished by making seperate half-potential measurements, $\overline{MO}$ and $\overline{ON}$, on each side of the center of the array.

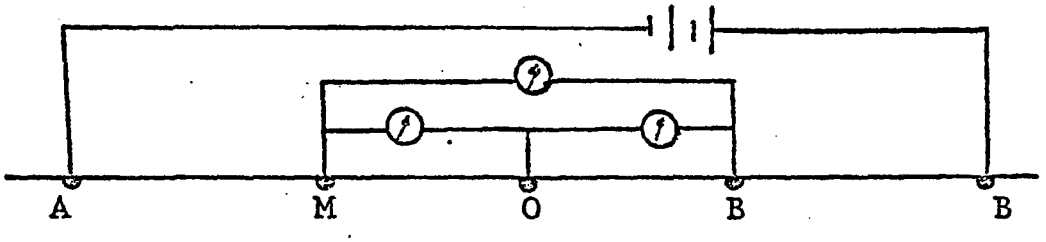

Lee Array Configuration

Monopole Method

The Monopole array is shown in the figure below. The

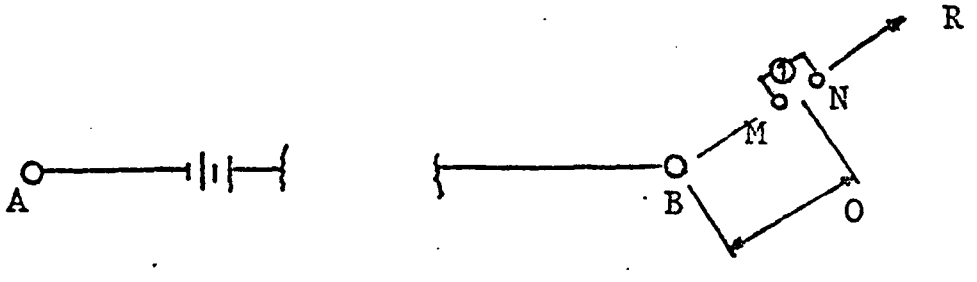

Monopole Array Configuration

distance AB is very large (assumed to be infinite) compared to the distance MN. Similarly, the distance AB is very large (assumed to be infinite) compared to the distance OB. The apparent depth of penentration in a homogeneous earth is increased directly as OB is increased. The separation MN is increased as the requirement for detectable signal dictates.

Dipole Arrays

The dipole arrays utilize an effective source dipole, $\overline{AB}$, and an effective receiver dipole, $\overline{MN}$. The dipole approximations are maintained by keeping $\overline{AB}$ and $\overline{MN}$ small compared to the source-receiver separation, R. See the figures below. Because two dipoles are used, the gradient of the $\vec{E}$ field is measured at $\overline{MN}$. The depth of penetration, DP, varies with each array used. The dipole arrays normally used are as follows:

Radial Dipole Array
$0.5R \leq DP \leq 0.67R$

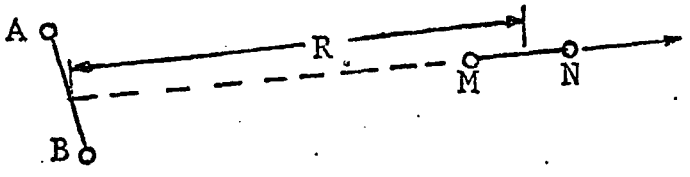

Tangential Dipole Array
$0.67R \leq DP \leq R$

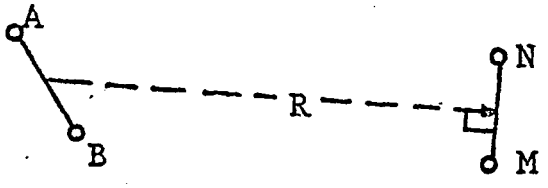

Parallel Dipole Array
$0.5R \leq DP \leq R$

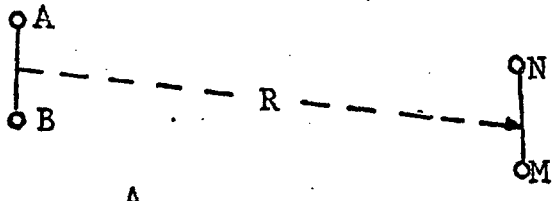

Perpendicular Dipole Array
$DP = 0.67\ R$

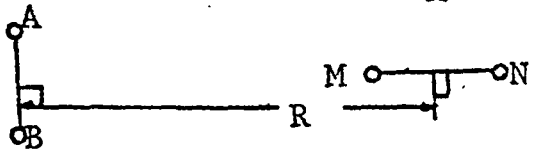

Polar Dipole Array
$DP = 0.5R$

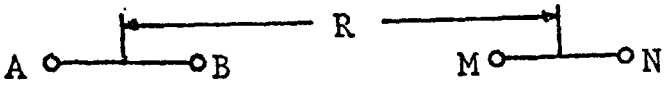

Equatorial Dipole Array
DP=R

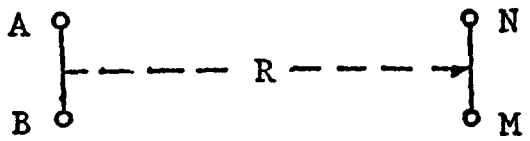

Equatorial Bipole-Dipole Array
(equivalent to Equitorial Dipole Array)
DP=R

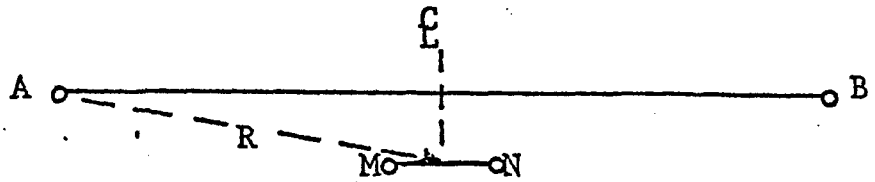

Modified Schlumberger Array

The Modified Schlumberger array is an expansion array of the receiver dipole, $\overline{MN}$, away from one of the source electrodes (monopole approximation) to the mid-point AB/2. See the figure below.

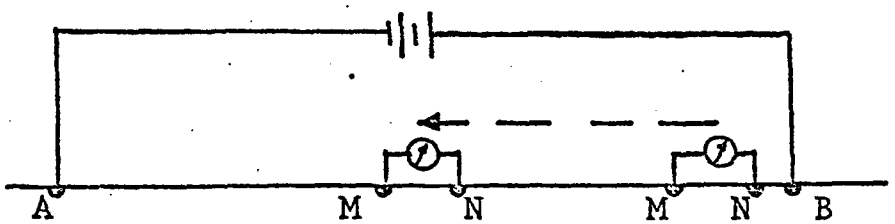

Modified Polar Dipole-Bipole Array

The Modified Polar Dipole-Bipole array is an expansion array of the receiver dipole, $\overline{MN}$, away from one of the surce electrodes (monopole approximation) outside and inline with the source bipole, $\overline{AB}$. Depth of effective penetration changes from the monopole depth of pentration toward the polar dipole depth of pentration as the array is expanded. See figure below.

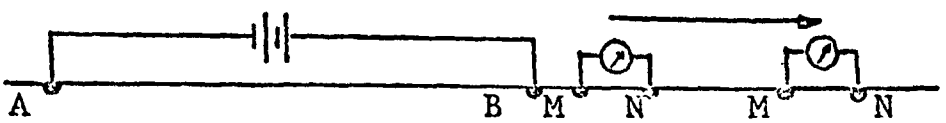

Some Considerations in the Interpretation of Resistivity Data

A permanent problem which must be routinely tackled in the interpretation of resistivity data is that of separating vertical effects from lateral effects. More correctly stated, one wants to discover both the lateral and depth distribution of resistivity in a geoelectric section.

A probable solution to the above ambiguities may be achieved by carrying out depth soundings at a high station density. However, such a solution is more often than not economically unacceptable.

One alternative to the costly high-density depth sounding approach is the use of combined modified Schlumberger soundings, monopole soundings, and equatorial soundings about a very long bipole source. This approach is very effective if the soundings are made about a crossed bipole source set-up as shown in Figure 1, although this approach is twice as costly as the single bipole source approach. The extra cost is offset by the following very positive interpretation features:

1. If an interpretation is totally correct from the sounding curves of one source, the interpretation for sounding from the other source will duplicate the interpretation found for the first source soundings. This seldom happens.

2. The multiple soundings from the two sources which provide depth of penetration to specific depths at different locations about the bipole source cross over point give one a very good interpretative handle on the lateral variation about the souce location. For examples of this, see Figures 2 - 6, as

to the interpretation capability.

It should be apparent that the use:of galvanic (dc) soundings about crossed long bipole sources is a very effective way of obtaining at least a qualitative description of the electrical resistivity distribution to depth and laterally within an area of interest in difficult interpretative sections such as are found in the Basin and Range Province. This sounding approach is relatively costly if done a random basis. Therefore, Electrodyne performs reconnaissance surveys using the less expensive telluric profiling and scalar AMT-MT sounding methods to locate areas of interest for detailing soundings such as the crossed bipole dc soundings and EM soundings.

As with the electromagnetic sounding detailing (which prevents one from overlooking important conductors below resistive screening layers, layers that prevent detection of the conductors by the dc sounding methods); dc soundings should be made to prevent one from interpreting layers having large vertical anisotropy and/or overlooking screening layers by the EM soundings. The EM sounding interpretations will forcast depths to conductive sections that are underestimated for both of the above. Simply stated, one has to make both dc soundings and EM soundings in detailing surveys, if they wish to obtain a good interpretation of the geoelectric section in areas such as the Basin and Range Province.

There are two considerations in dc soundings when their results are compared to EM sounding results. These are:

1. The dc sounding interpretation will lead one to conclude that an anomalous conductive zone at depth will have a much larger areal extent than the EM interpretations will indicate.

2. The dc sounding interpretations of layer resistivity and layer thickness will always be equal to or greater than those interpreted from EM soundings for a layered earth interpretation.

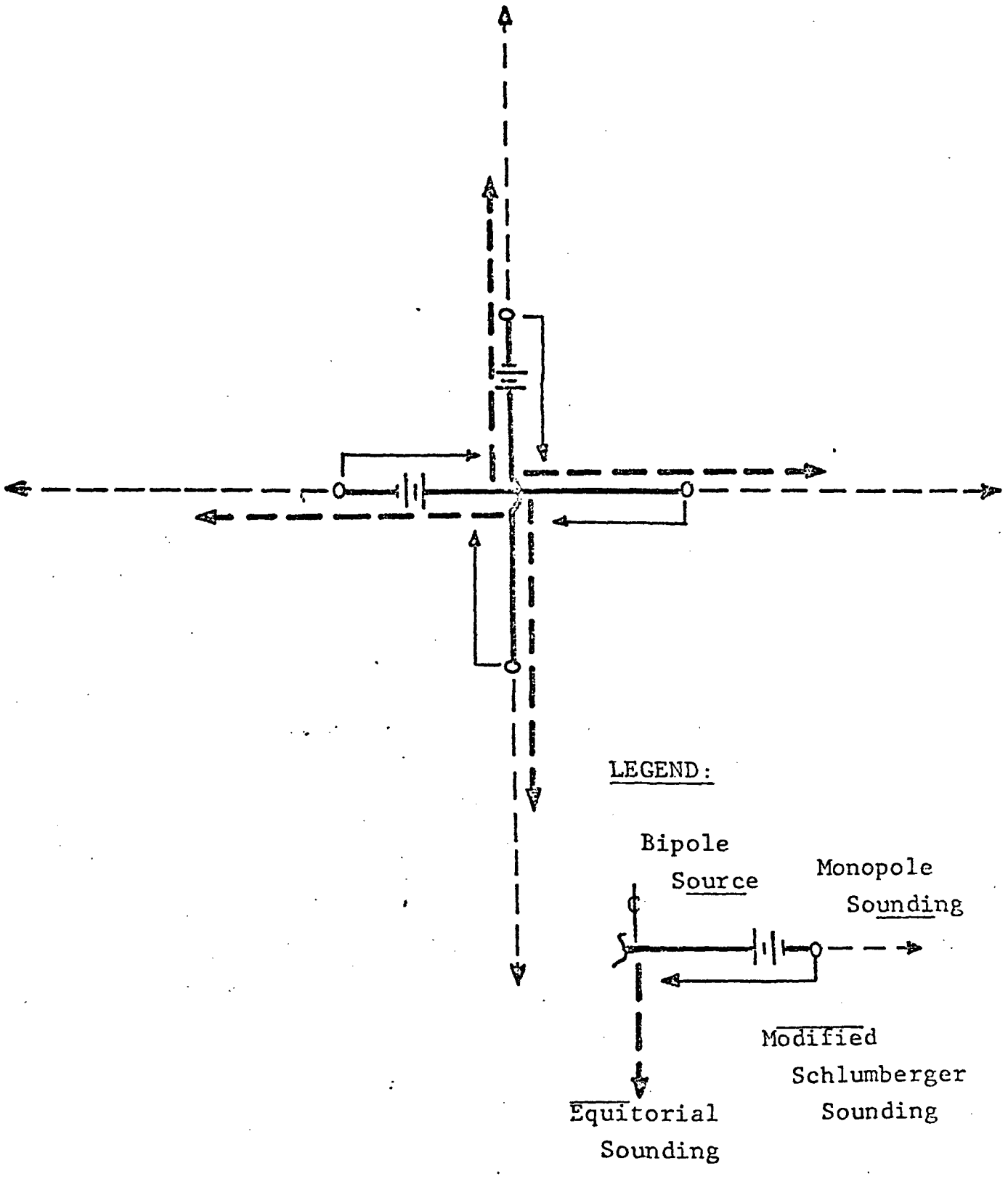

Figure 1. Cross Bipole Source--Modified Schlumberger, Monopole, and Equitorial Sounding Array Representation.

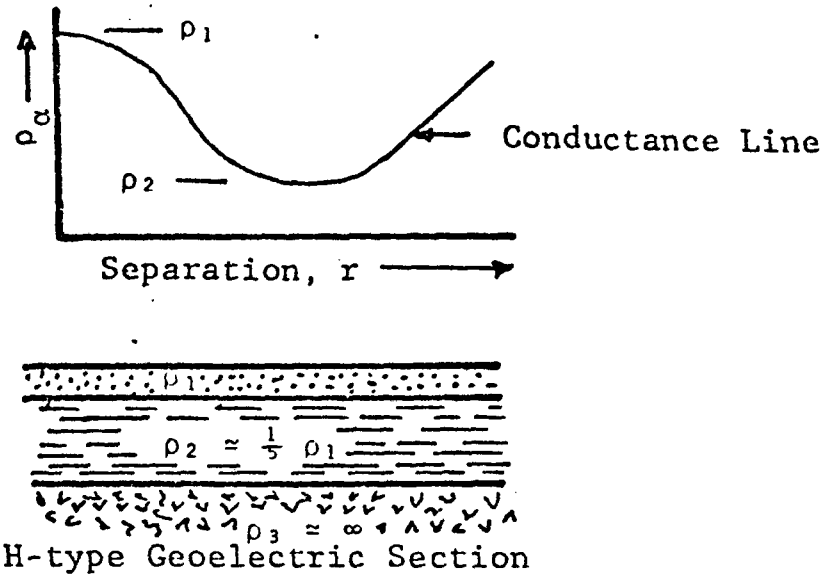

Figure 2. Typical 3-layer Geothermal Model and Sounding

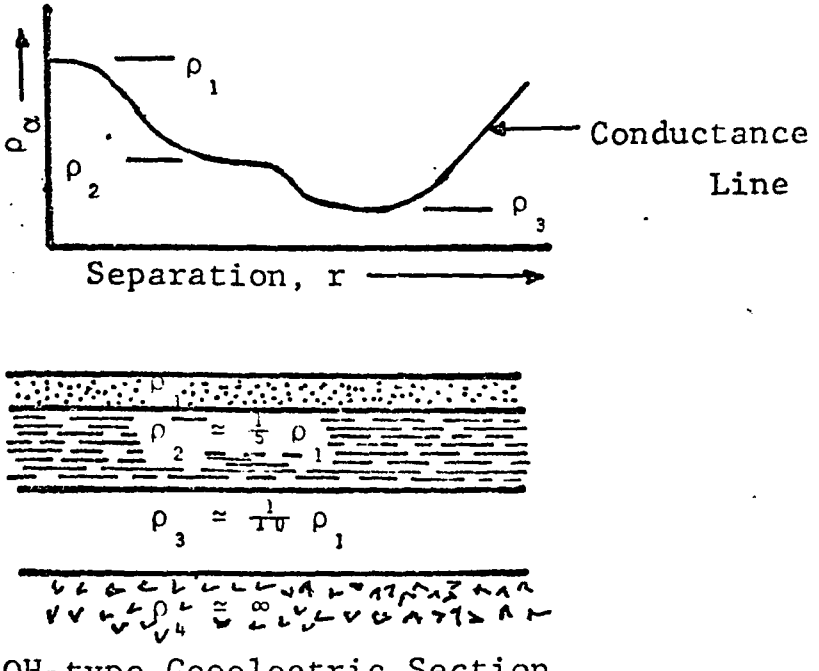

Figure 3. Typical 4-layer Geothermal Model and Sounding

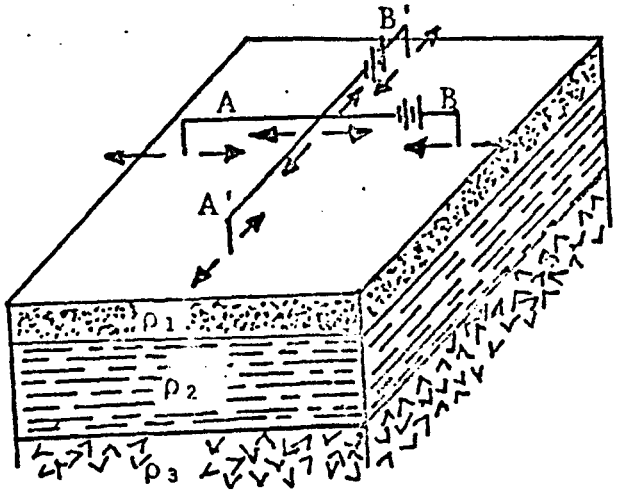

$\rho_1 > \rho_2 << \rho_3$

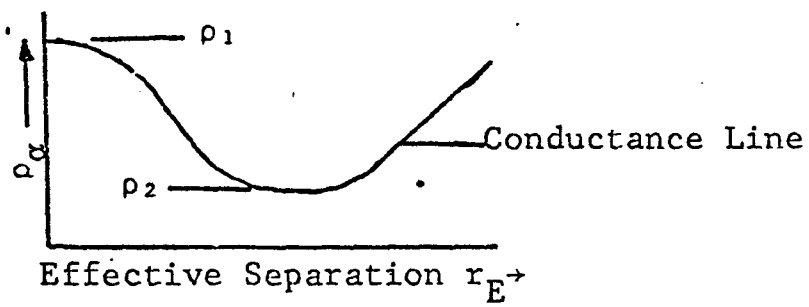

Typical Sounding Curve for All Electrical Resistivity Arrays:
Monopole,
Modified Schlumberger,
and Equitorial Arrays.

Figure 4. Typical Response Curves for a One-dimensional variation (vertical) in Electrical Resistivity

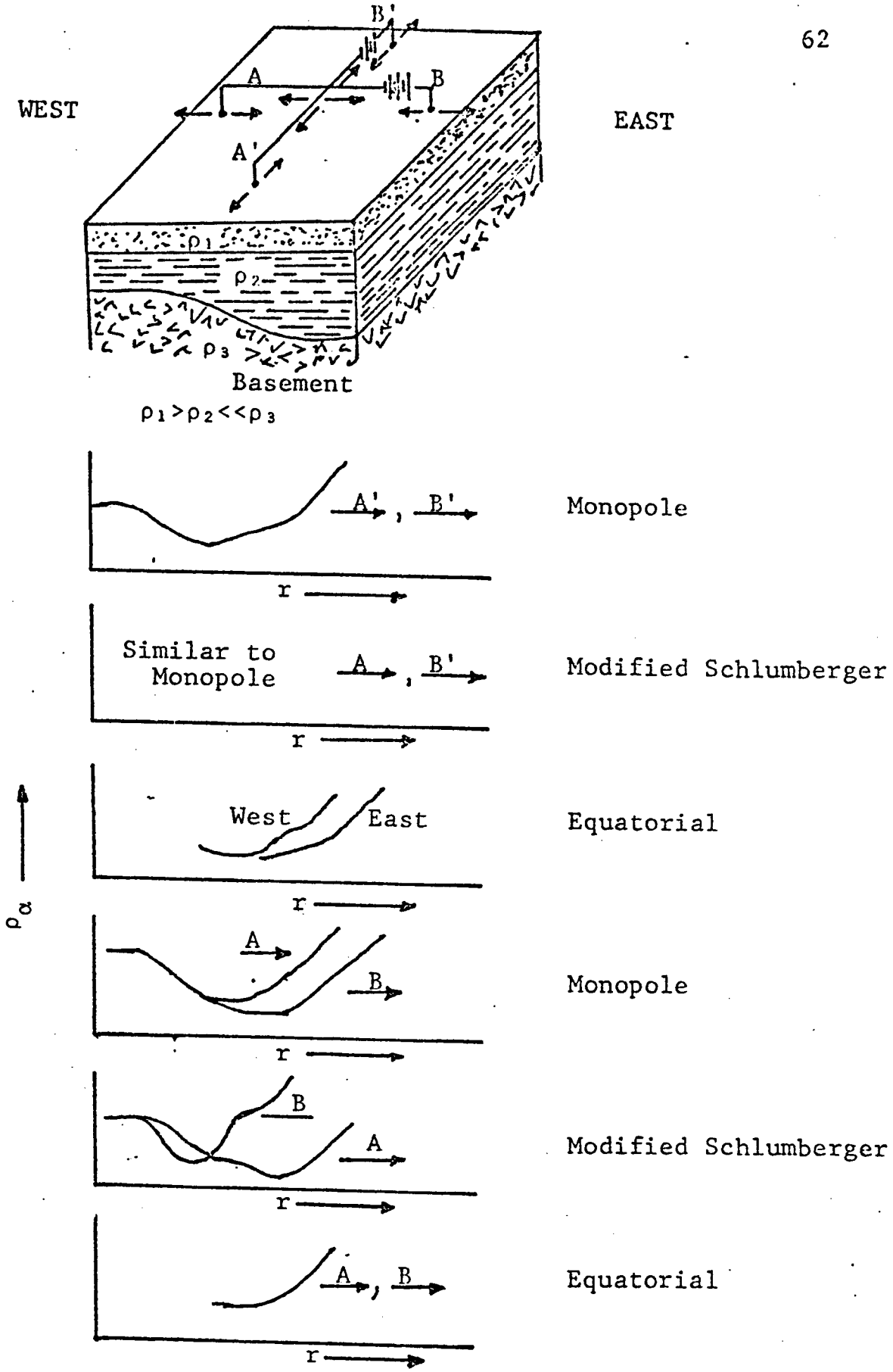

Figure 5. Typical Response Curves for a Basement Monocline

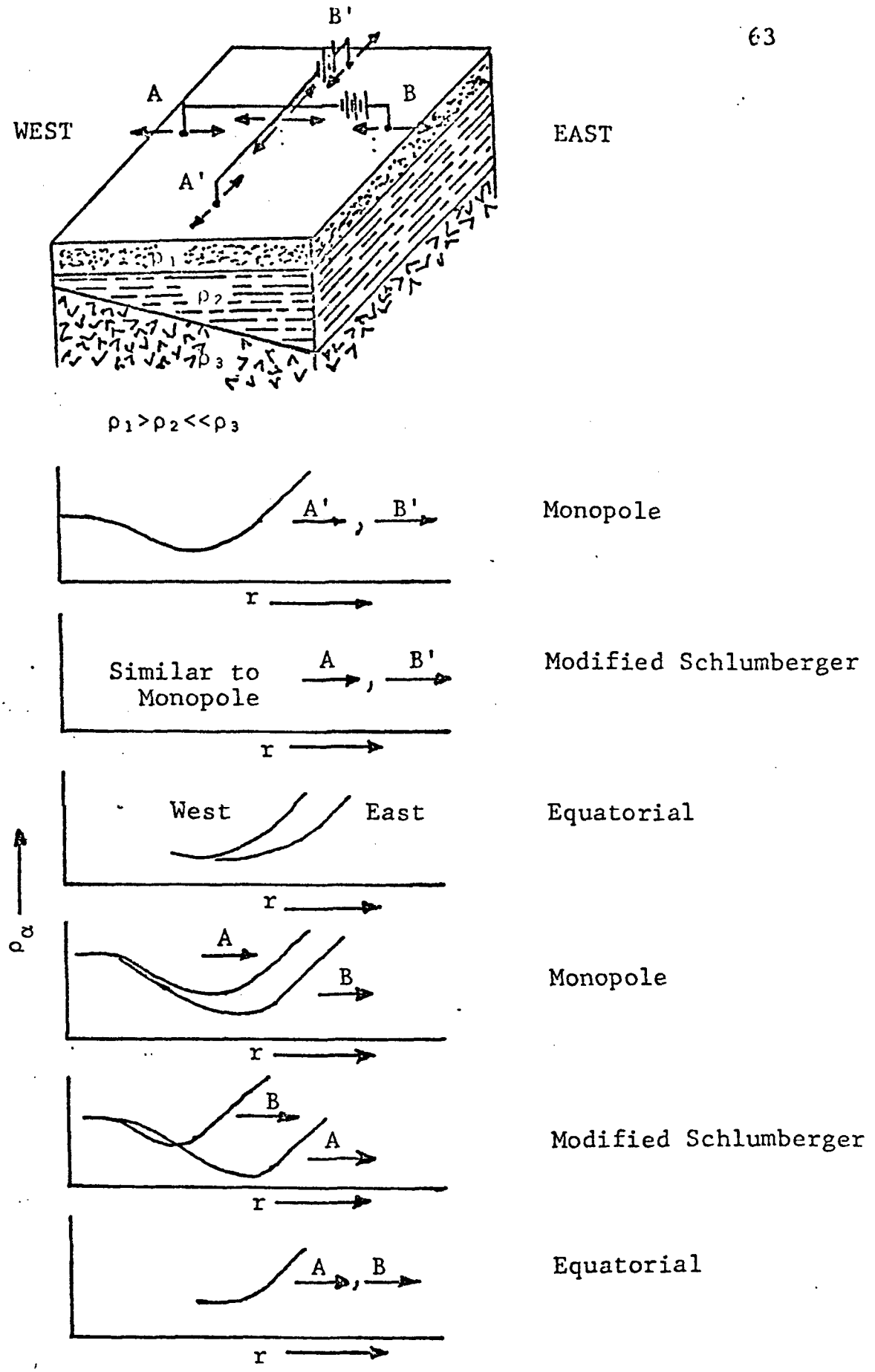

Figure 6. Typical Response Curves for a Dipping Basement Model

KEY TO SOUNDING ANNOTATION

C | R — Conductive--Resistive Contrast

ρ_i — Interpreted resistivity value for the ith layer.

h_i — Interpreted thickness value for the ith layer

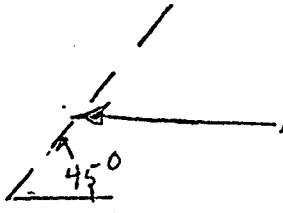

Apparent uniform conductance line

$h_i \cong$ x-depth Sounding did not penetrate into electrical basement.

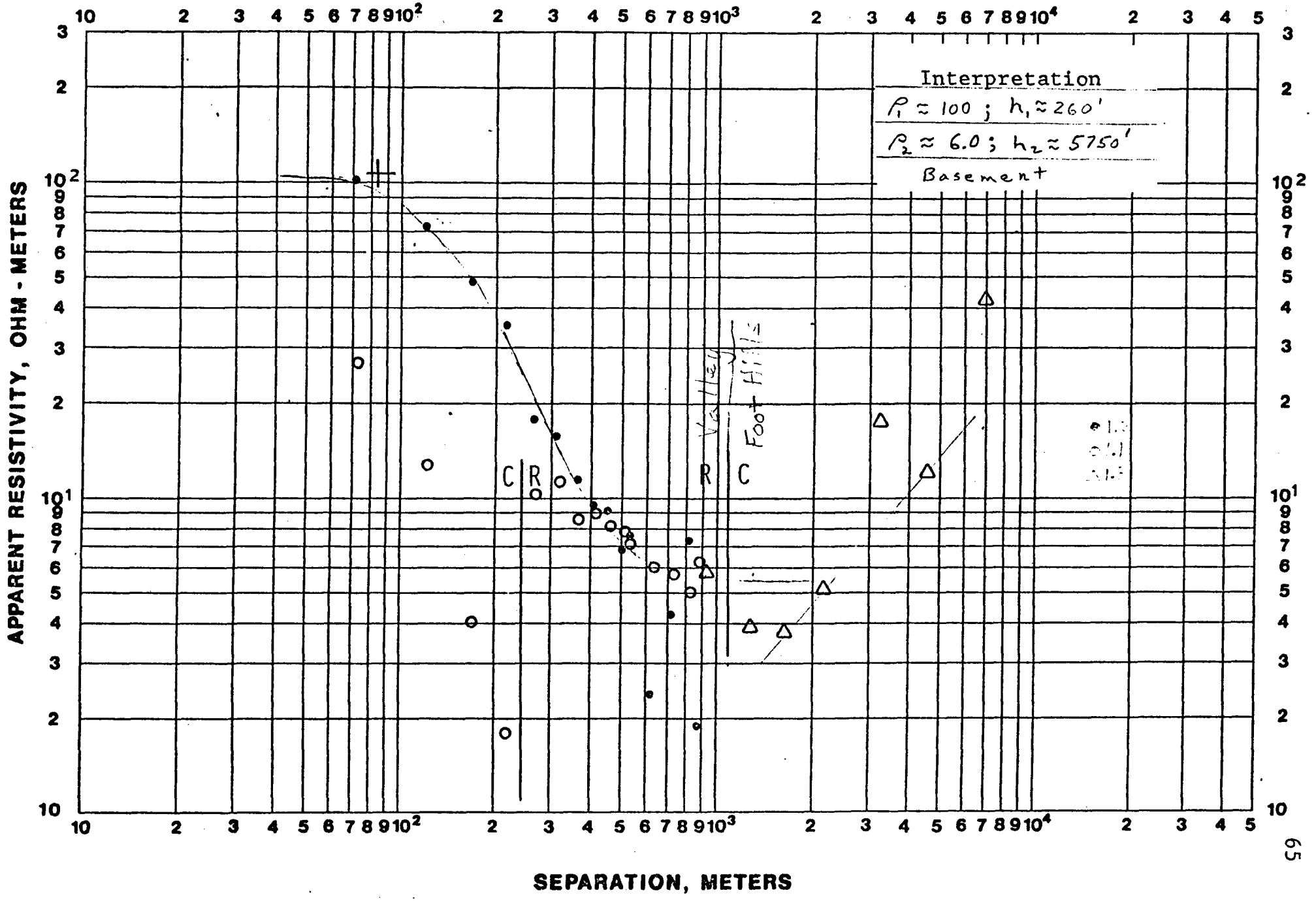

Figure V-1. Soundings 1.1, 1.2, and 1.3,
Combined Modified Schlumberger and Equatorial Soundings

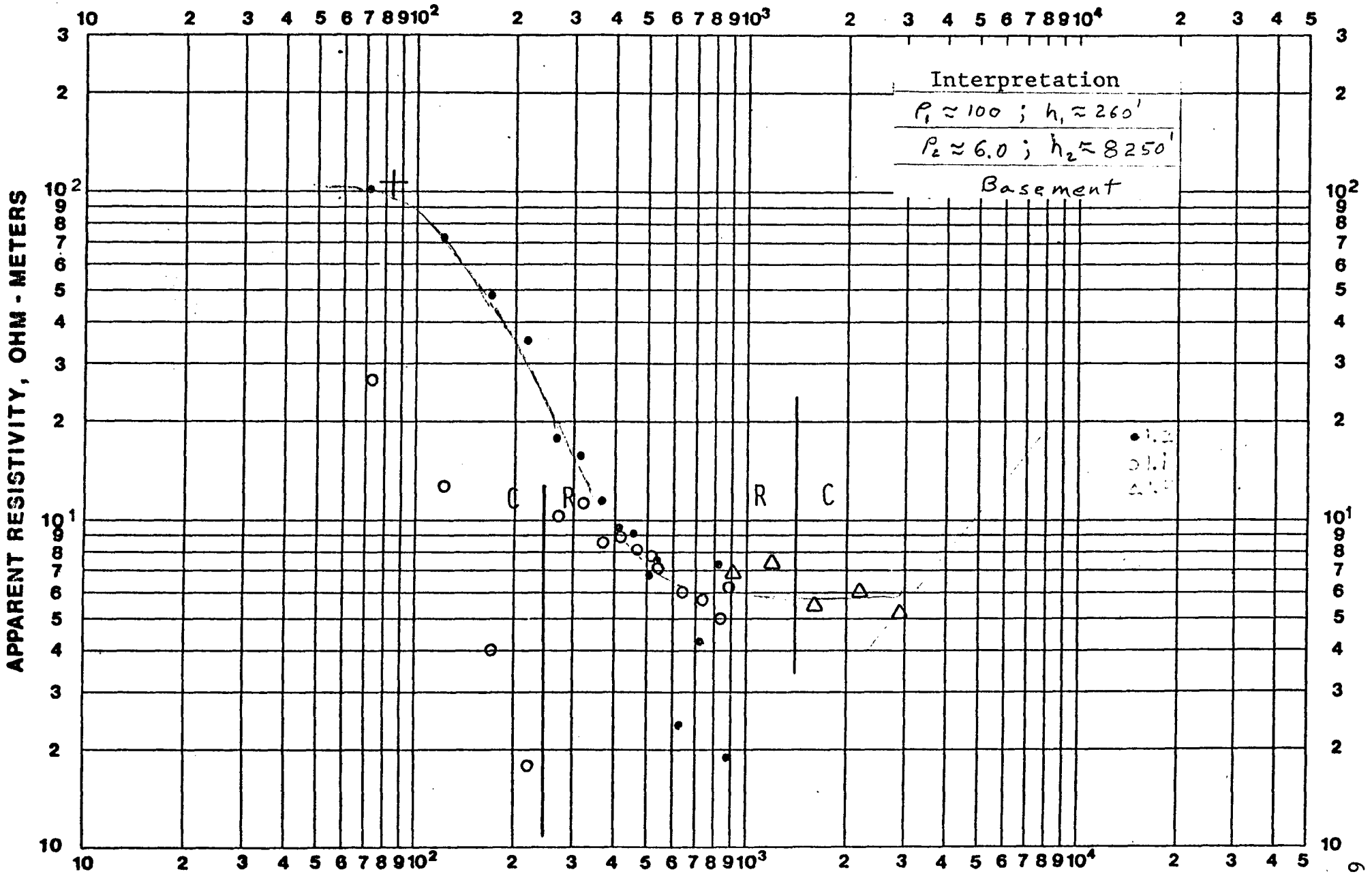

Figure V-2. Soundings 1.1, 1.2, and 1.4,
Combined Modified Schlumberger and Equatorial Soundings

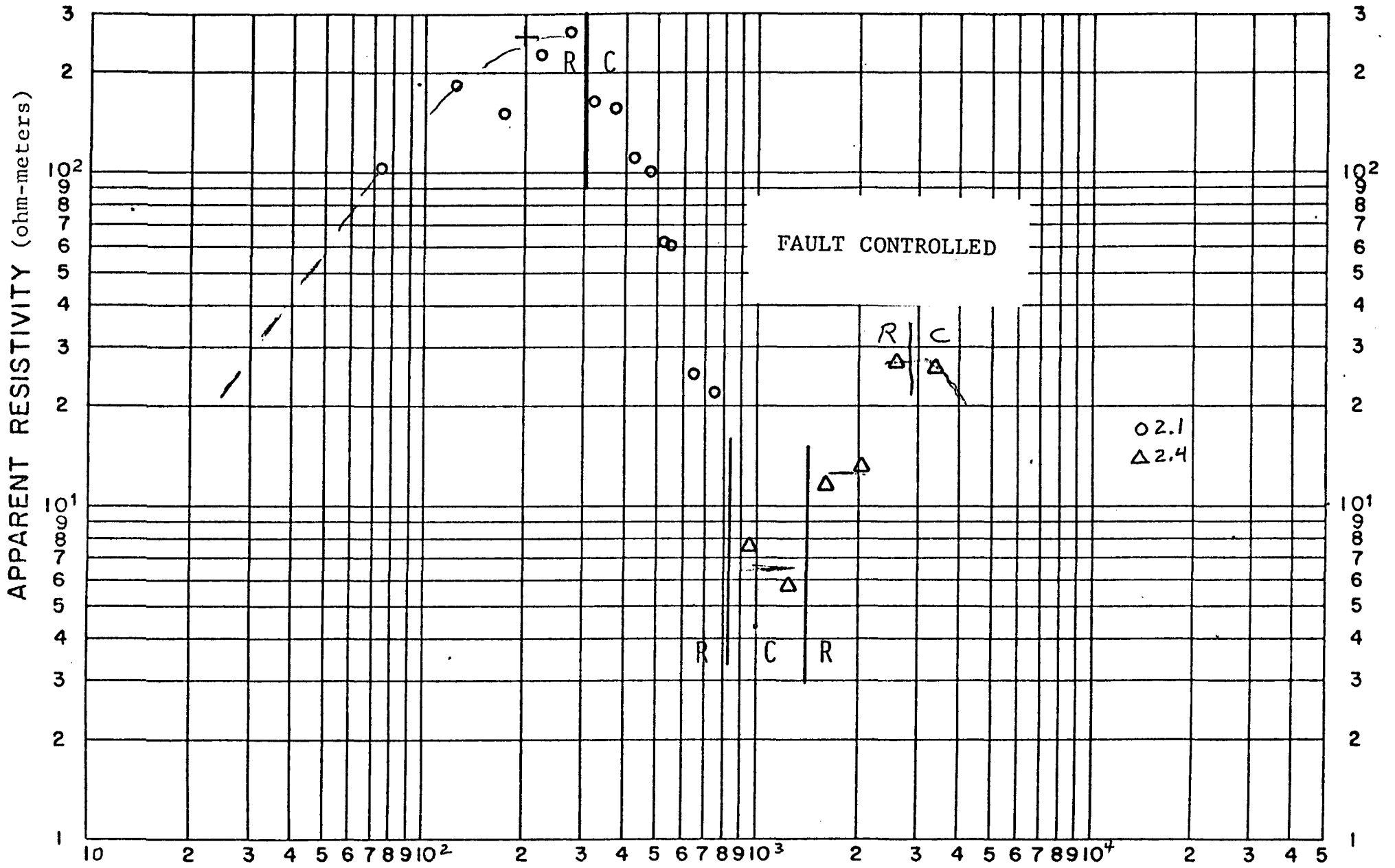

Figure V-3 . Soundings 2.1 and 2.4,
Combined Modified Schlumberger and Equatorial Soundings

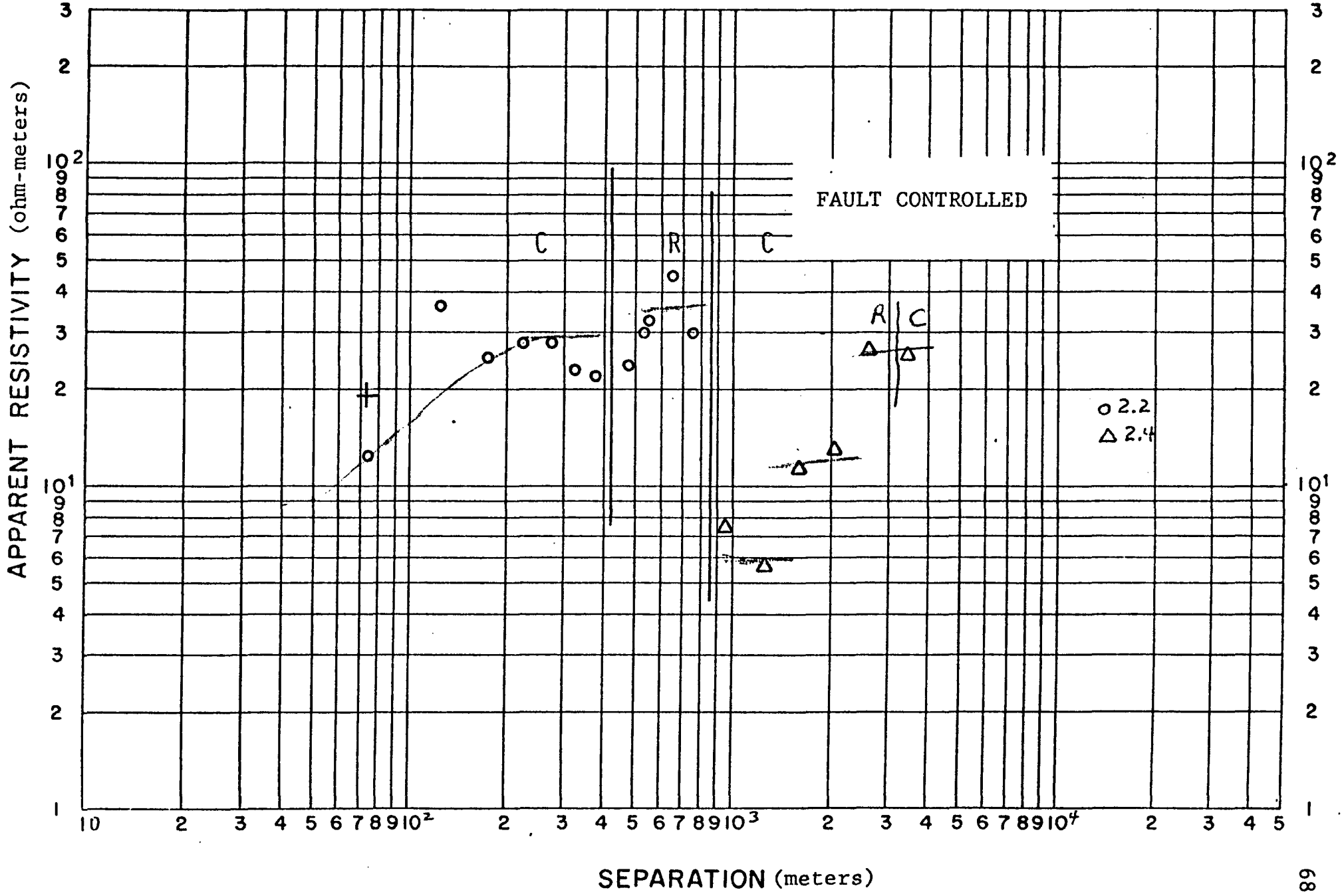

Figure V-4. Soundings 2.2 and 2.4,
Combined Modified Schlumberger and Equatorial Soundings

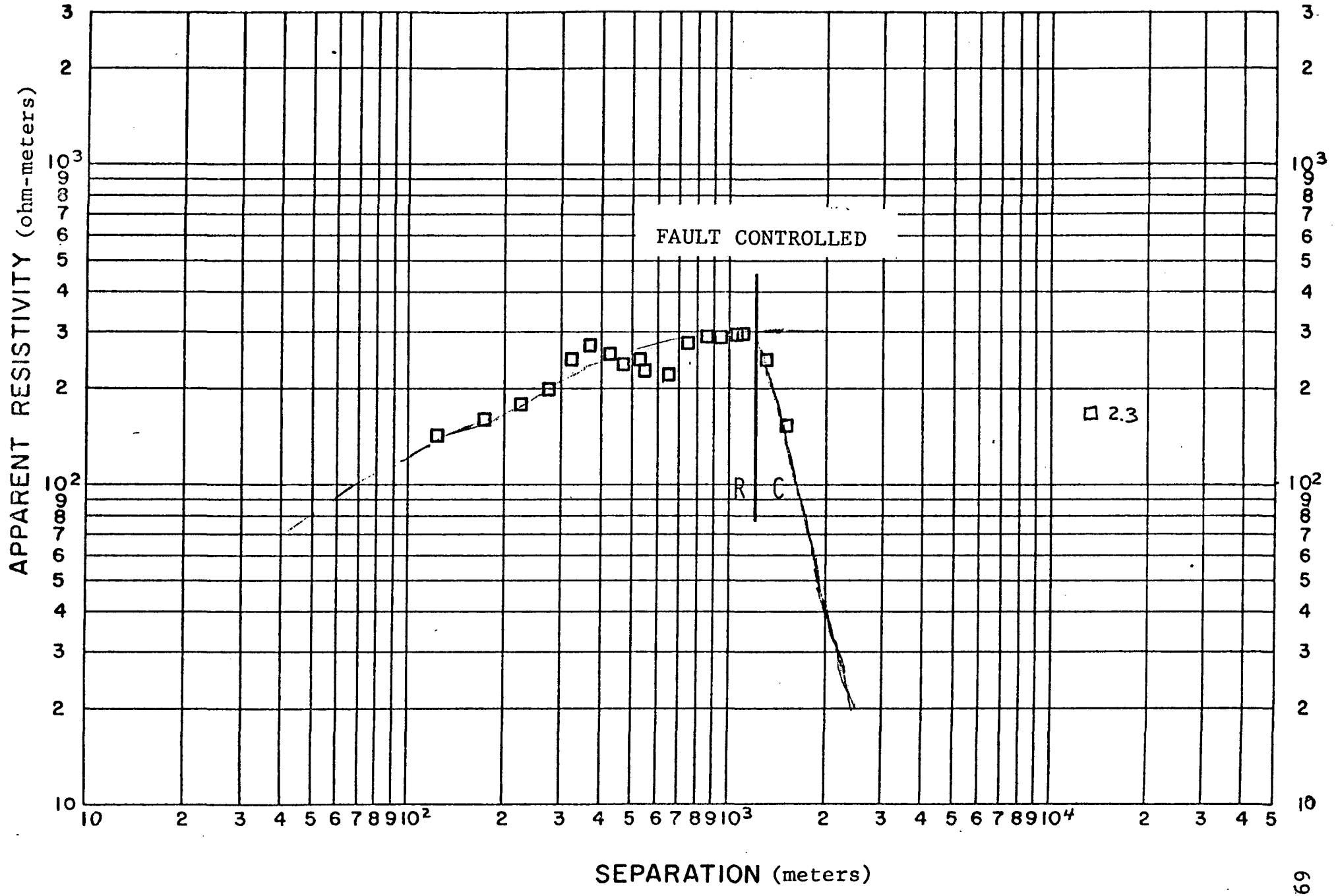

Figure V-5. Sounding 2.3
Monopole Sounding

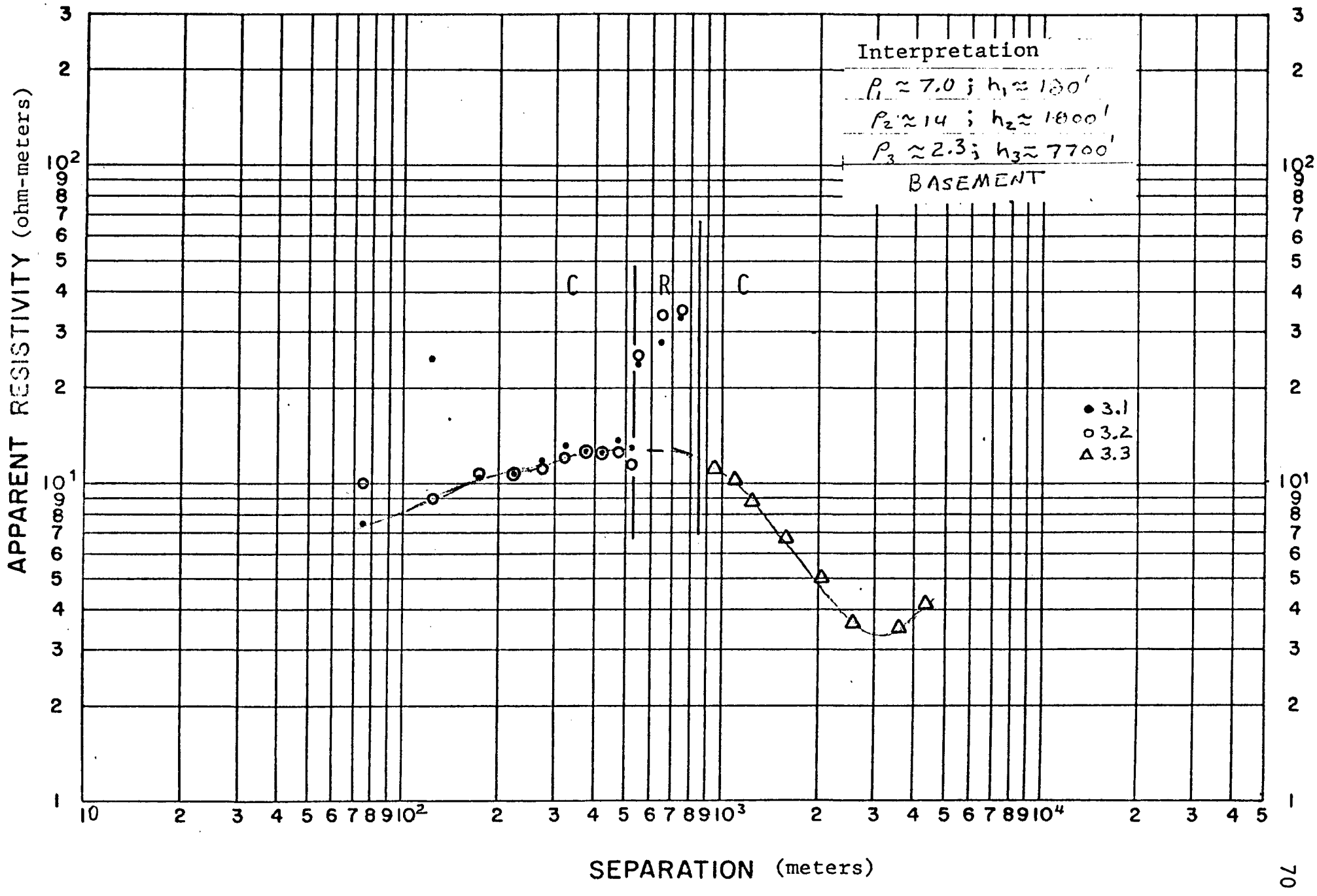

Figure V-6. Soundings 3.1, 3.2, and 3.3,
Combined Modified Schlumberger and Equatorial Soundings

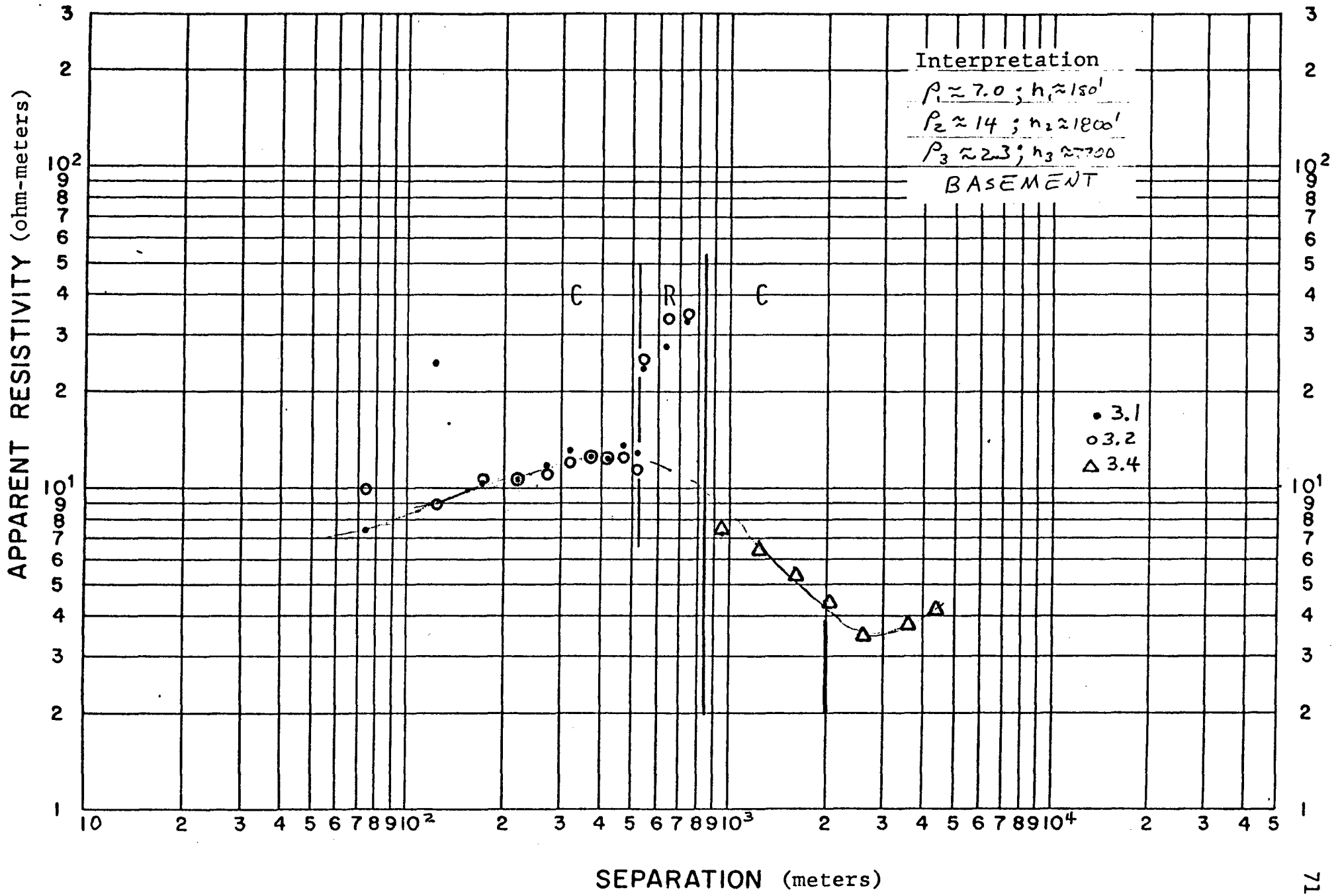

Figure V-7. Soundings 3.1, 3.2, and 3.4,
Combined Modified Schlumberger and Equatorial Soundings

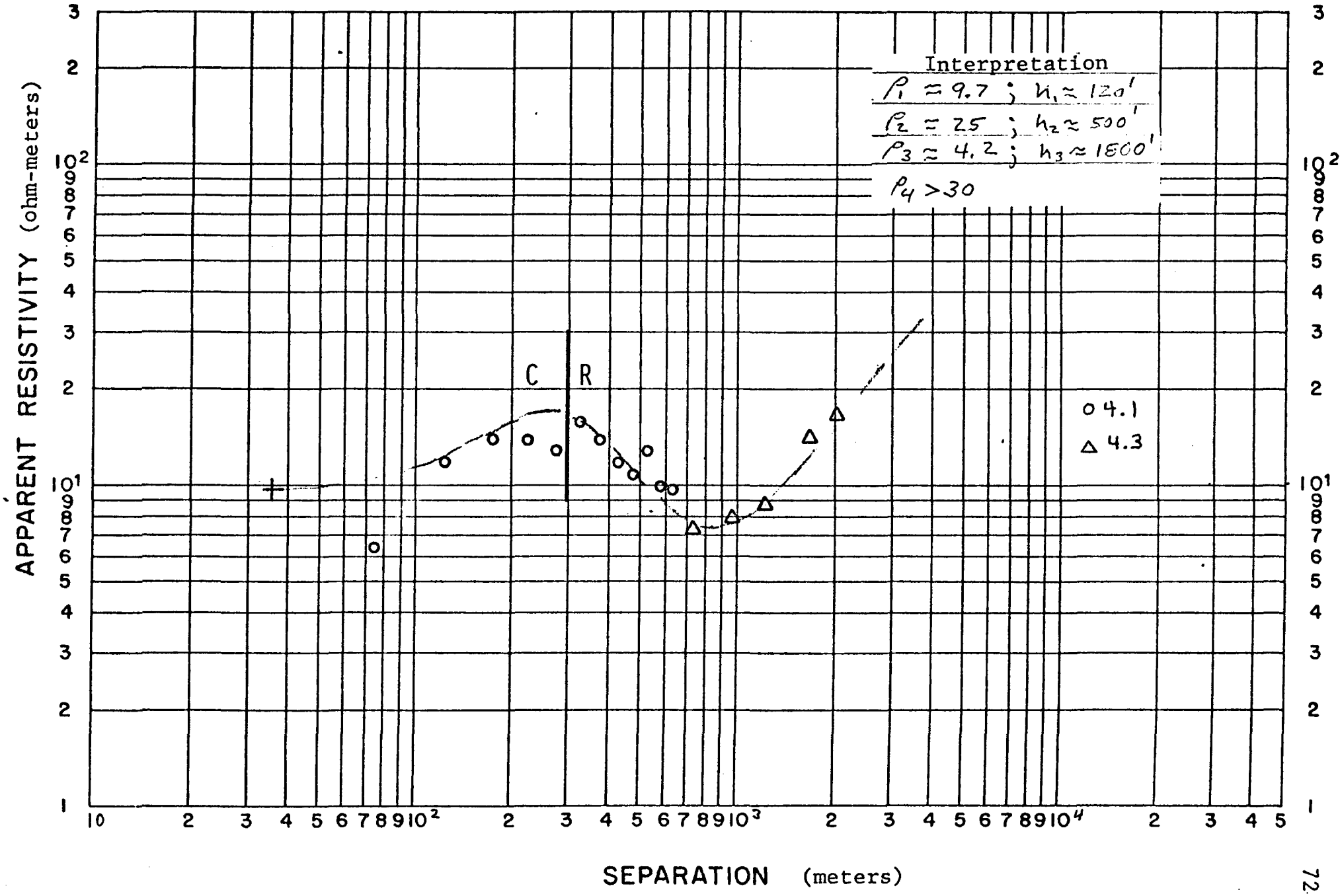

Figure V-8. Soundings 4.1 and 4.3,
Combined Modified Schlumberger and Equatorial Soundings

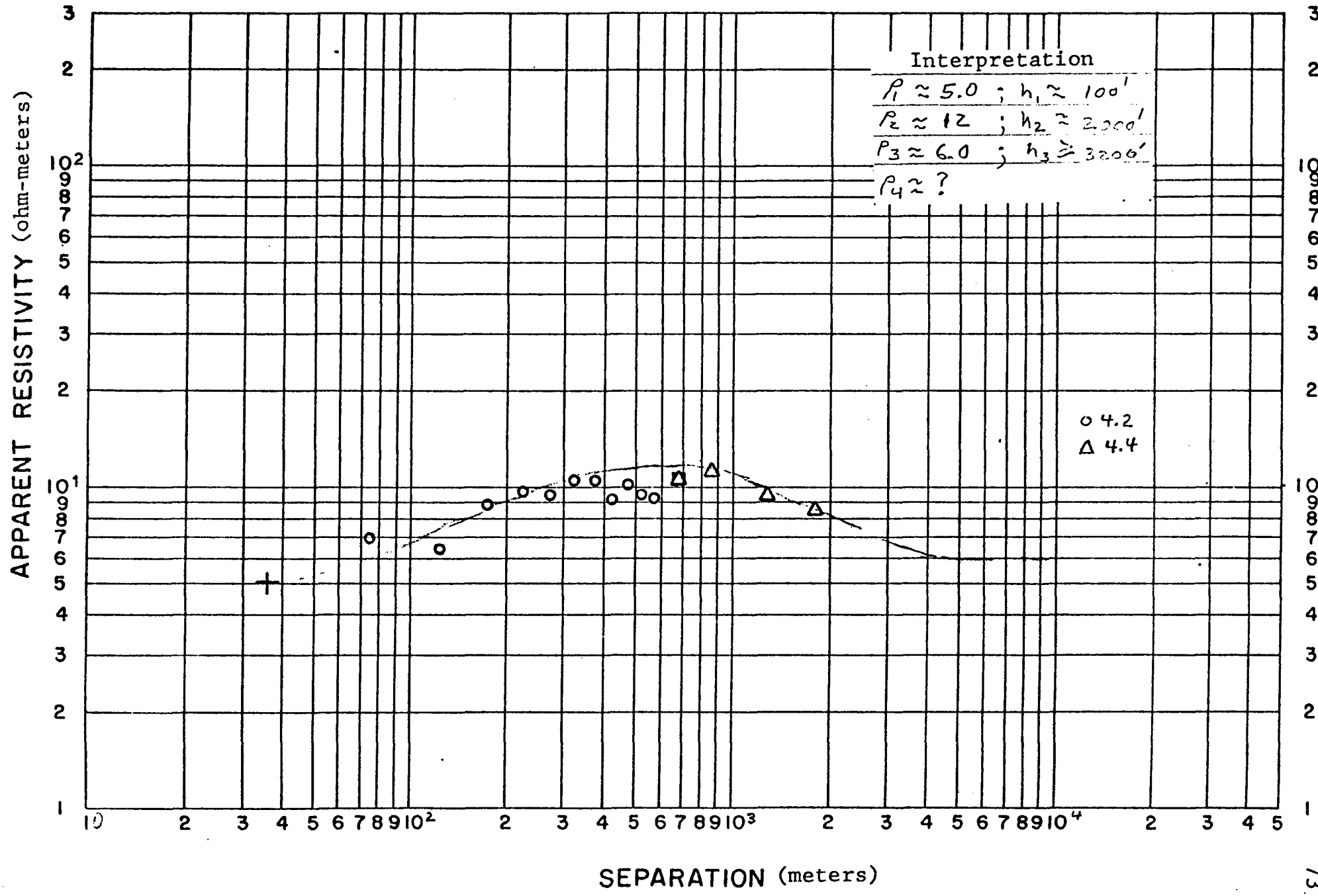

Figure V-9. Soundings 4.2 and 4.4,
Combined Modified Schlumberger and Equatorial Soundings

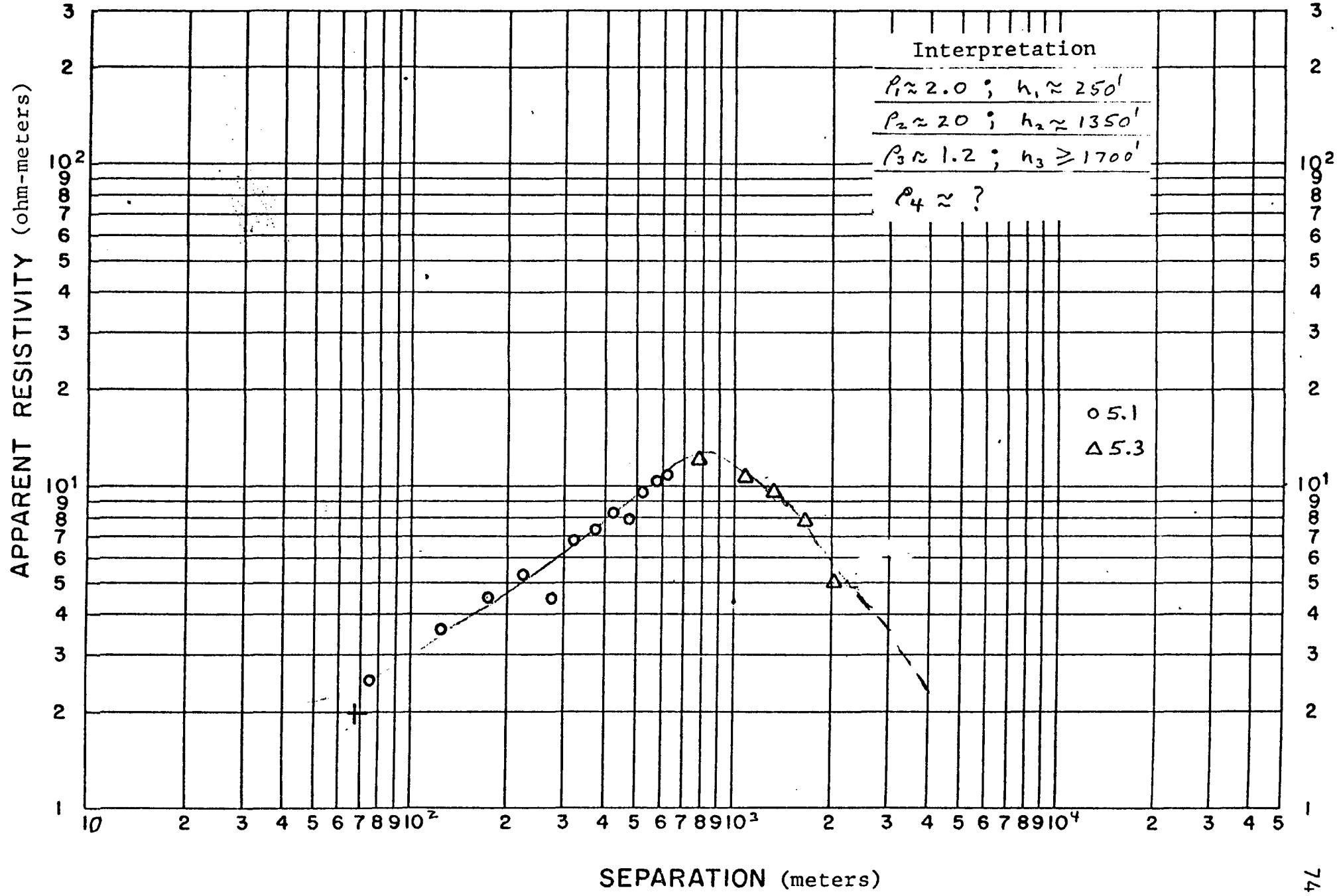

Figure V-10. Soundings 5.1 and 5.3,
Combined Modified Schlumberger and Equatorial Soundings

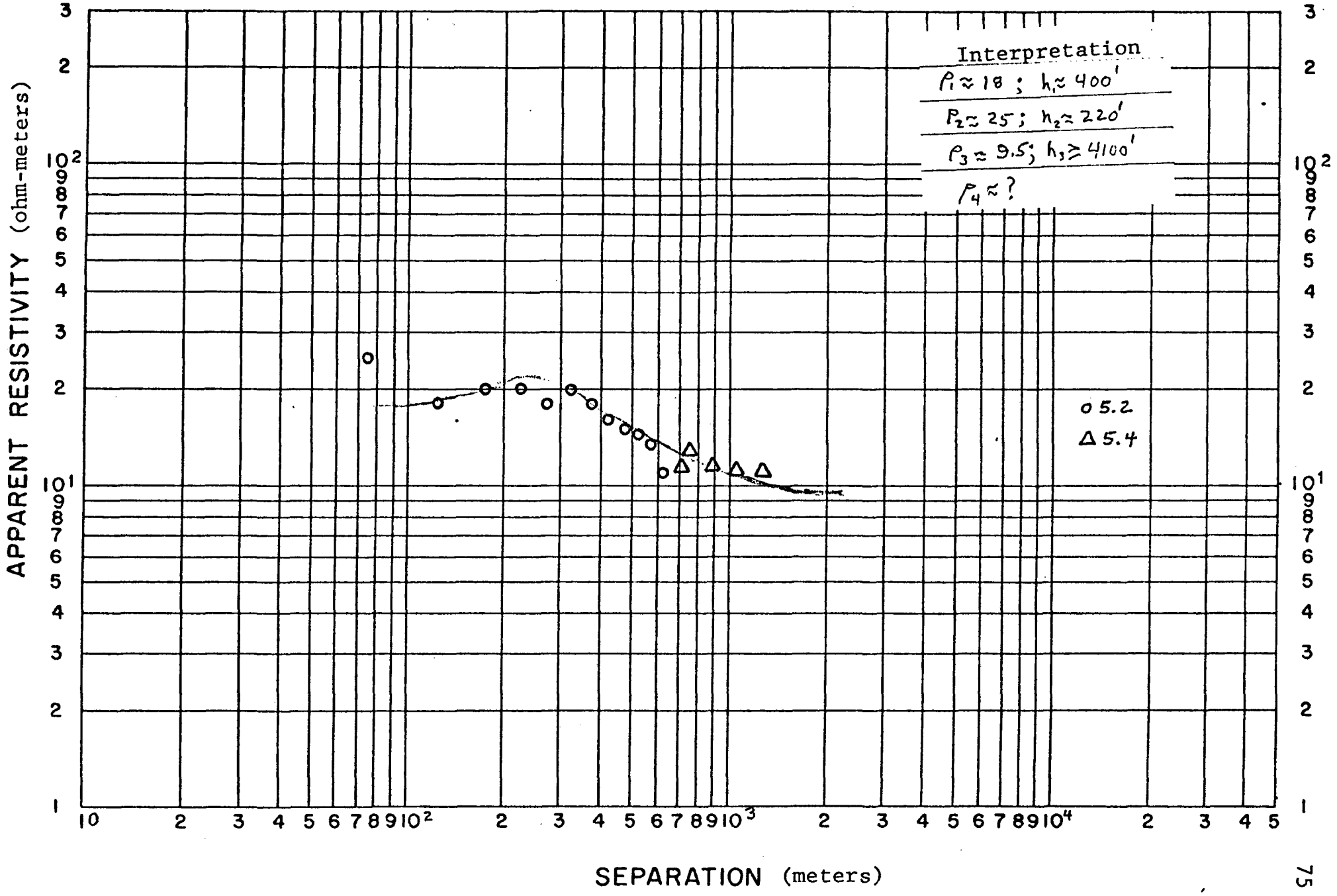

Figure V-11. Soundings 5.2 and 5.4,
Combined Modified Schlumberger and Equatorial Soundings

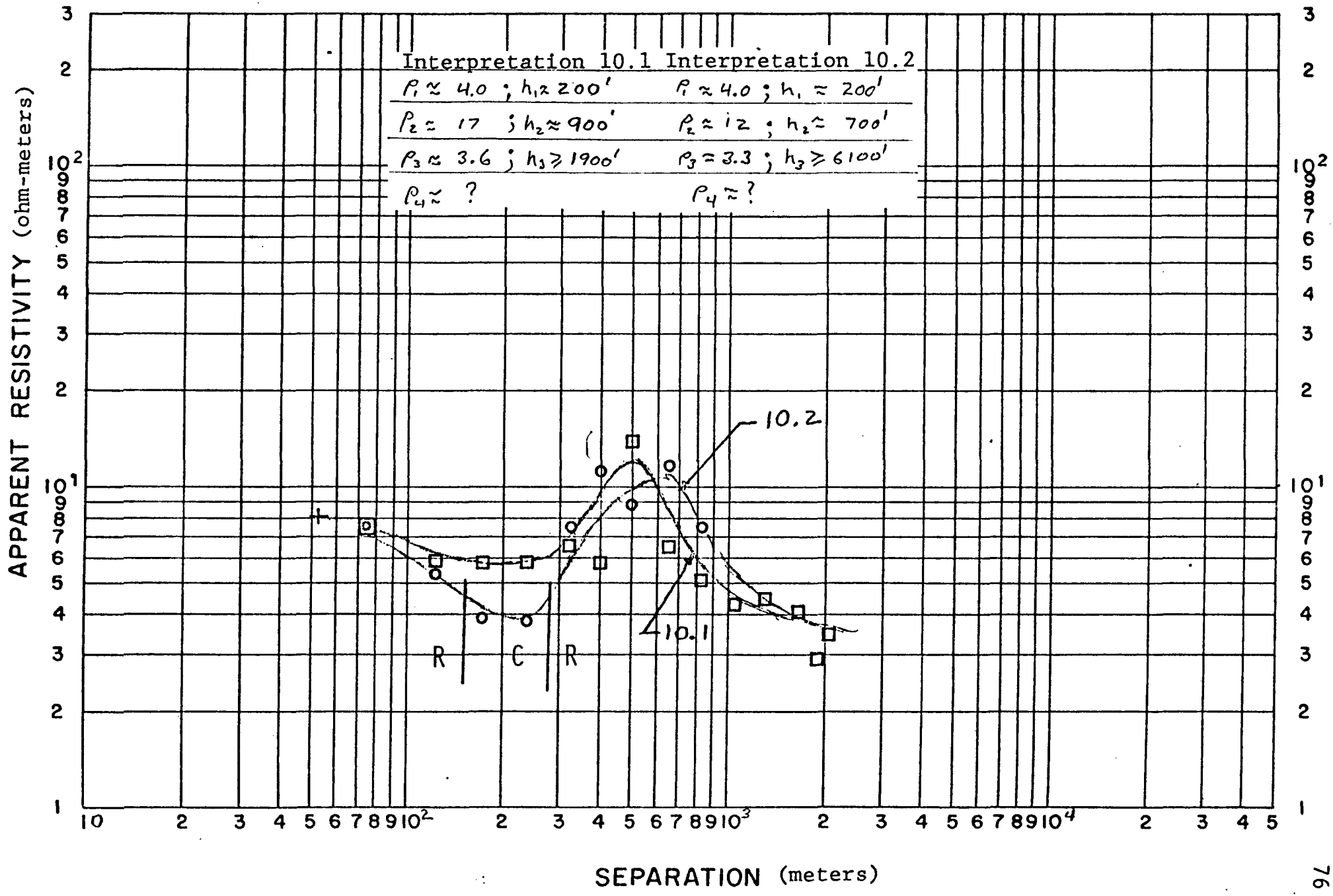

Figure V-12. Soundings 10.1 and 10.2,
Combined Modified Schlumberger and Monopole Soundings

APPENDIX VI

Parallel (dc) Electrical Resistivity Profiles

Contents:

Description of the Method

The parallel electric field dipole receiver--bipole source method is a relatively unknown galvanic resistivity technique. We do not know of it being described in the literature, either as a general survey method nor as a geothermal prospect survey method. The layout of the bipole source and the multiple receivers is shown in the figure below.

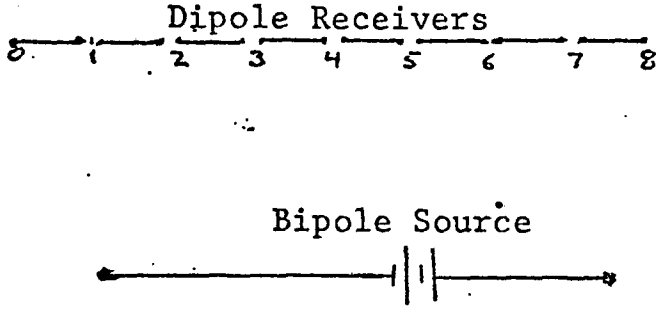

Figure 1. Layout of the parallel dipole receiver--bipole source.

The objectives of these parallel profile measurements are multi-fold. They are:

a. To discover the lateral limits of geothermal zones at depth.

b. To discover fault-like expressions which may contain geothermal fluids.

and

c. To discover anomalously conductive (low resistivity value) areas that are continous over economic geometry considerations.

To acheive the above objectives, the separation between the bipole source and the line of the dipole receivers is optimized to provide penetration depth to or into features of interest. The parallel dipole measurements approximate equatorial measurements of the equitorial dipole array. Therefore, for an H-type geoelectric section, penetration for source-receiver separations less than the depth to basement will approximate the source-

receiver separation. For source-receiver separations greater than the depth to basement, the parallel dipole method may be used to profile the variations in conductance along the profile. The interpretation of the results of the parallel electric field dipole receiver--bipole source measurements is guided by the interpretations described in Appendix V.

A consideration of the angle between a line connecting the receiver to the source and the direction of the source must be considered. The result, similar to those of a parallel dipole receiver array,will occur at an angle approximately equal to one radian. The electric field approximates zero and the geometric factor, K, approximates infinity for measurements over a uniform or one-dimensional (vertically changing) earth. For the dipole receiver-- bipole source array, such a condition will occur when the receiver orientation is perpendicular to the general current flow in the earth.

TABLE VI-1

Parrallel Electric (dc) Field
Apparent Resistivity Values

PROFILE 8.2		PROFILE 8.3	
STATION NUMBER	APPARENT RESISTIVITY (ohm-meter)	STATION NUMBER	APPARENT RESISTIVITY (ohm-meter)
1	13	1	6.4
2	12	2	6.0
3	16	3	5.8
4	15	4	6.4
5	11	5	7.9
6	16	6	9.0
7	17	7	7.9
8	17	8	8.7
		9	8.7

TABLE VI-2

Parrallel Electric (dc) Field

Apparent Resistivity Values

PROFILE 9.1		PROFILE 9.2		PROFILE 9.3	
STATION NUMBER	APPARENT RESISTIVITY (ohm-meter)	STATION NUMBER	APPARENT RESISTIVITY (ohm-meter)	STATION NUMBER	APPARENT RESISTIVITY (ohm-meter)
1	4.9	1	69	1	1.7
2	2.8	3	44	2	2.0
3	3.9	4	24	3	4.1
4	3.2	5	14	4	13
5	3.2	6	15	5	7.3
6	3.4	7	6.7	6	7.9
7	4.0	8	6.6	7	7.7
8	3.7	9	5.2	8	7.2
9	3.7	10	7.6	9	7.0
10	3.9	11	3.8	10	8.6
11	4.0	12	5.6	11	8.5
12	8.9	13	4.8	12	9.4
13	21	14	6.8	13	11
14	34	15	6.6	14	9.6
15	20	16	7.3	15	10
16	6.6	17	7.8	16	11
		18	5.9		
		19	4.6		
		NO VALUE STATION 2			

TABLE VI-3
Parrellel Electric (dc) Field
Apparent Resistivity Values

PROFILE 9.4			PROFILE 9.5	
STATION NUMBER	APPARENT RESISTIVITY (ohm-meter)		STATION NUMBER	APPARENT RESISTIVITY (ohm-meter)
1	10		1	7.1
2	8.2		2	5.8
3	6.2		3	8.1
4	7.1		4	11
5	8.0		5	N.V.
6	11		6	N.V.
			7	21
			8	20
			9	9.5
			10	N.V.
			11	6.1
			12	4.1
			13	4.1
			14	4.0
			15	3.8
			16	3.6
			17	3.4
			18	3.6

N.V. – NO VALUE

APPENDIX VII

Time-Domain Electromagnetic Soundings

E_p (parallel) & H_z (vertical) Components

Contents:

TABLE VI-4

Parallel Electric (dc) Field
Apparent Resistivity Values

PROFILE 10.1		PROFILE 10.2		PROFILE 10.3	
STATION NUMBER	APPARENT RESISTIVITY (ohm-meter)	STATION NUMBER	APPARENT RESISTIVITY (ohm-meter)	STATION NUMBER	APPARENT RESISTIVITY (ohm-meter)
1	3.7	1	0.6	1	11
2	6.0	2	2.1	2	15
3	13	3	1.1	3	27
4	22	4	7.0	4	7.1
5	29	5	3.8	5	5.5
6	1.0	6	3.9	6	6.1
7	2.4	7	3.5	7	14
8	4.8	8	2.1	8	3.4
9	5.3	9	2.7	9	3.9
10	4.4	10	5.7	10	4.9
11	0.8	11	3.4	11	4.1
12	4.3	12	3.1	12	4.3
13	3.8	13	3.1	13	4.7
14	3.0	14	3.8	14	4.7
15	3.7	15	7.1	15	4.1
16	3.8	16	HIGHLY SKEWED	16	4.1
17	2.7	17	" "		
18	0.6	18	16		

TABLE VI-5

Parrallel Electric (dc) Field

Apparent Resistivity Values

PROFILE 11.1		PROFILE 11.2		PROFILE 11.3	
STATION NUMBER	APPARENT RESISTIVITY (ohm-meter)	STATION NUMBER	APPARENT RESISTIVITY (ohm-meter)	STATION NUMBER	APPARENT RESISTIVITY (ohm-meter)
1	9.5	1	5.2	1	1.7
2	1.6	2	2.6	2	1.9
3	0.7	3	1.2	3	1.3
4	1.0	4	3.0	4	3.2
5	1.3	5	4.2	5	3.6
6	1.1	6	7.5	6	4.4
7	1.0			7	4.7
8	1.6			8	3.8
9	1.5			9	3.5
10	2.4			10	9.6
11	2.6				
12	2.0				

Discussion and Description

Controlled Source EM Methods

For some years, electromagnetic controlled source, vertical magnetic field receiver soundings have been used in geothermal exploration in the United States and other parts of the world. The U.S.S.R. and Eastern Block Countries' literature describes their use in various geophysical surveys, particullarly for surveying geologic sections having thick resistive sections in them.

Much less widely known and discussed in the free-world are the horizontal electric field EM soundings from grounded dipole or grounded bipole sources. There are numerous articles written in the Soviet and Eastern Block Countries" literature, but, the only interest to date in the United States seems to come out of studies at the Colorado School of Mines (CSM) and the USGS. There has been reported success in the use of the "Electroflex Technique" (a rather primative approach to EM soundings) in surveying carbonate sections (reef problems, etc.) where the parameter of control is resistivity.

Published works by G. V. Keller (Chairman of the Geophysics Department), Pritchard and other graduate students at CSM show that the grounded source--electric field receiver soundings will provide interpretative data for resolution of:

1. Vertical anisotropy of layers within the geologic section, and
2. The thickness and resistivity of resistive screening layers

(screen dc electrical resistivity soundings from penetrating to depth and are virtually undetectable by mangnetic receiver soundings, MT soundings, and all magnetic source soundings).

Knowledge of screening layers and vertical anisotropy are very important in making correct depth interpretation in survey investigations of geothermal areas. Further, we believe that resolution of vertical anisotropy will become an important parameter in geothermal investigations as drilling tests qualify the results in areas of large anisotropy versus no anisotropy.

Electrodyne Data Acquisition

The source-receiver layout is shown in the figure below. Electrodyne's receiver system is comprised of a parallel electric field dipole and a multiturn vertical d /dt receiver. The signal is preconditioned by a filter-amplifier system and recorded on analogue tape. The tape recorder used a four channel Hp recorder.

The total transient response and an "early time" amplitude clipped response is recorded for each component. The source signal input into theground is square-waves of 12.8 seconds period and 2.0 seconds period to give an equivalent frequency domain band of 0.08 Hz to 32.0 Hz.

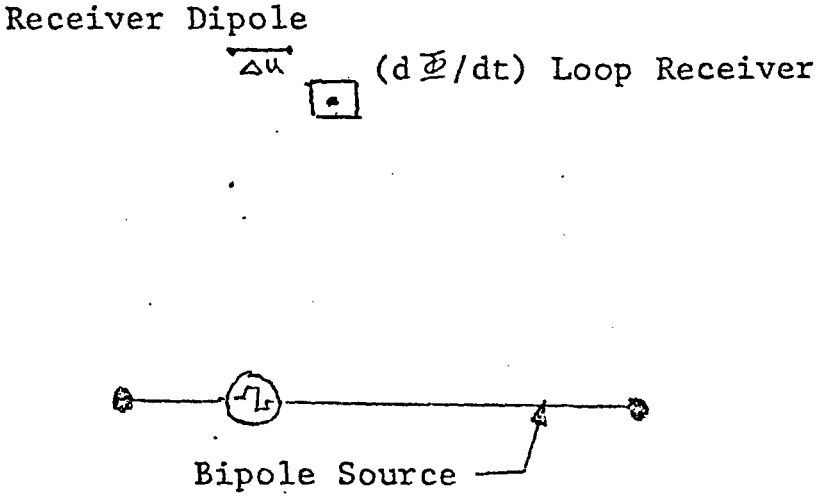

Typical Electrodyne EM Sounding Layout

Electrodyne Data Interpretation

Electrodyne performs a preliminary partial curve matching interpretation of the sounding curves. The assumption made is that all data corresponds to two frequency domain responses, plane-wave and static field responses. The incorporation of the quasistatic respnse is incorporated when the inversion modeling is performed in the computer inversion interpretation process. The inversion interpretation is not performed if the preliminary partial curve matching indicates that the sounding is two or three dimensionally cotrolled.

Interpretation Considerations

Electrodyne is in the preliminary stages of developing the full interpretation capability of the combined E_p and H_z EM soundings. At this time, a pseudo-anisotropy is determined by by taking the ratio of the E_p resistivity value of a layer to the H_z resistivity of a layer. The E_p soundings are used to interpret the layer thickness. The H_z soundings are used to interpret the true resistivity of the conductive layers of interest.

Electrodyne Data Reduction

Electrodyne uses a wave analyser to transform the total transient response signal from a square-wave input to the frequency domain. This done in a manner similar to the AMT-MT data reduction, i. e., a number of visulally inspected time windows are transformed and these are stacked to give the best average amplitude spectra. The system response is removed and the data are ready for frequency domain interpretation. Electrodyne does not transform back to the time domain for interpretation.

To date signal to noise relationships have been high enough that we have not had to bring up additional resolution from the stacking of the clipped amplitude transient recording.

KEY TO SOUNDING ANNOTATION

The apparent resistivity on the sounding curves is derived by the plane-wave formula

FAULT CONTROLLED --Two or three dimensional control on the sounding

E_p Soundings

ρ_i---ith layer resistivity value
h_i---ith layer thickness

S_R--- Residual conductance --- determined by taking the difference between the (dc) total conductance and the E_p total conductance

H_zSoundings

ρ_i---ith layer resistivity value
h_i---ith layer thickness

λ_i--- $\rho_{i_{E_p}} / \rho_{i_{H_z}}$

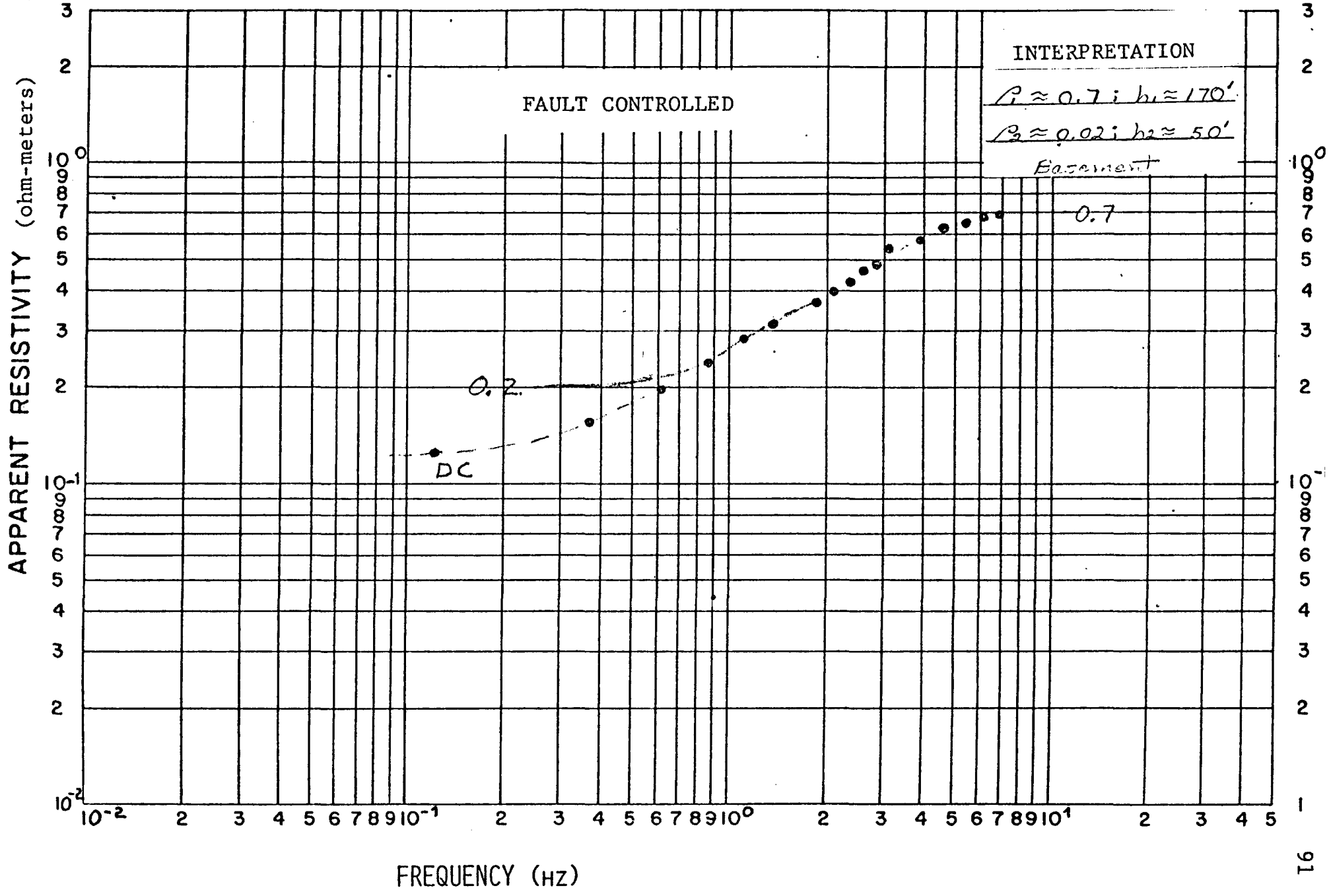

Figure VII-1. TDEM Ep Sounding 3.02.

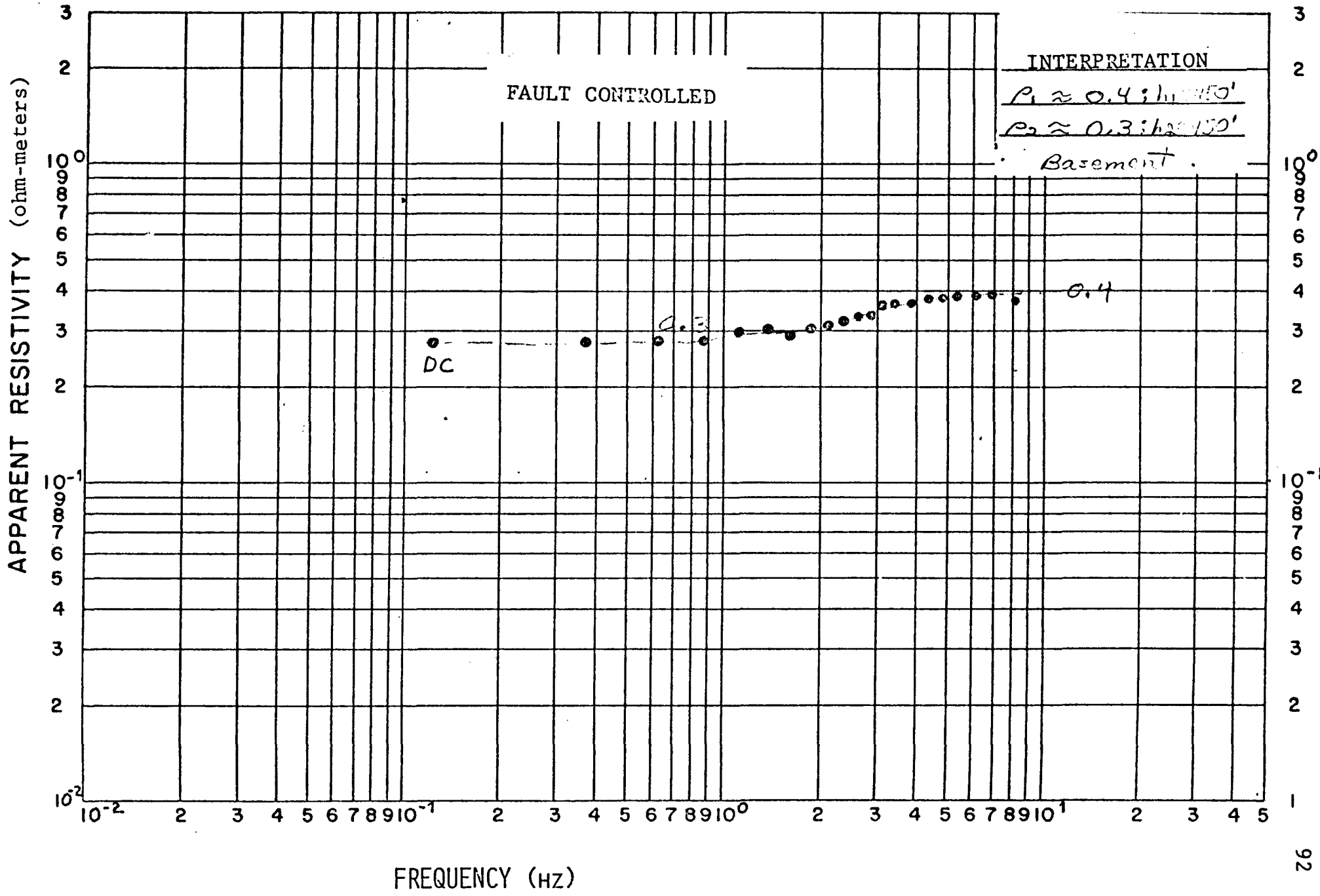

Figure VII-2. TDEM Ep Sounding 6.01.

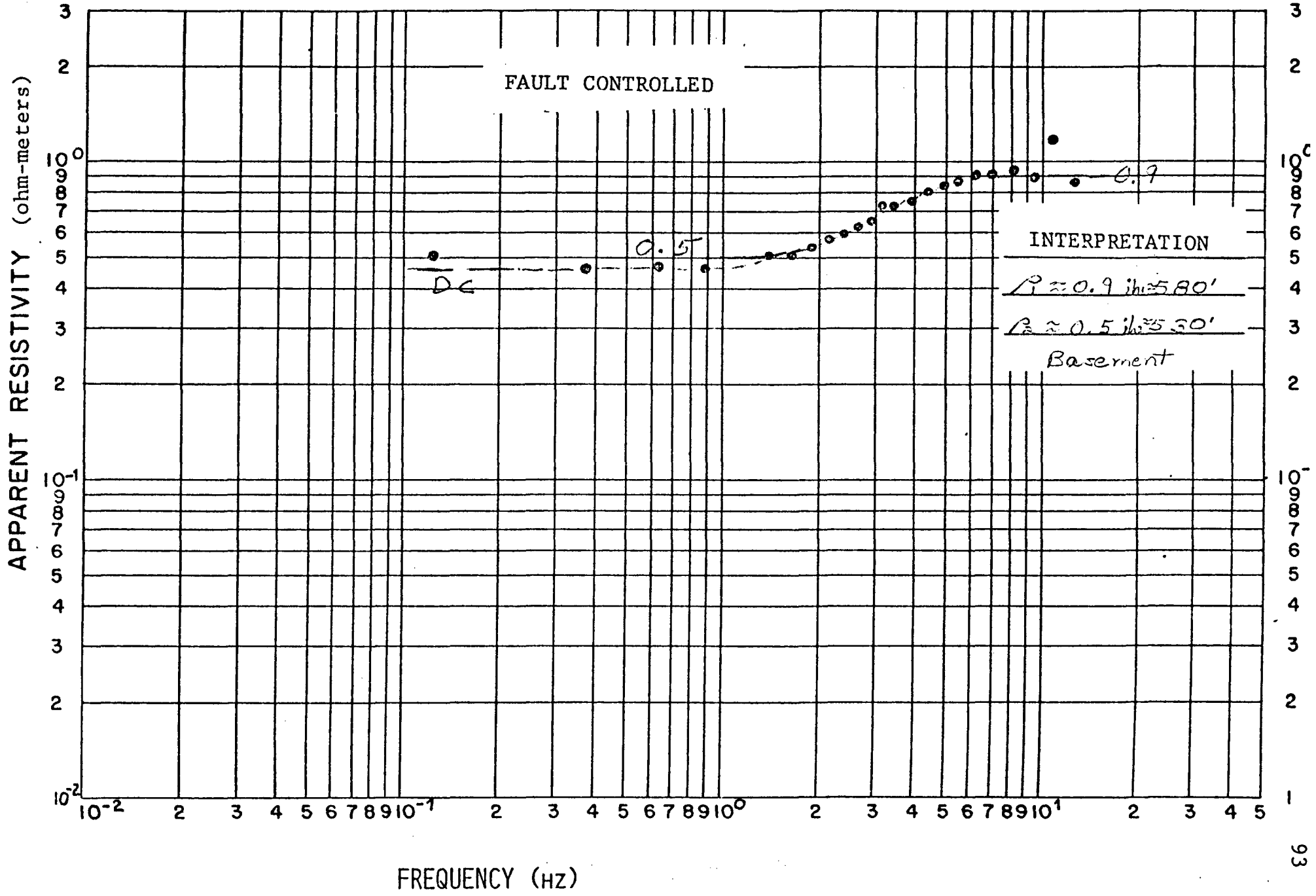

Figure VII-3. TDEM Ep Sounding 6.02.

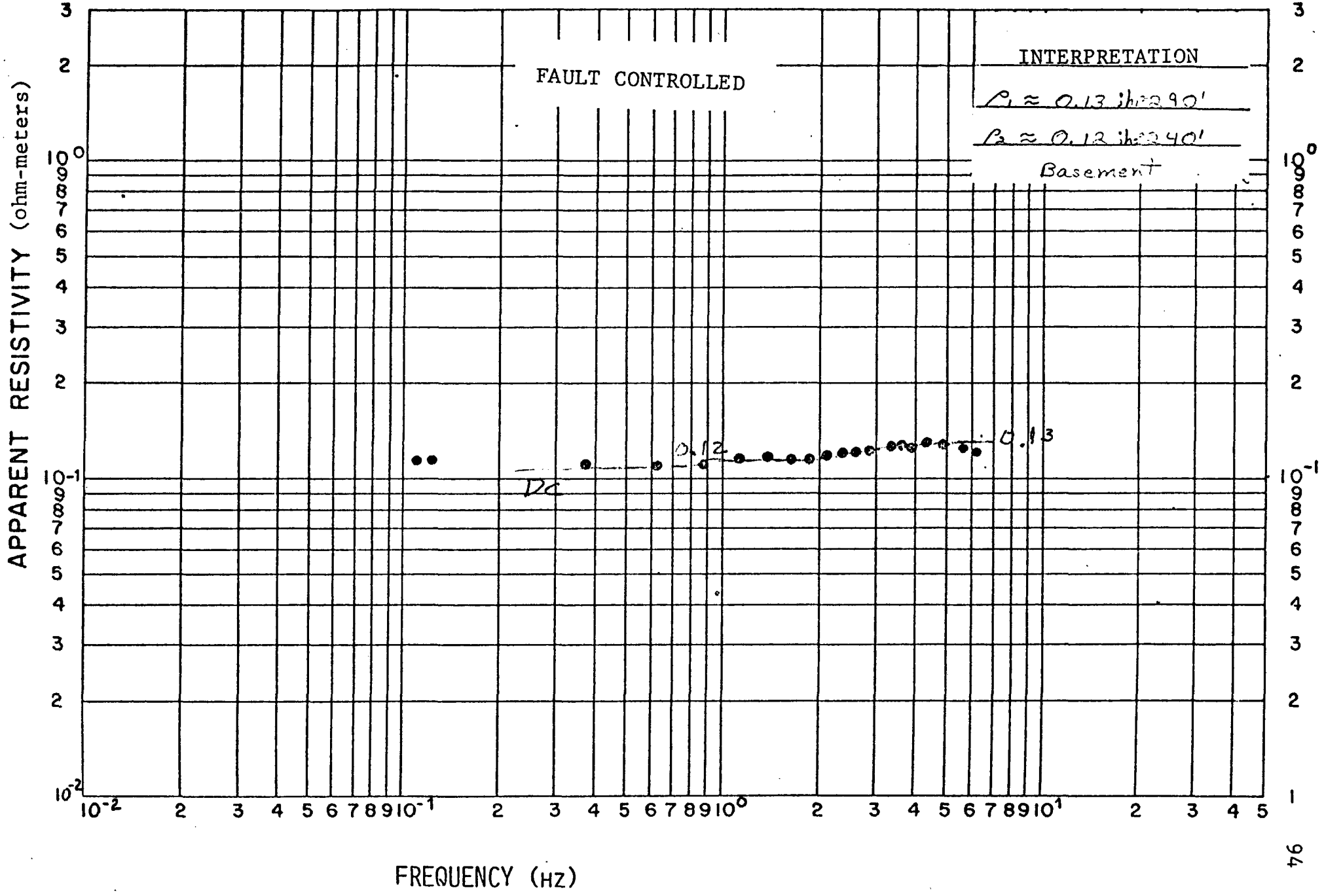

Figure VII-4. TDEM Ep Sounding 6.03.

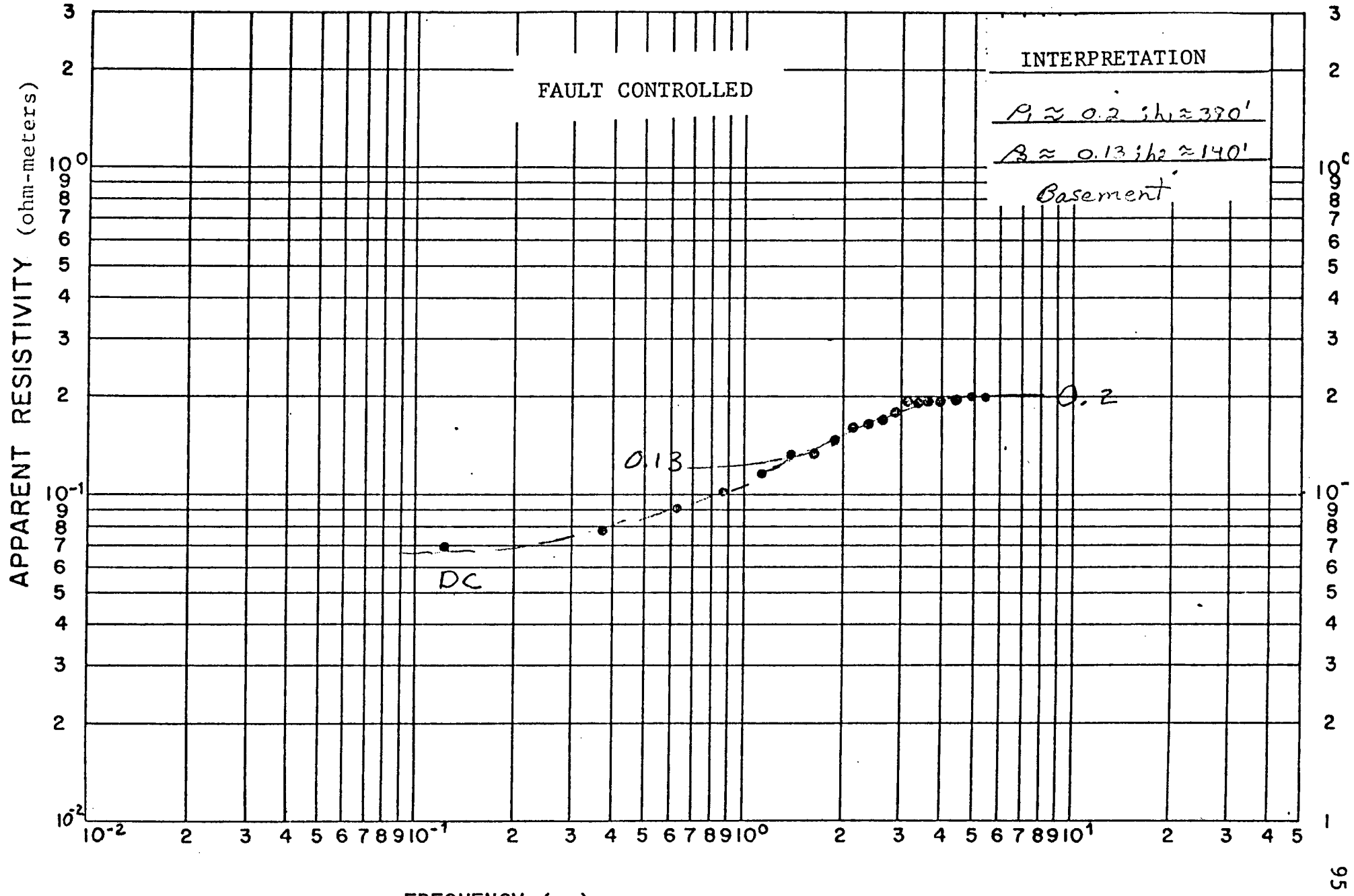

Figure VII-5. TDEM Ep Sounding 6.04.

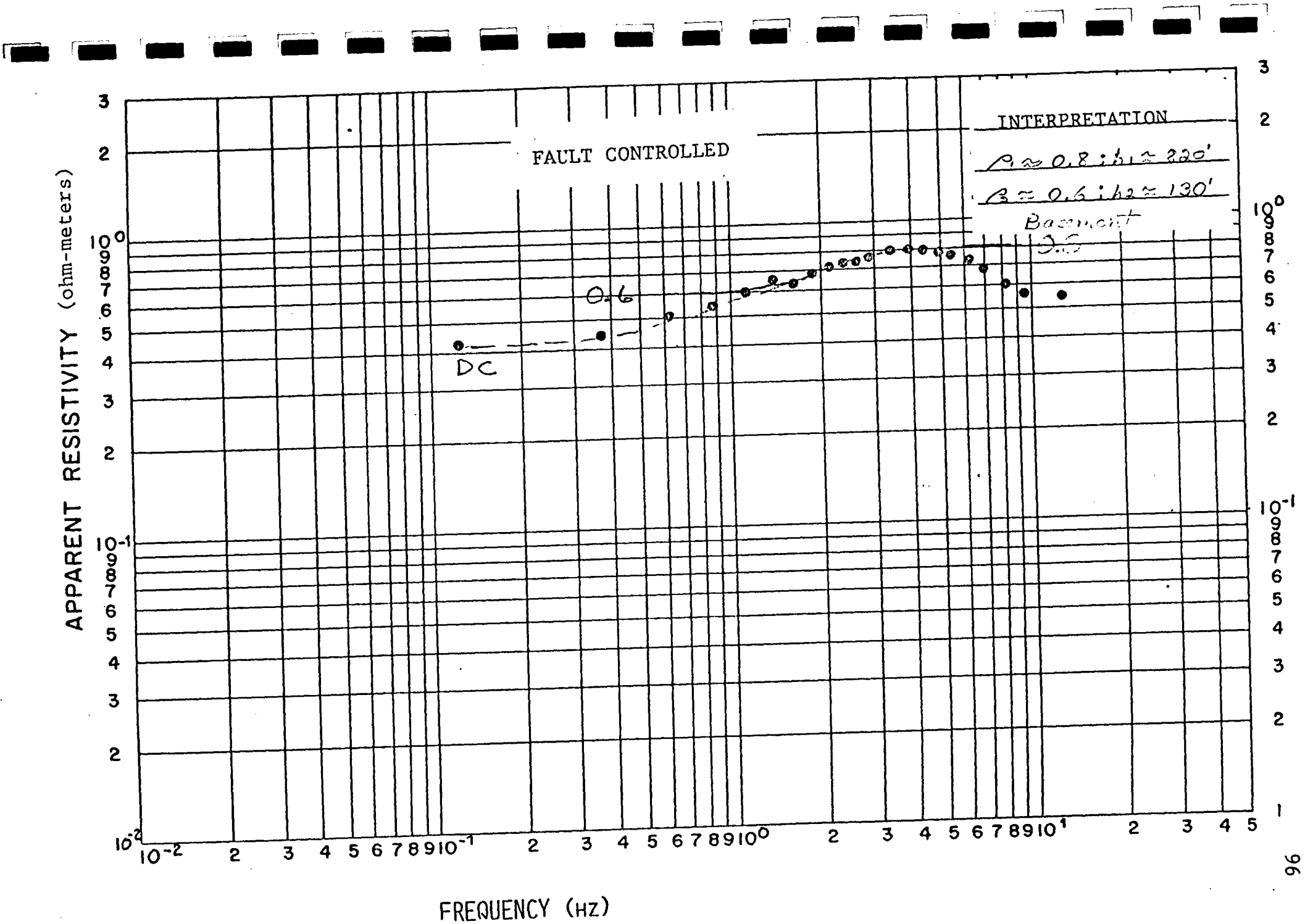

Figure VII-6. TDEM Ep Sounding 6.05.

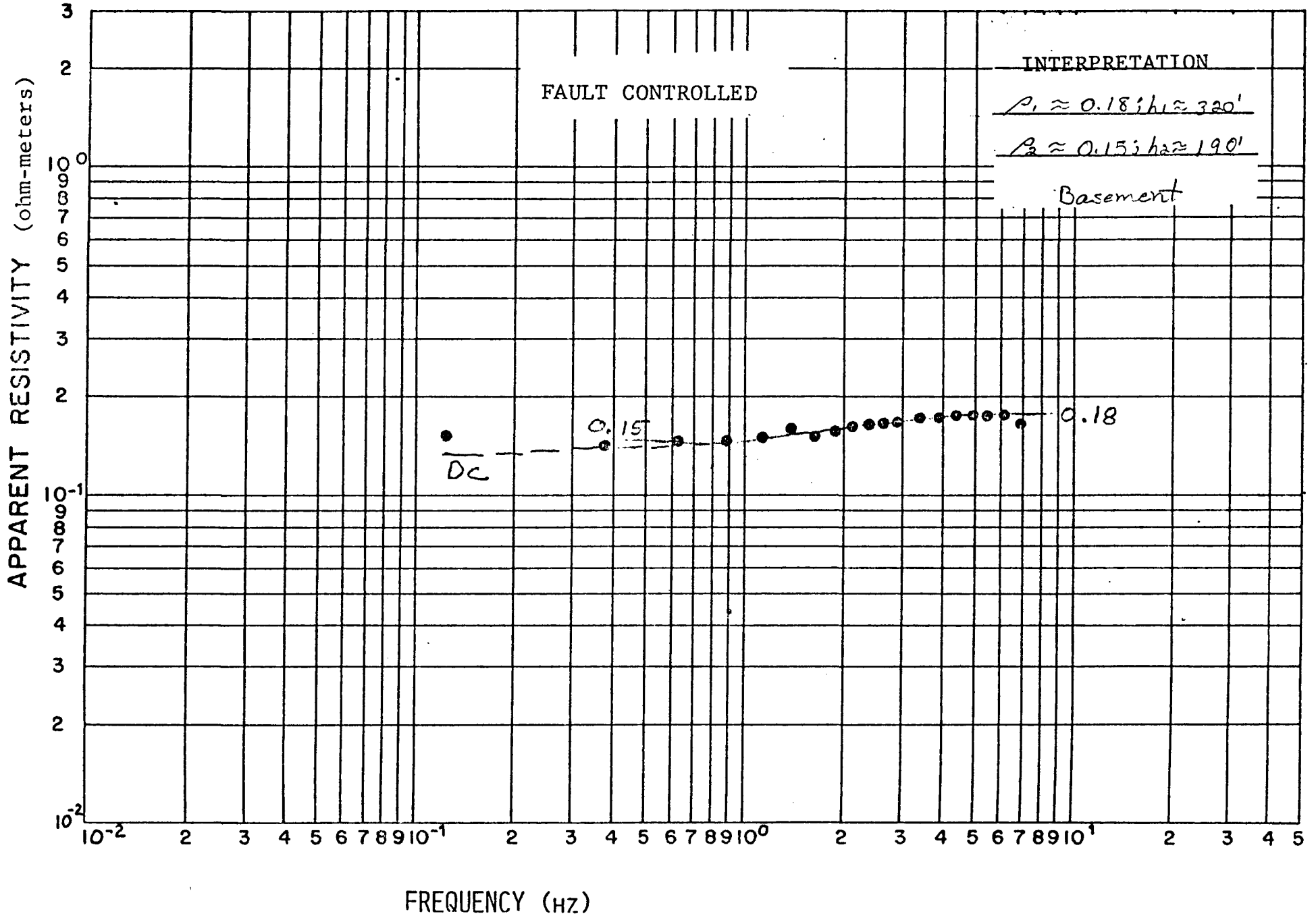

Figure VII-7. TDEM Ep Sounding 7.01.

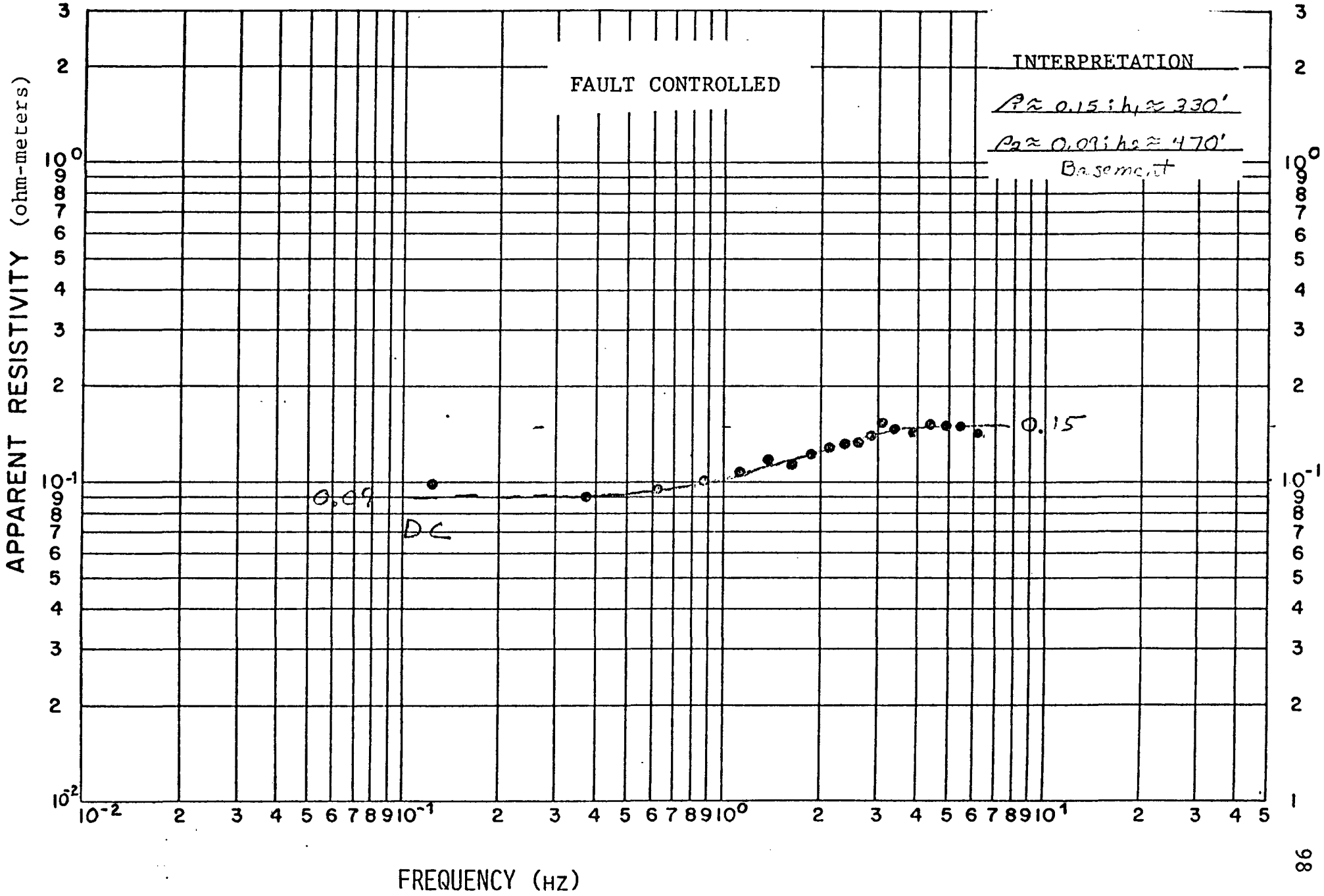

Figure VII-8. TDEM Ep Sounding 7.02.

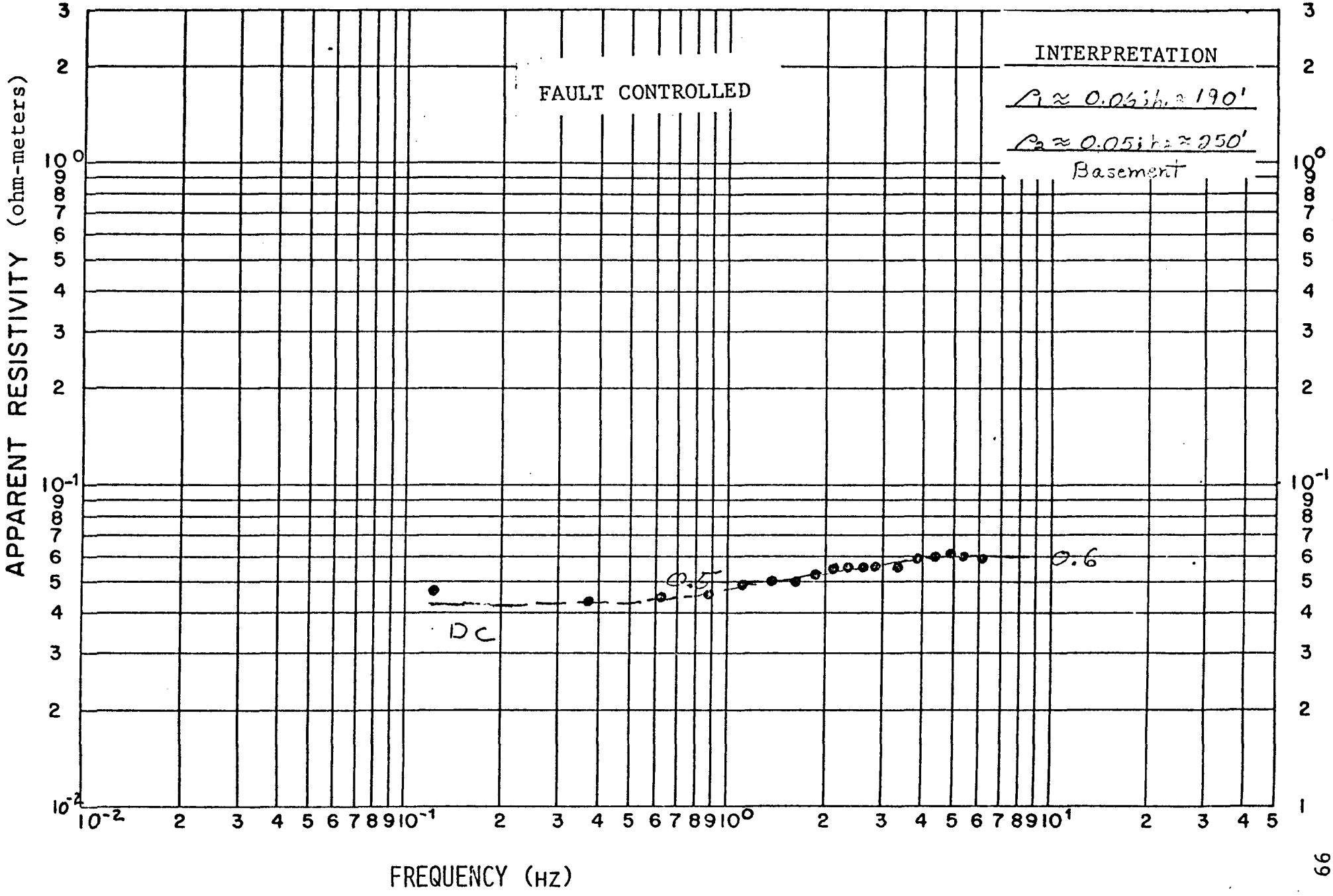

Figure VII-9. TDEM Ep Sounding 7.03

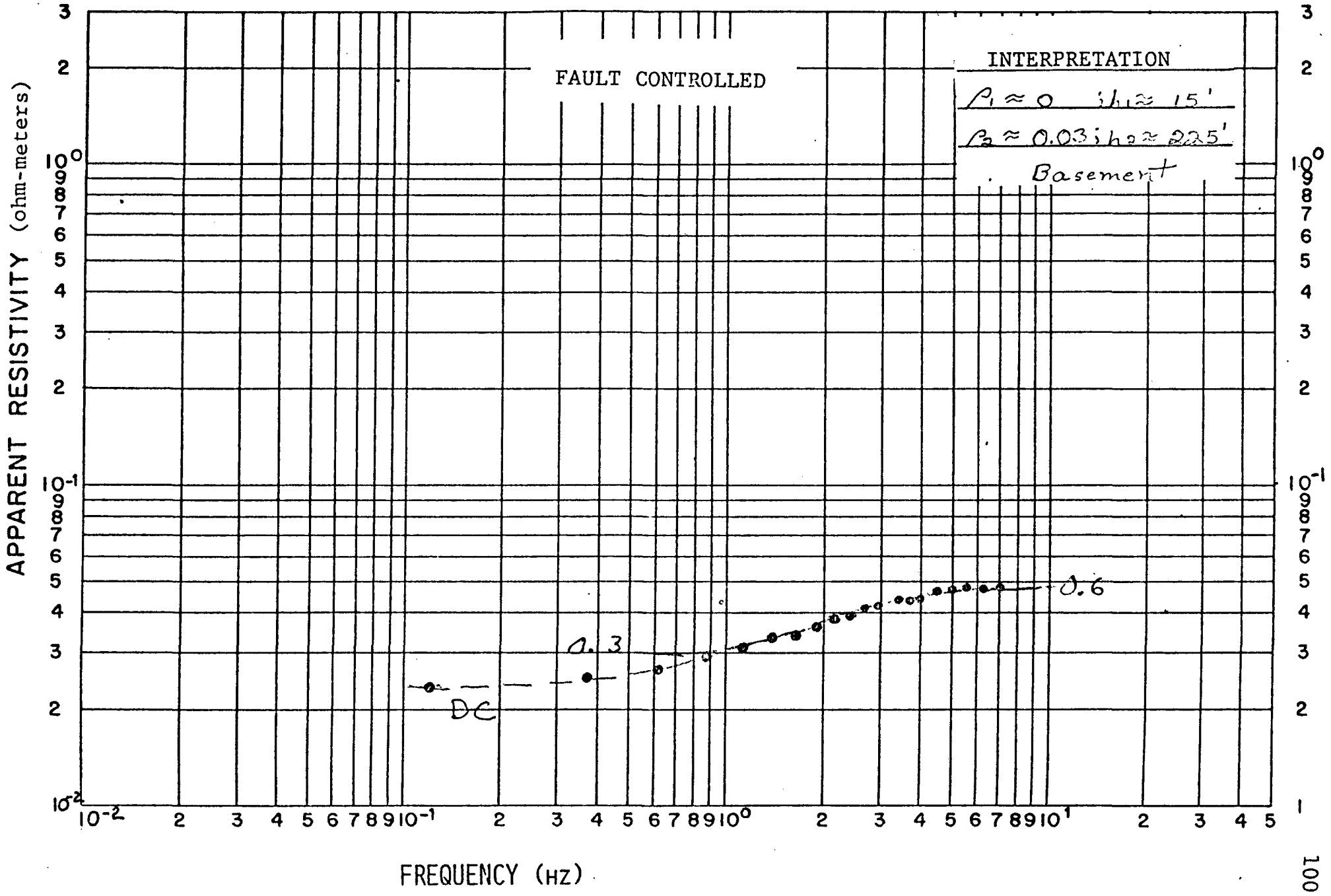

Figure VII-10. TDEM Ep Sounding 7.04

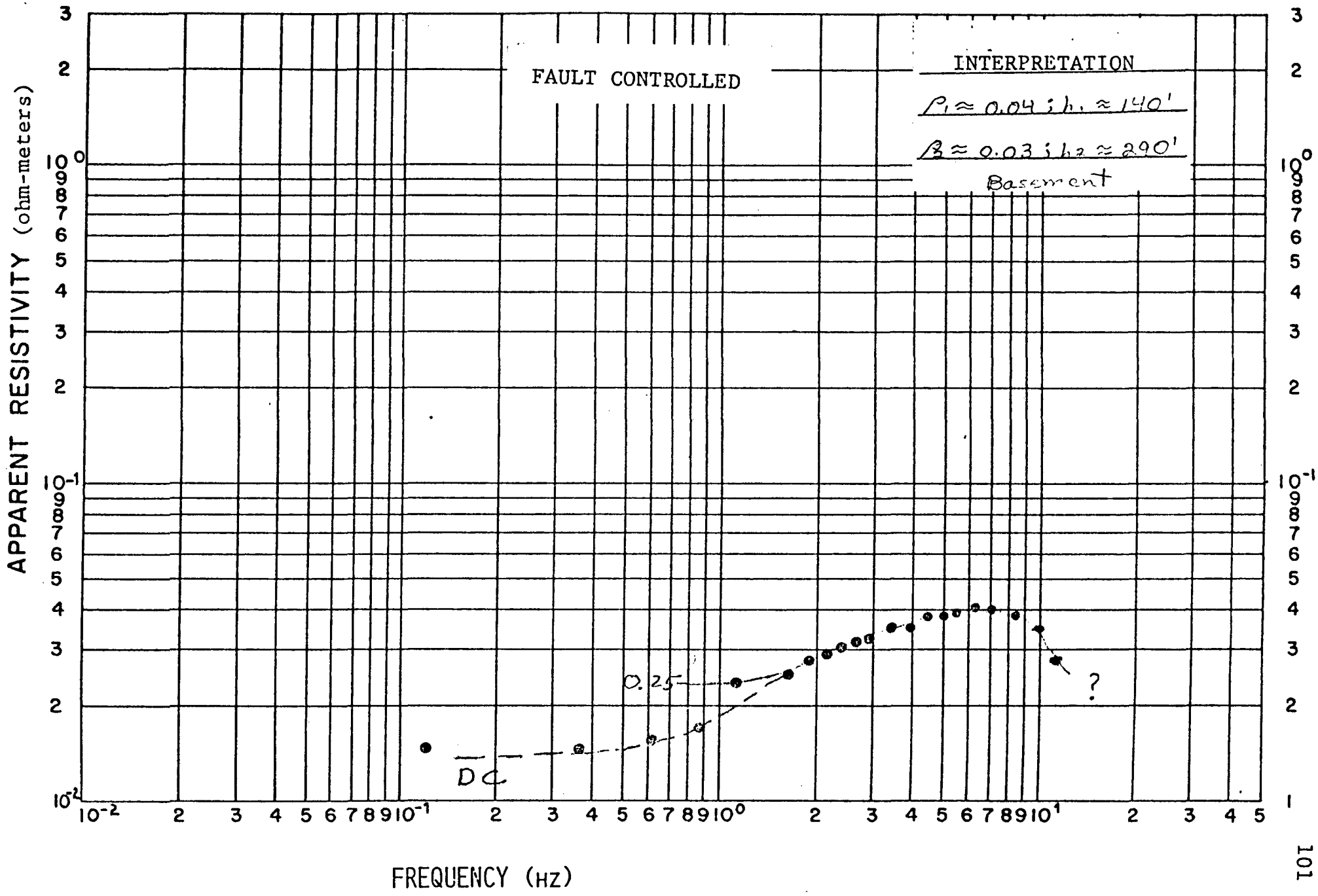

Figure VII-11. TDEM Ep Sounding 7.05

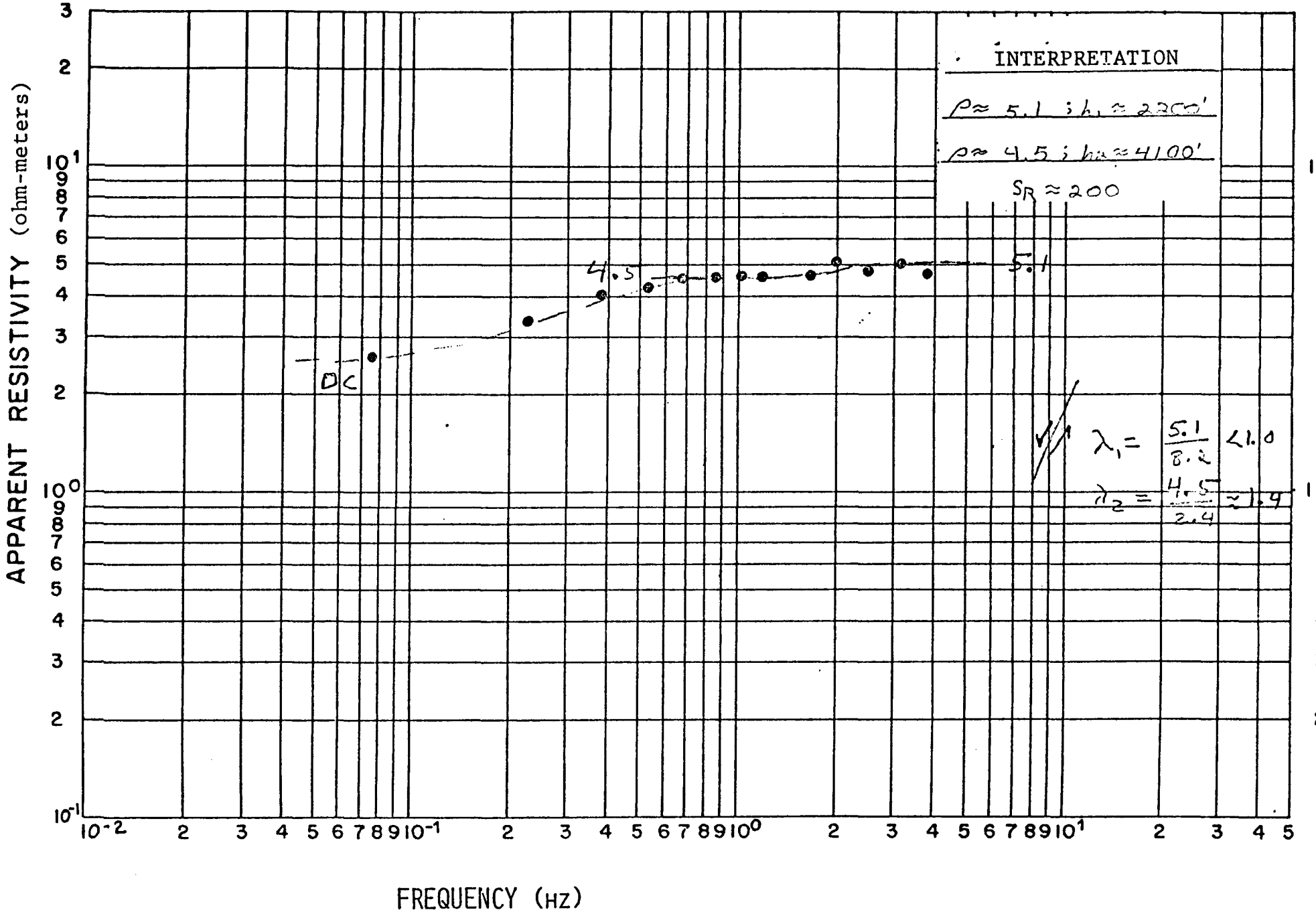

Figure VII-12. TDEM Ep Sounding 8.02

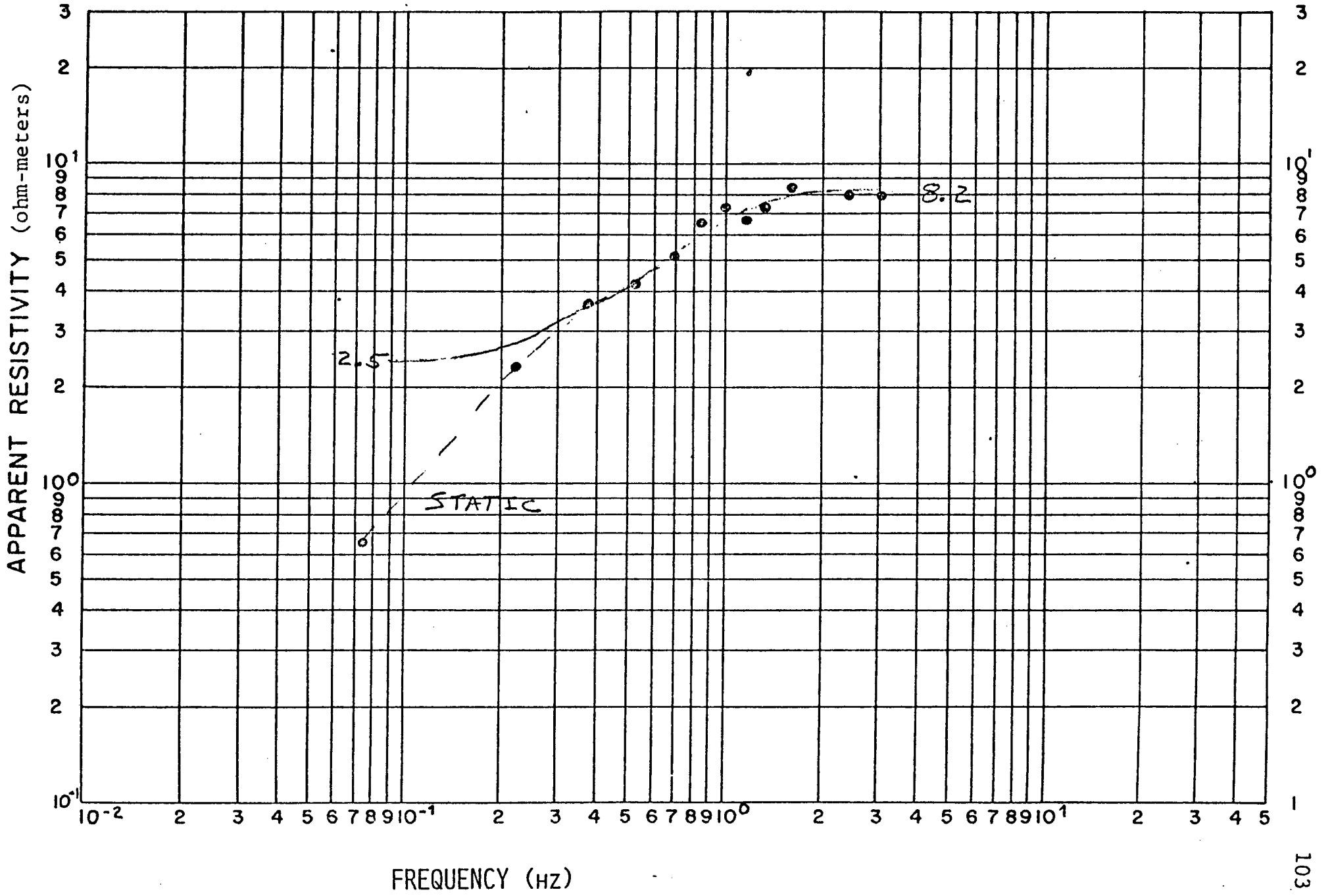

Figure VII-13. TDEM Hz Sounding 8.02

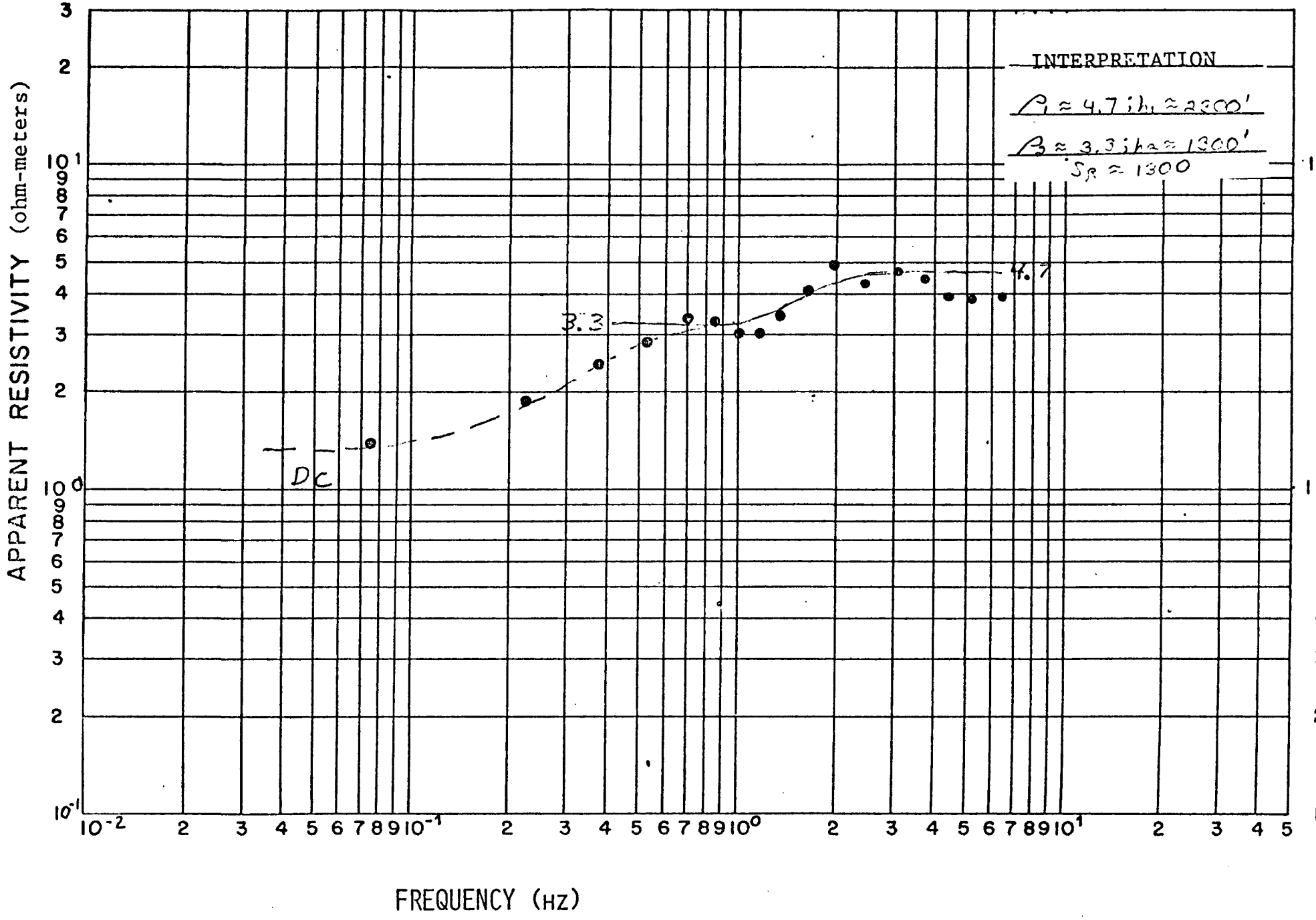

Figure VII-14. TDEM Ep Sounding 8.03

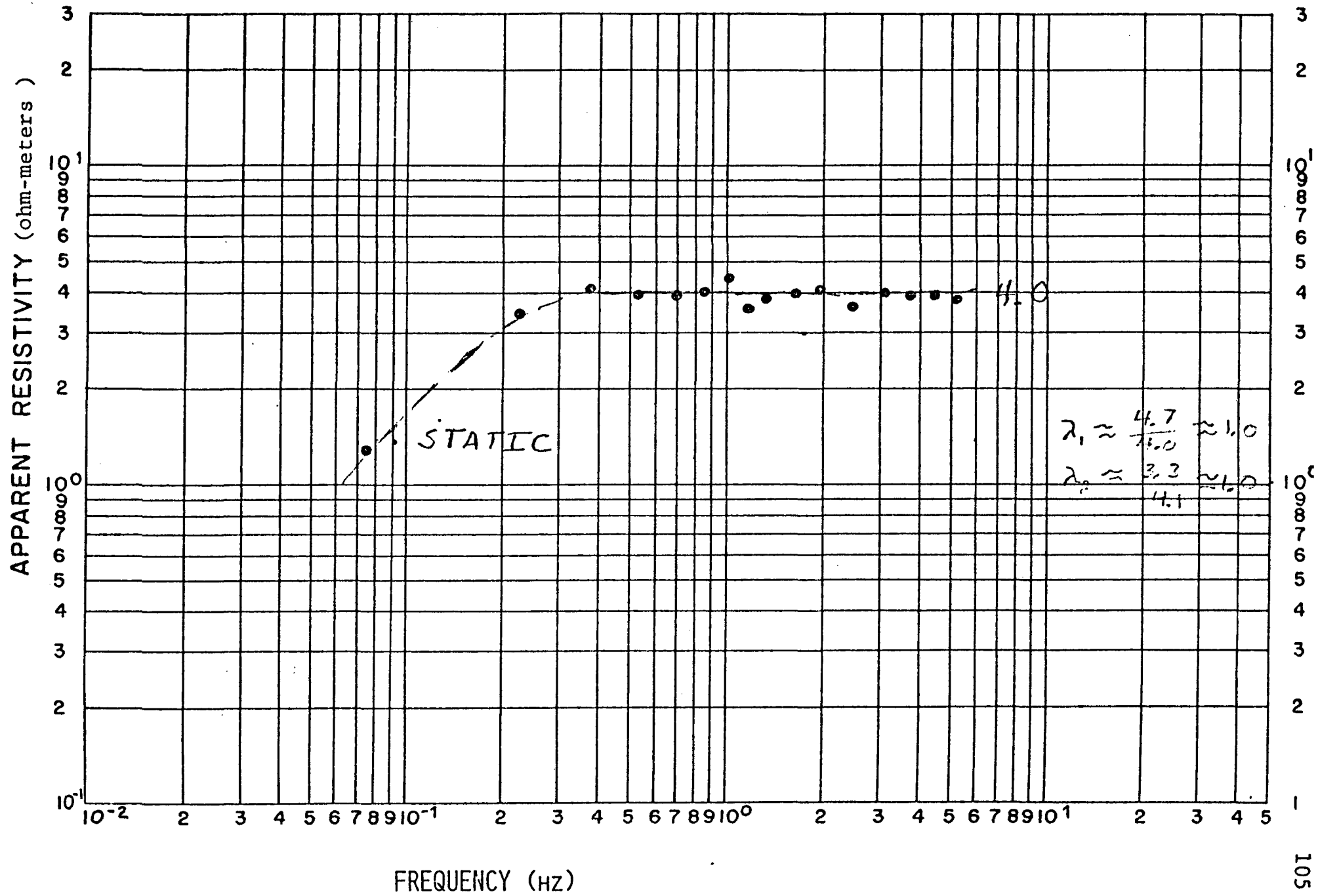

Figure VII-15. TDEM Hz Sounding 8.03

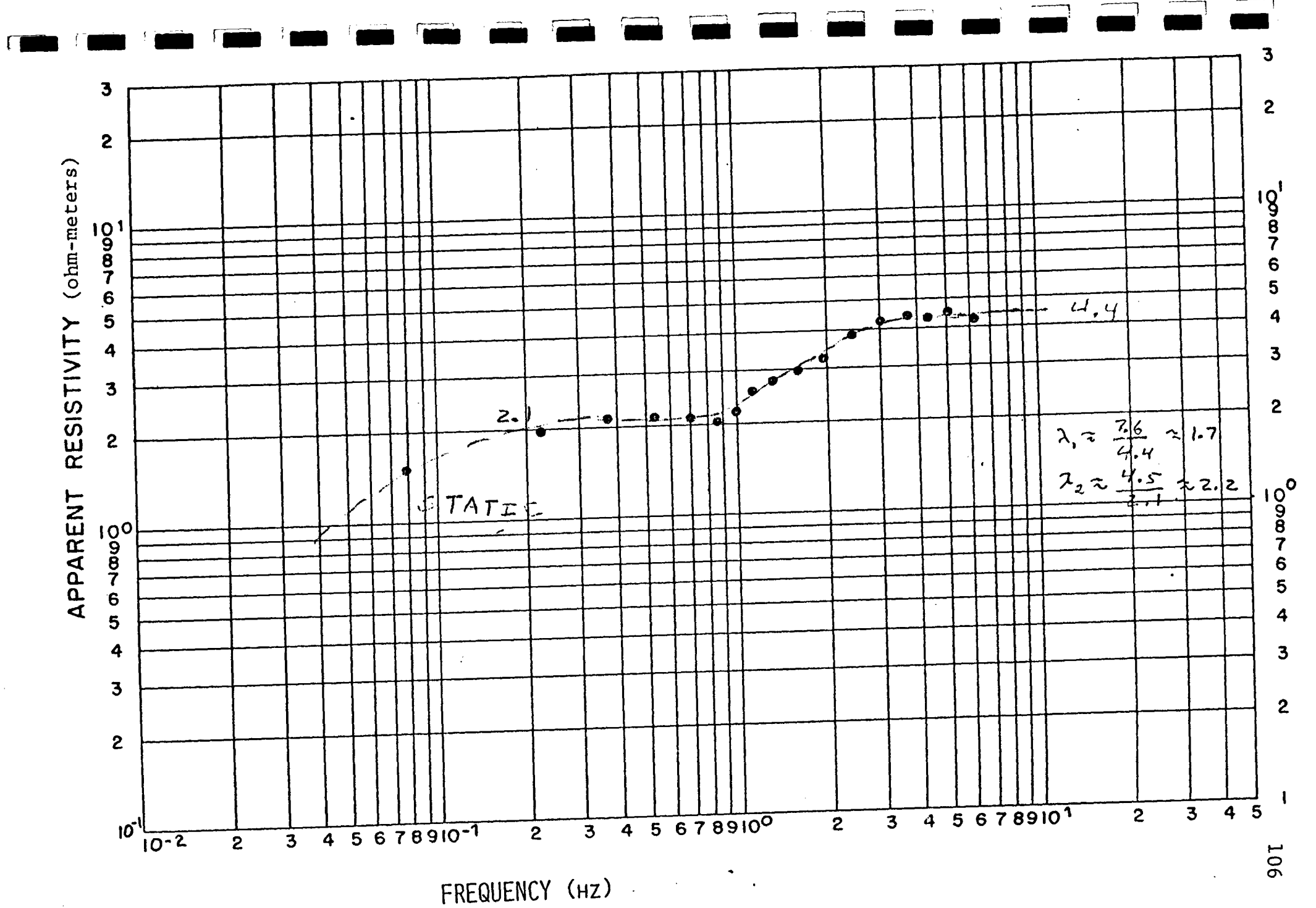

Figure VII-16. TDEM Hz Sounding 9.01

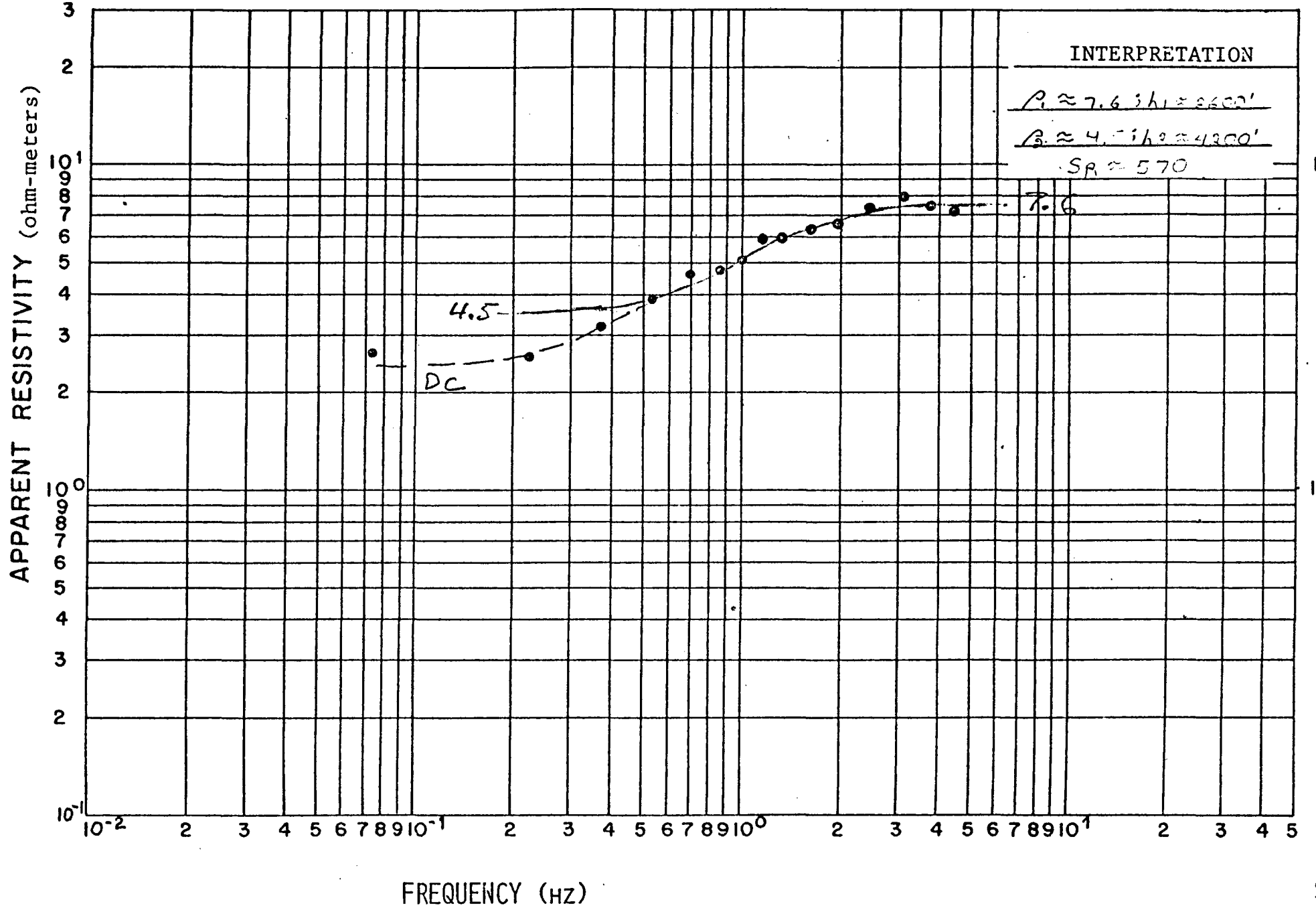

Figure VII-17. TDEM Ep Sounding 9.01

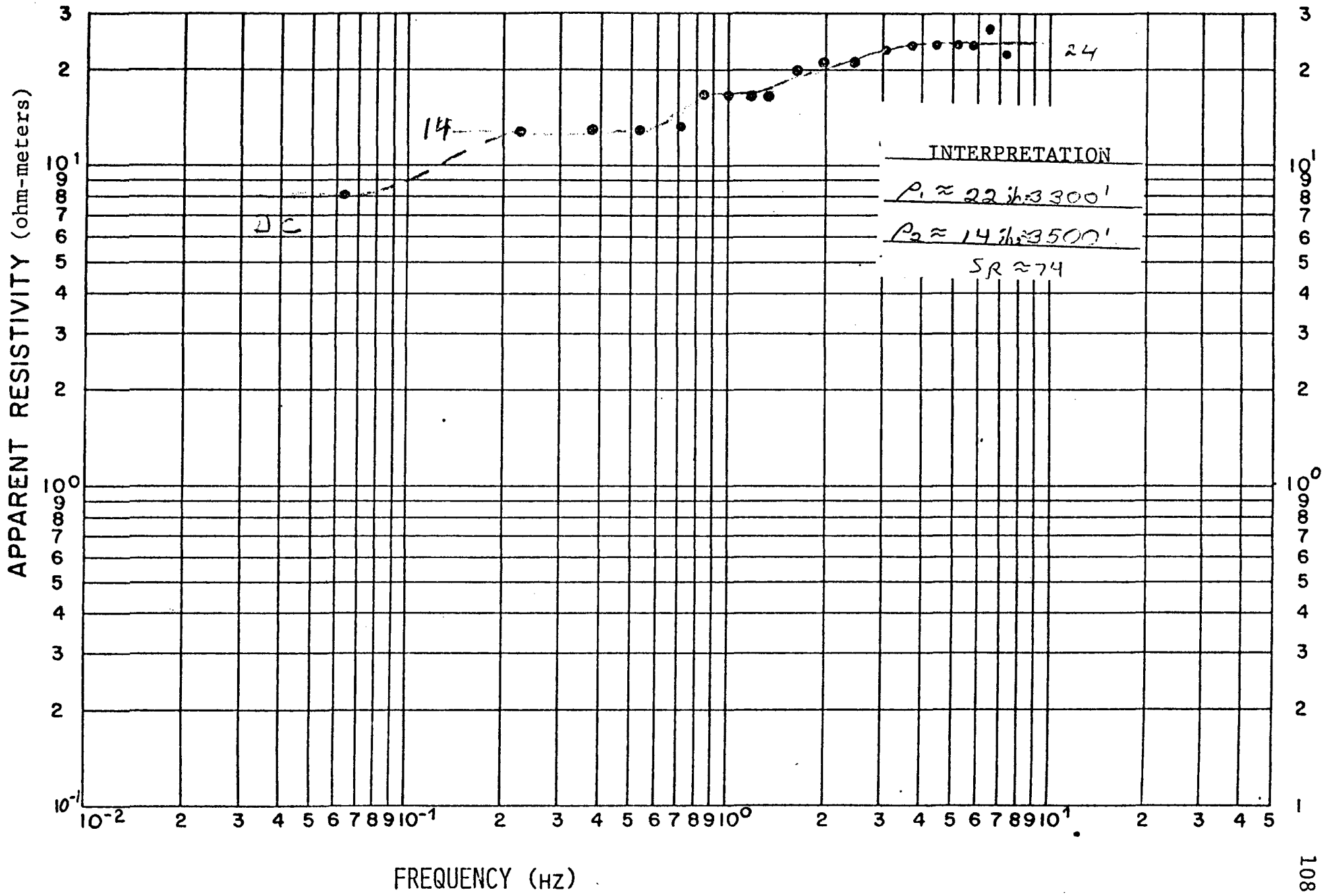

Figure VII-18. TDEM Ep Sounding 9.02

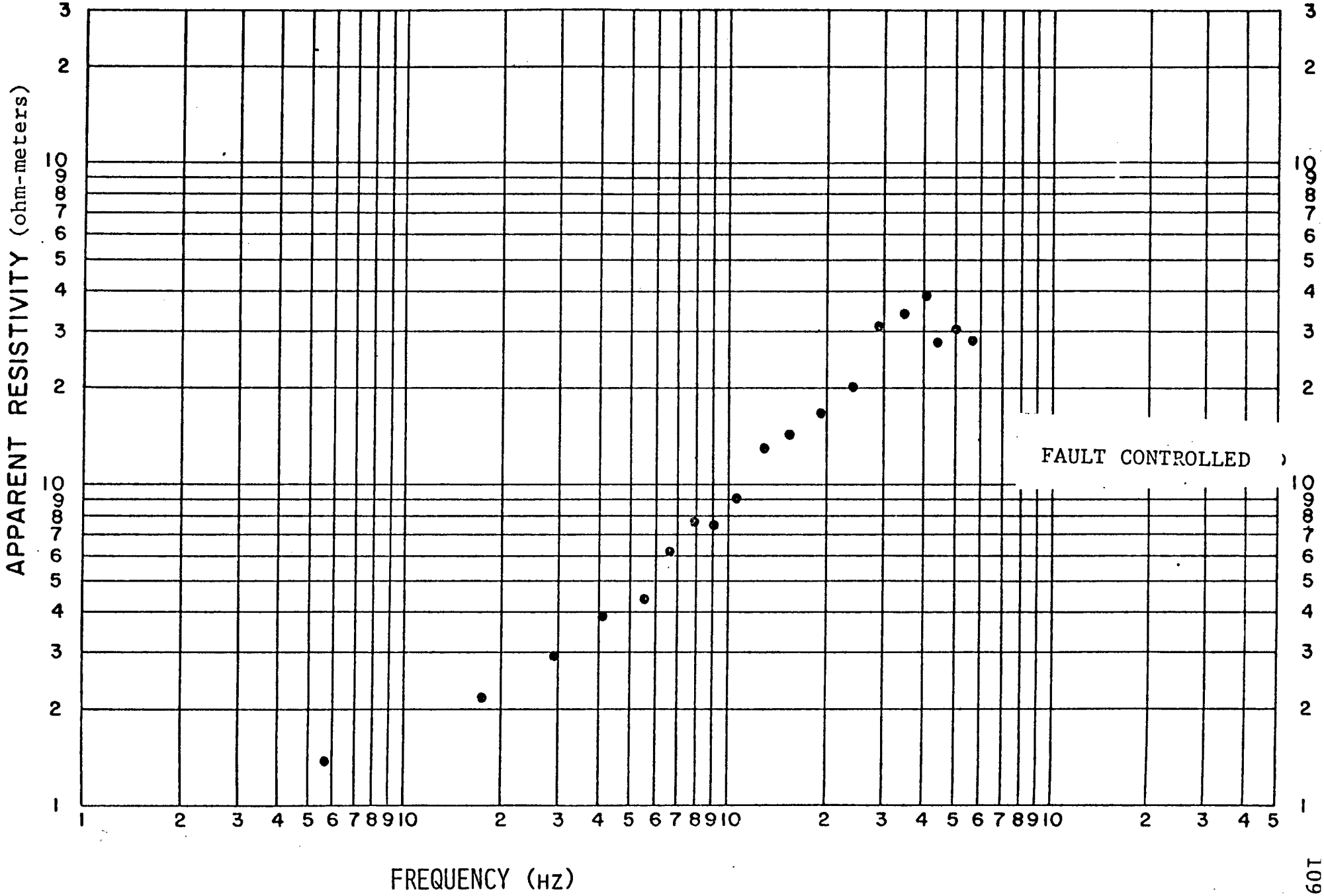

Figure VII-19. TDEM Hz Sounding 9.02

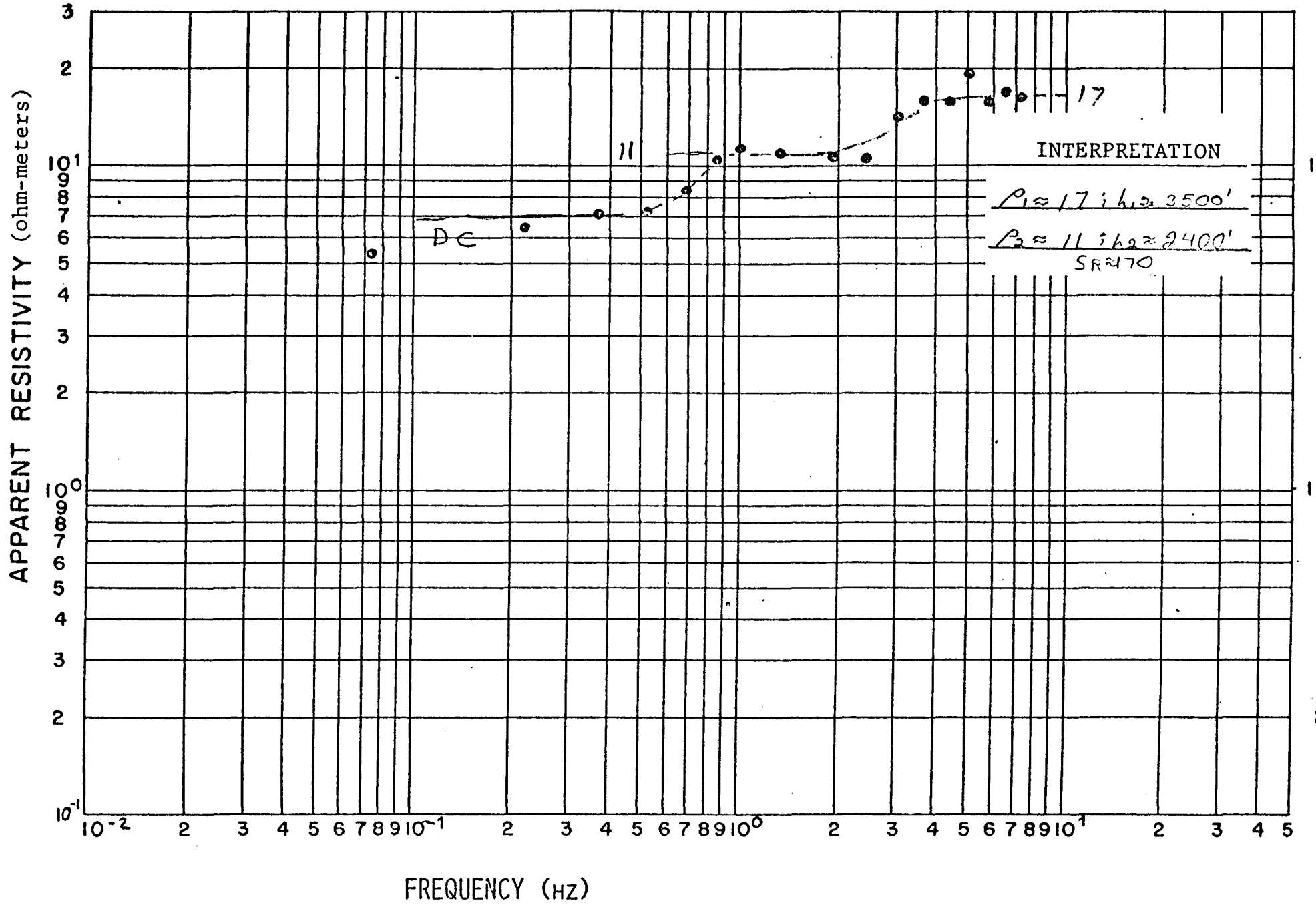

Figure VII-20. TDEM Ep Sounding 10.01

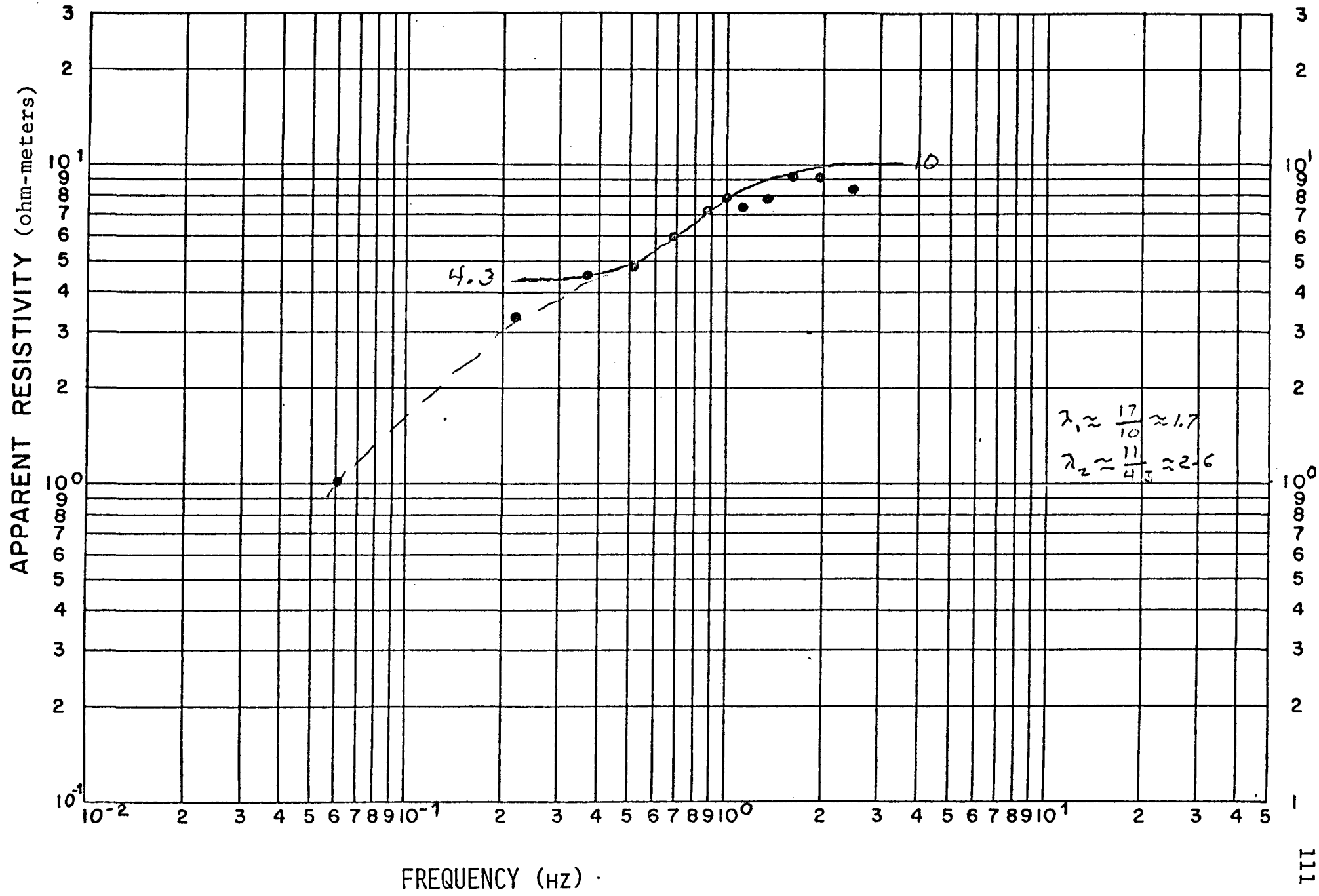

Figure VII-21. TDEM Hz Sounding 10.01

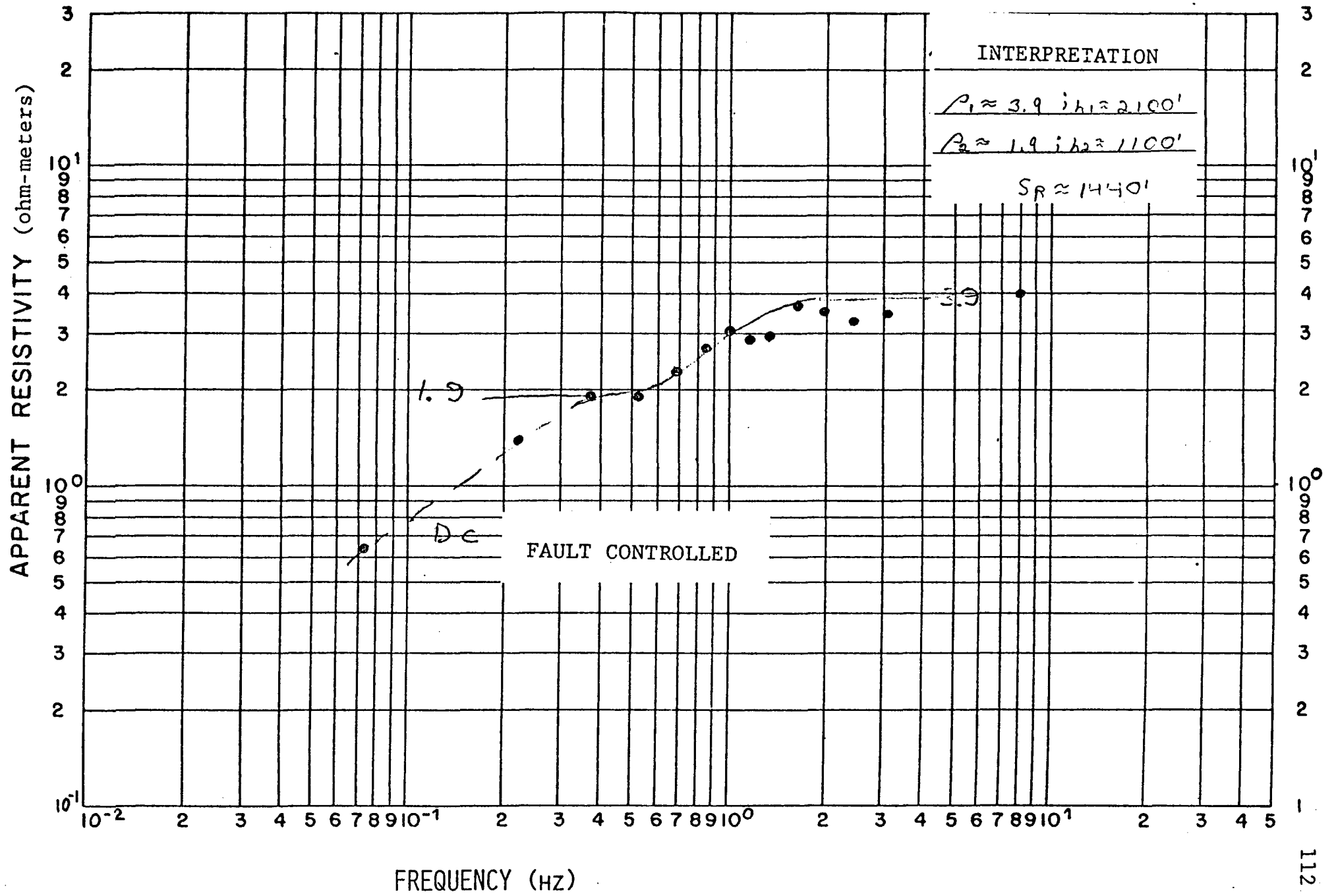

Figure VII-22. TDEM Ep Sounding 11.01

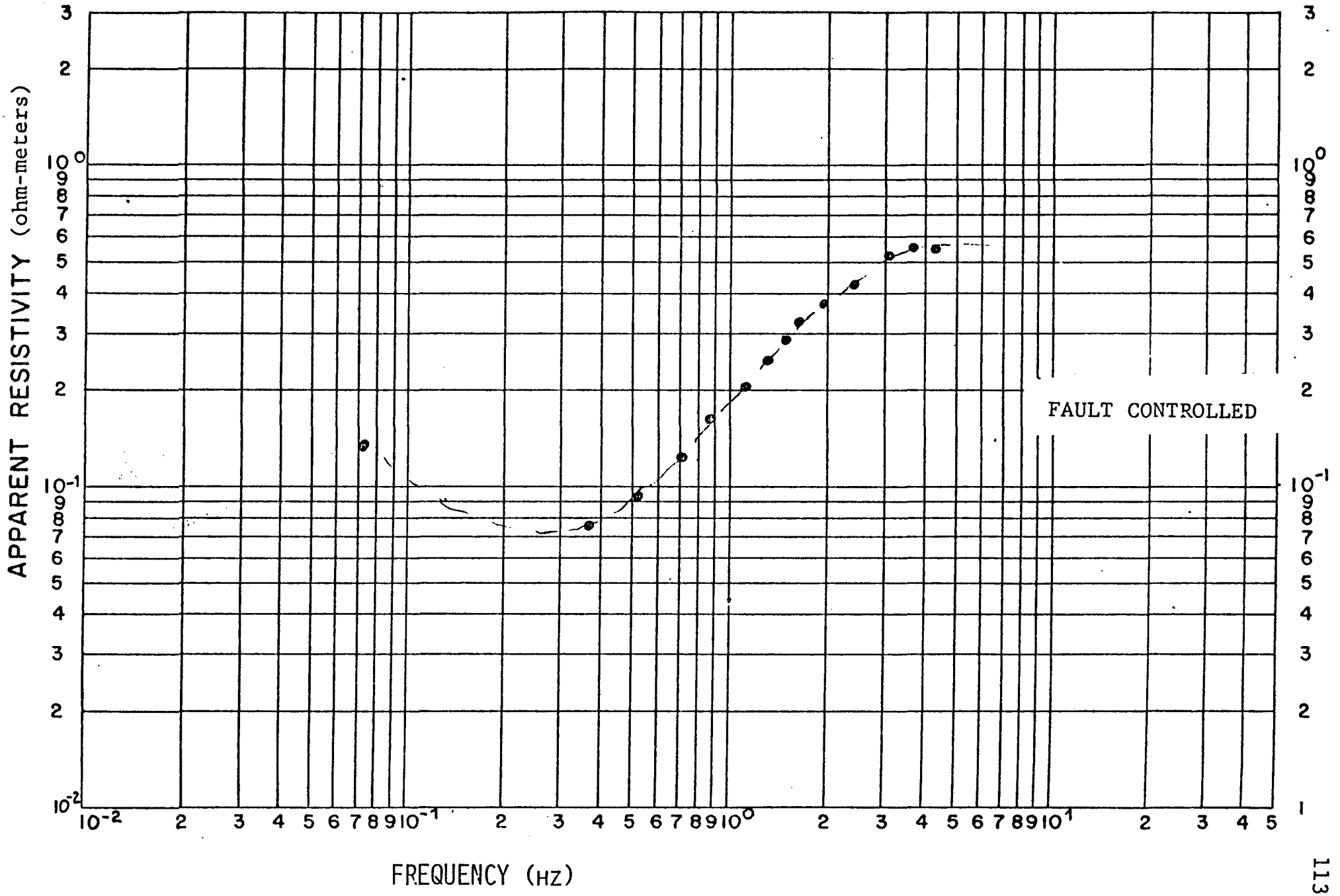

Figure VII-23. TDEM Hz Sounding 11.01

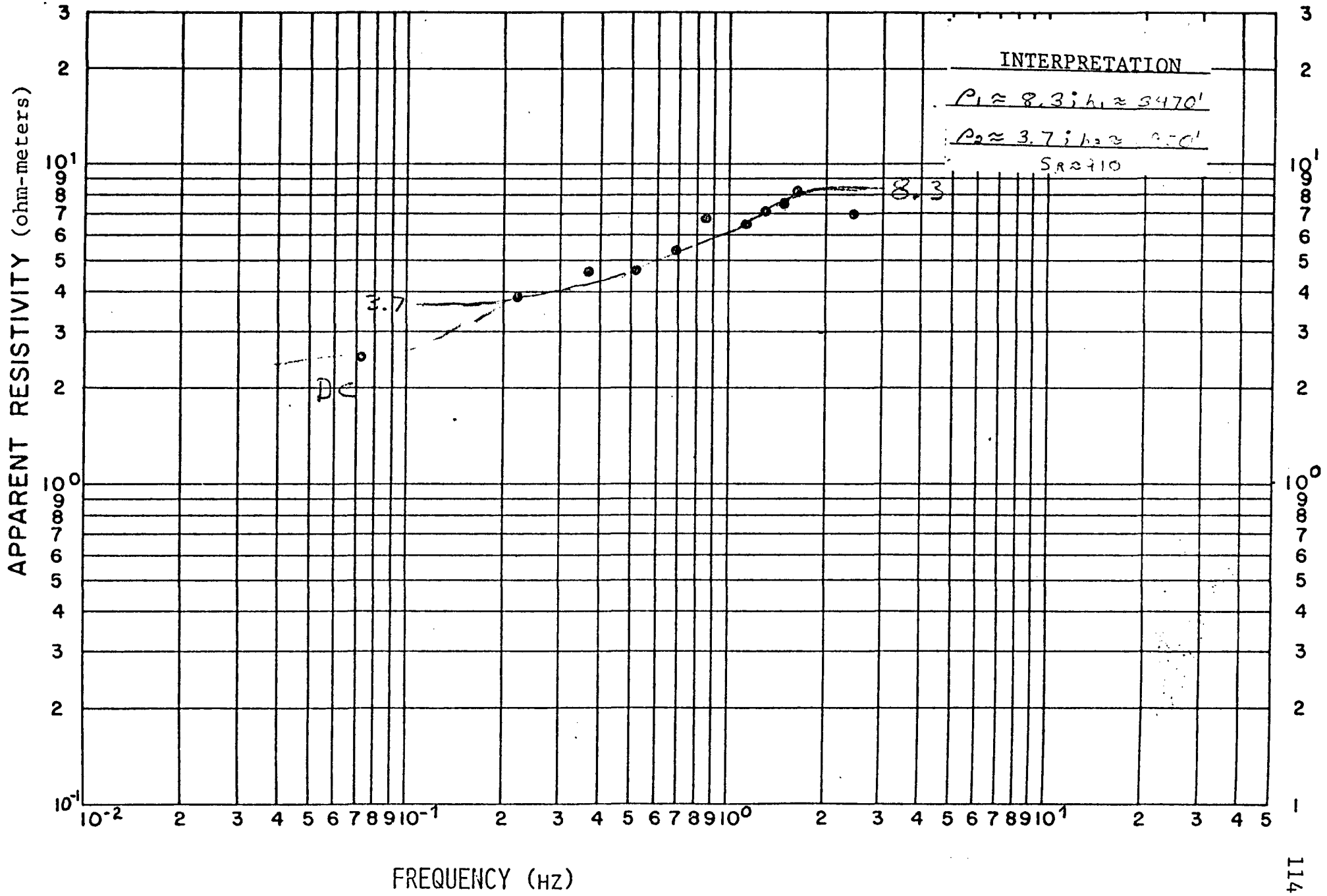

Figure VII-24. TDEM Ep Sounding 11.02

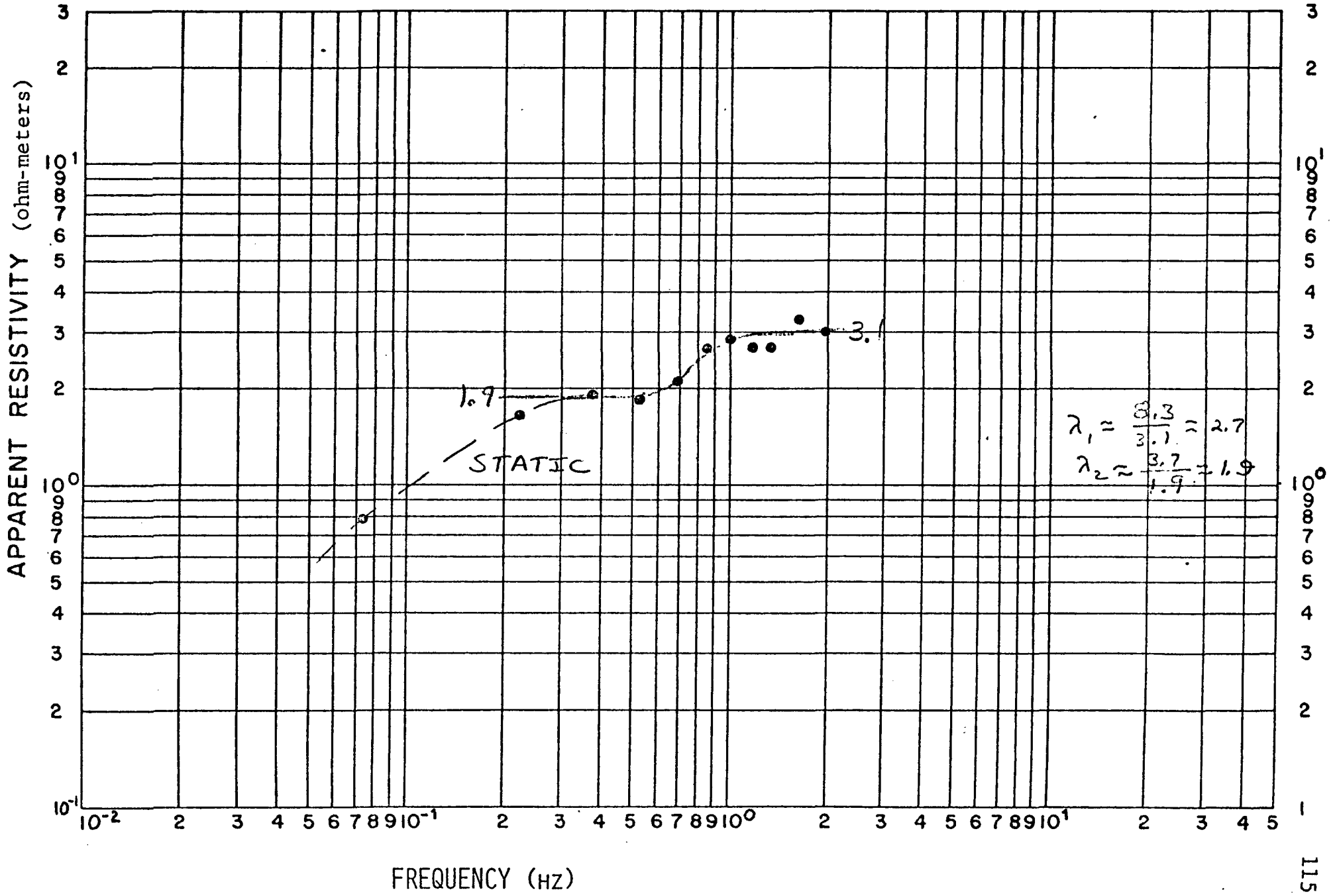

Figure VII-25. TDEM Hz Sounding 11.02

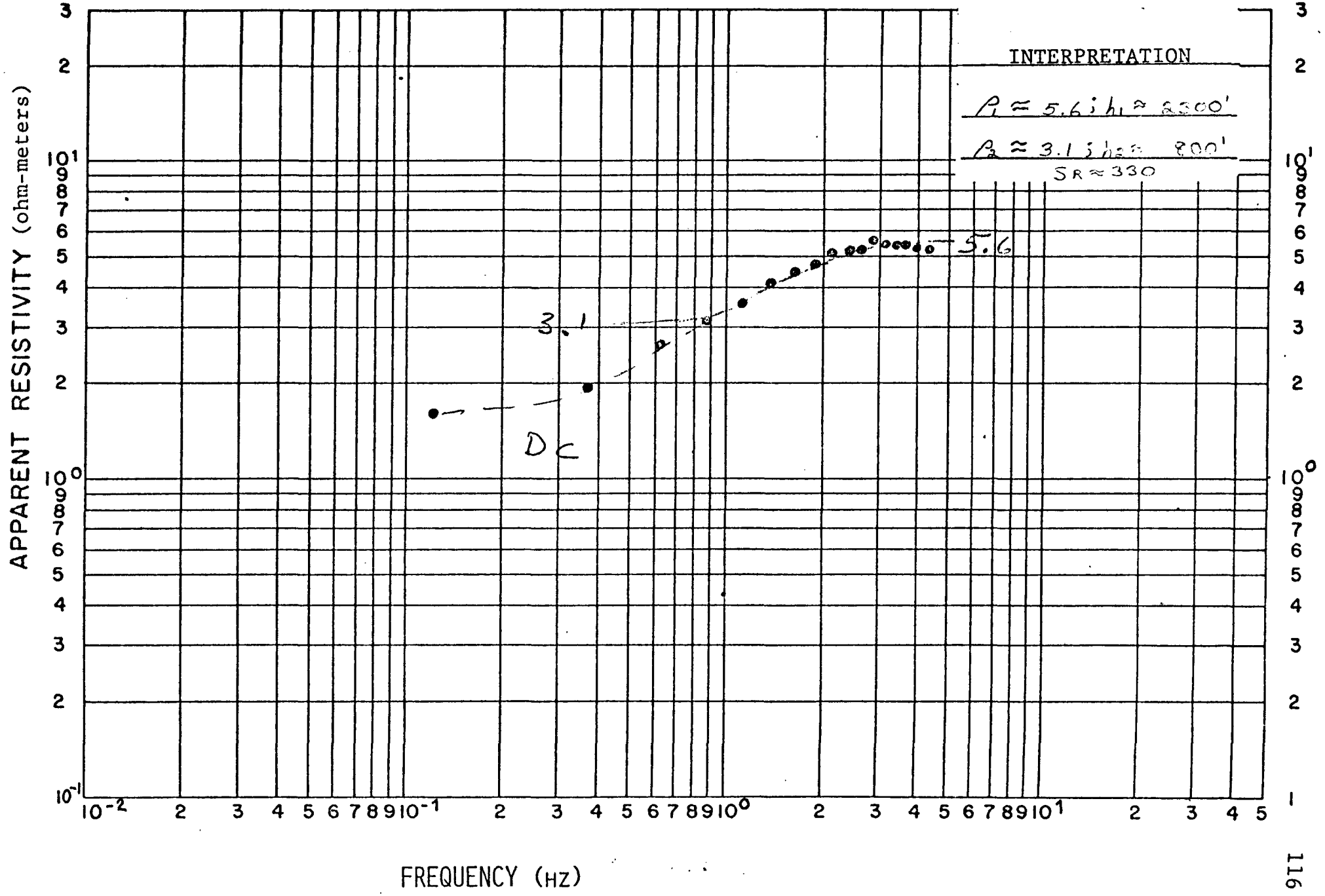

Figure VII-26. TDEM Ep Sounding 12.01

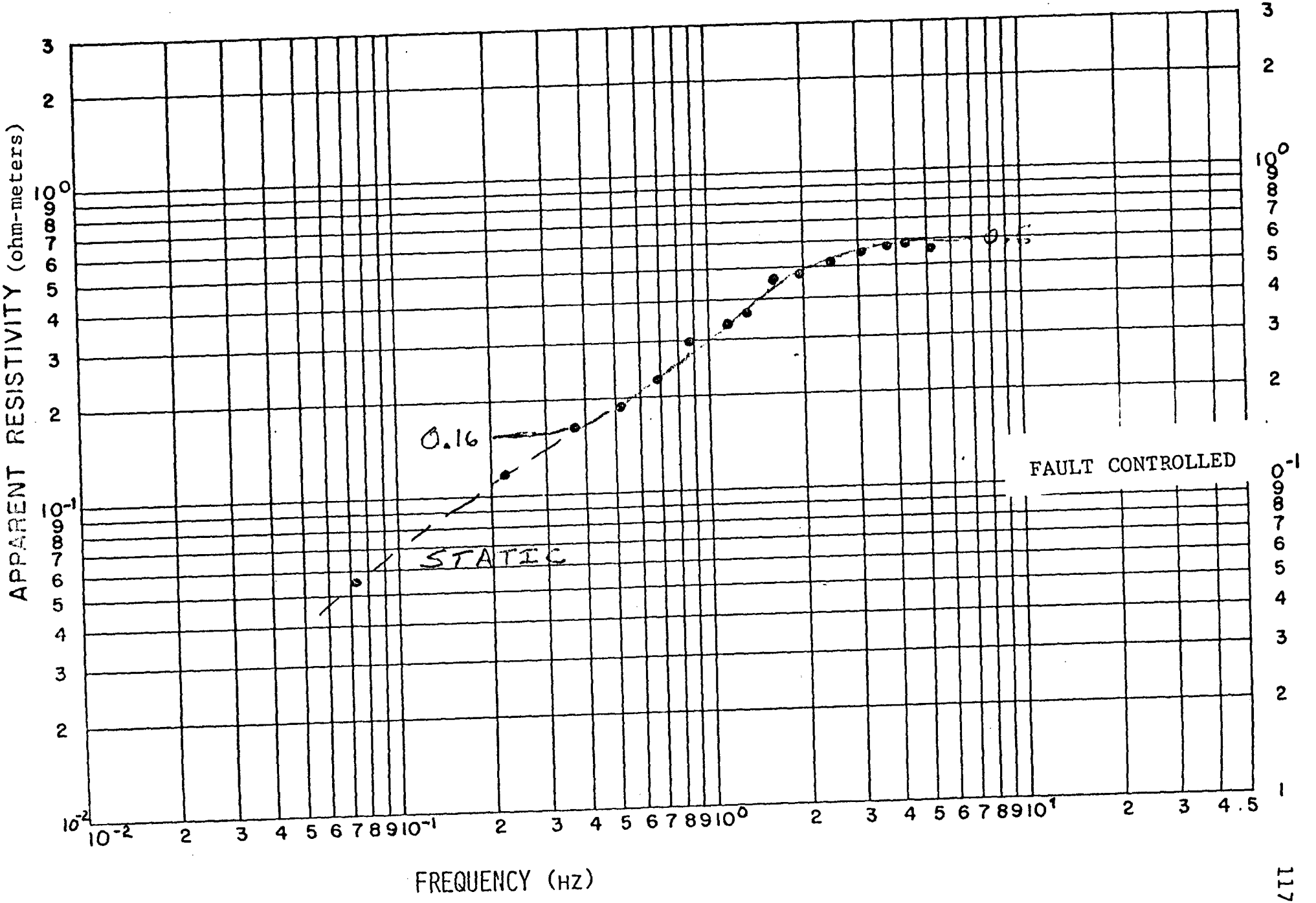

Figure VII-27. TDEM Hz Sounding 12.01

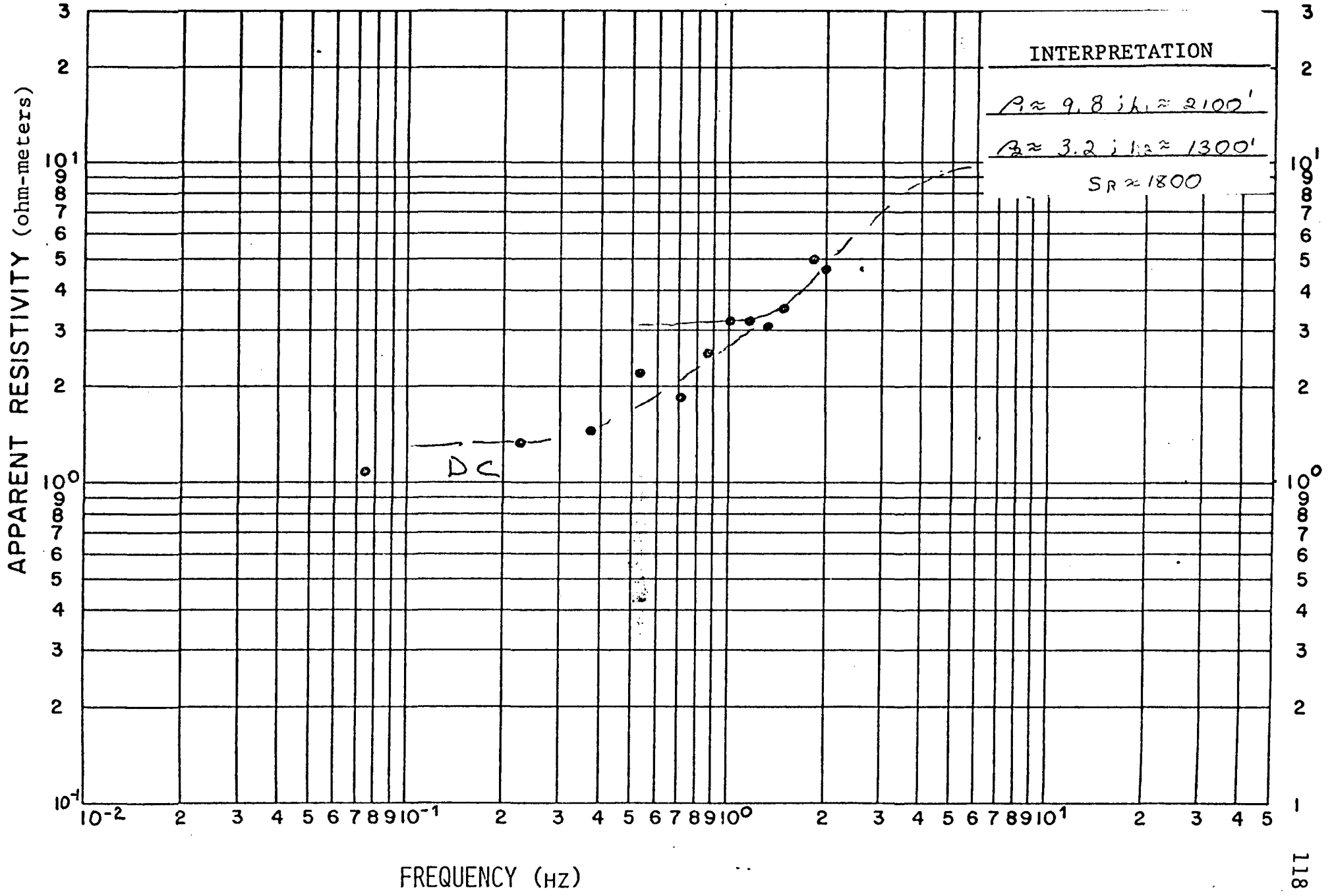

Figure VII-28. TDEM Ep Sounding 12.02

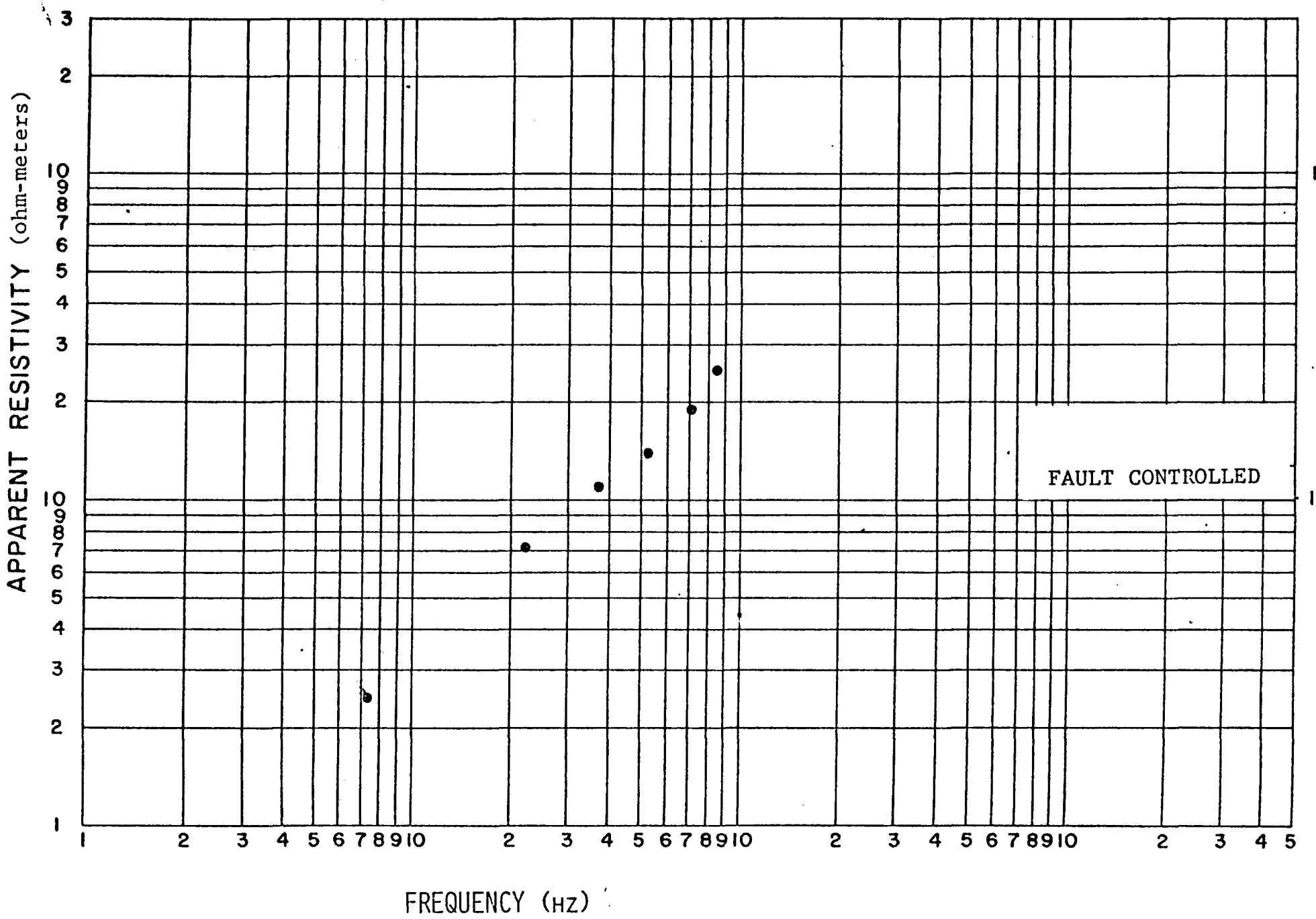

Figure VII-29. TDEM Hz Sounding 12.02

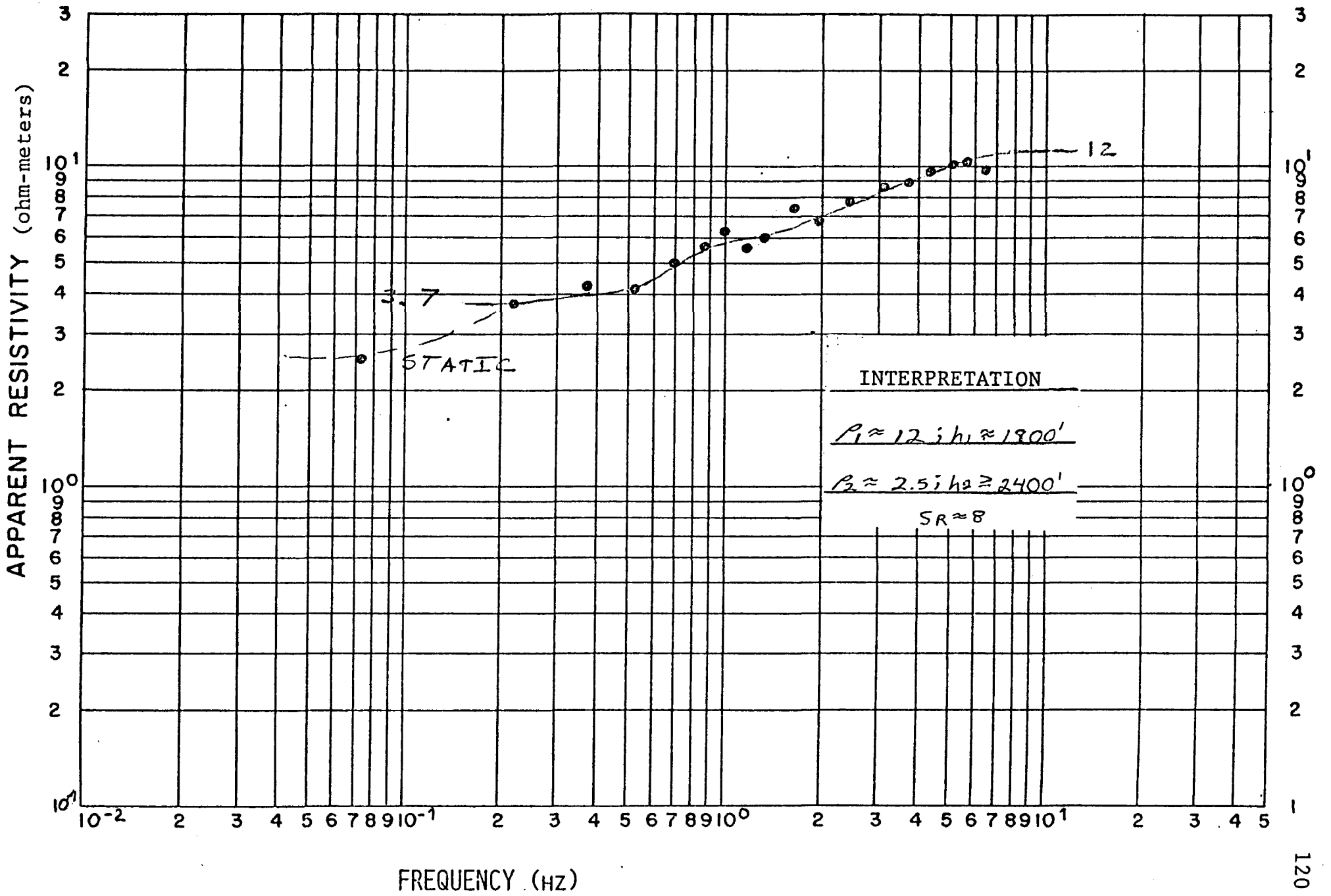

Figure VII-30. TDEM Ep Sounding 12.03

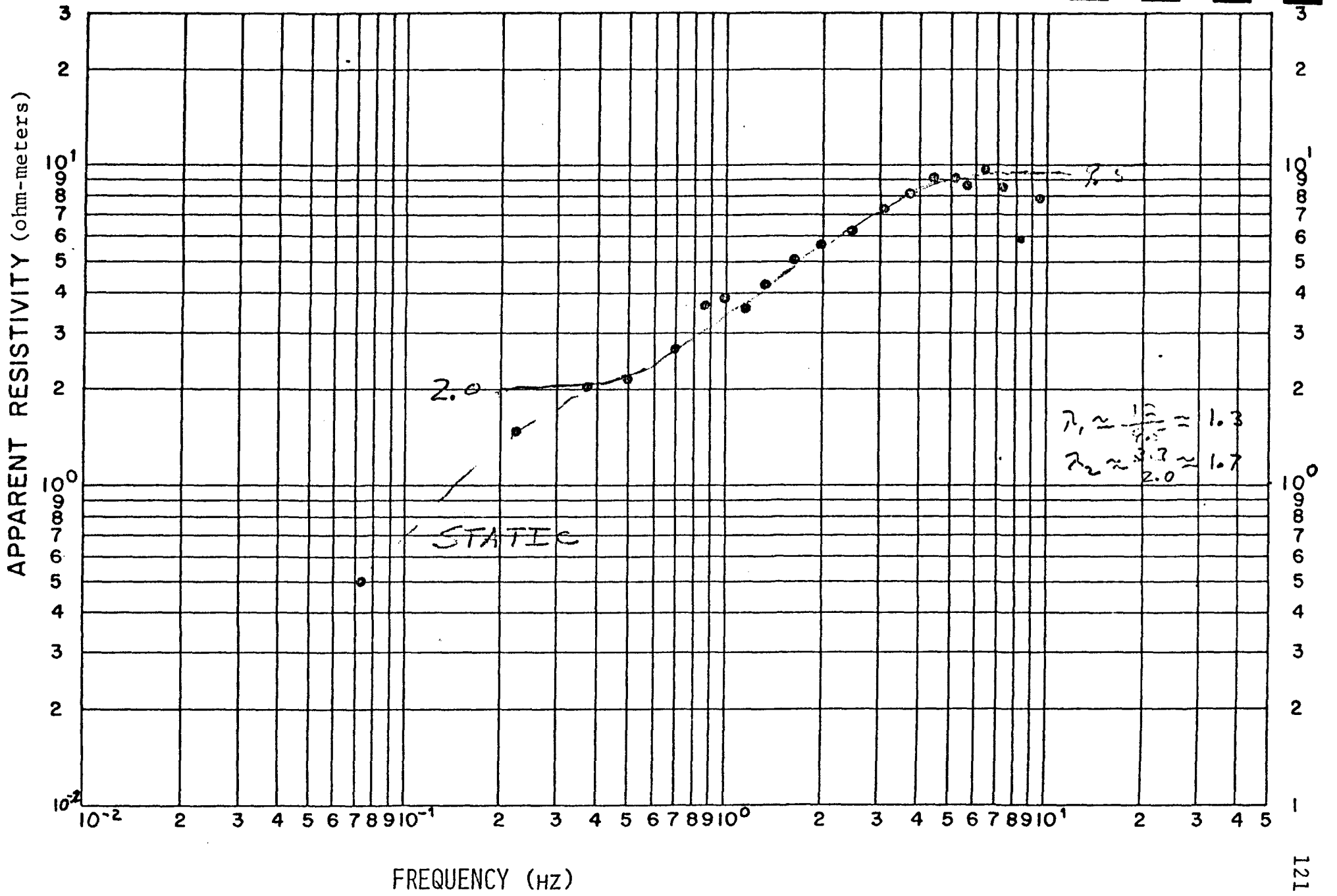

Figure VII-31. TDEM Hz Sounding 12.03

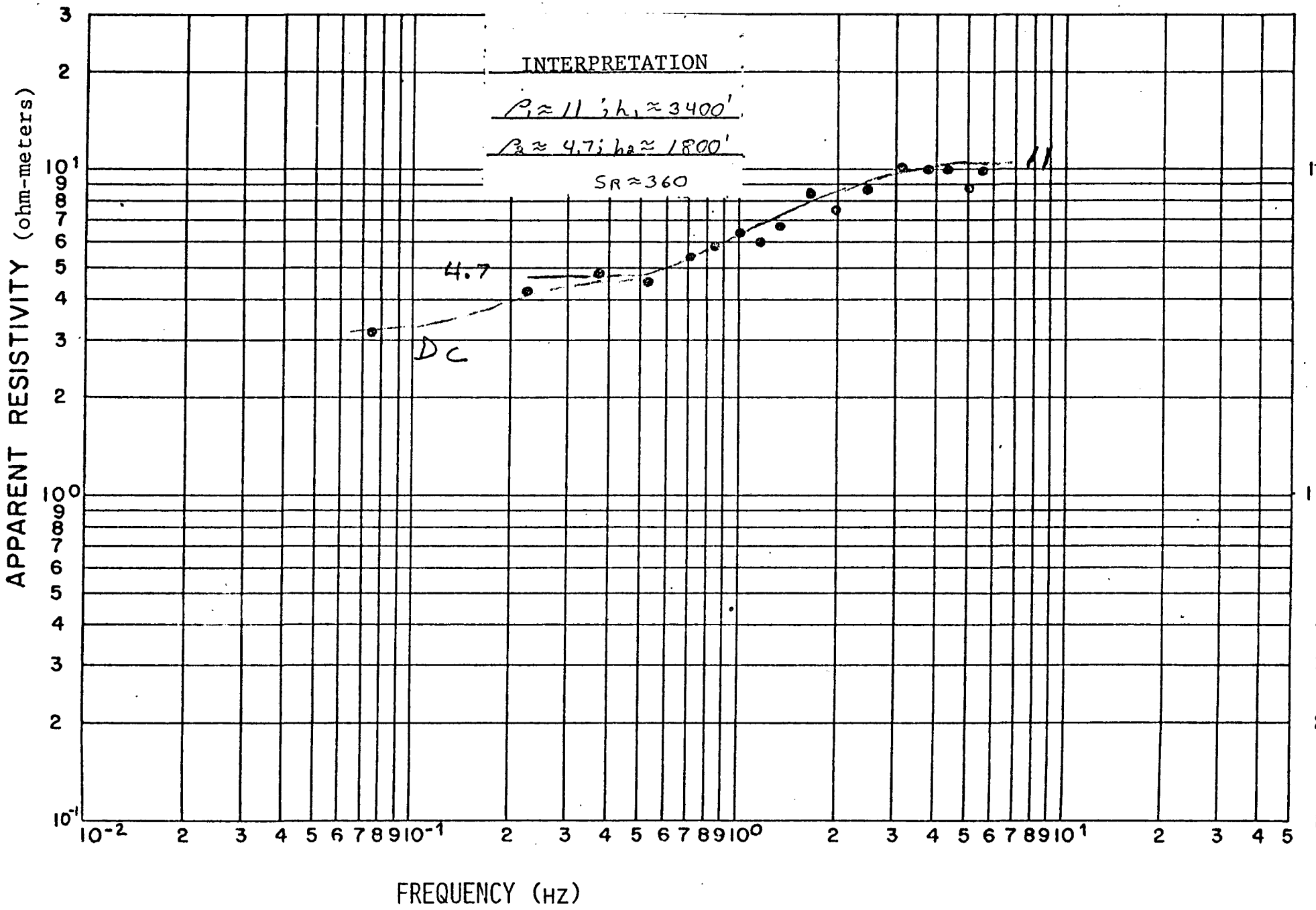

Figure VII-32. TDEM Ep Sounding 12.04

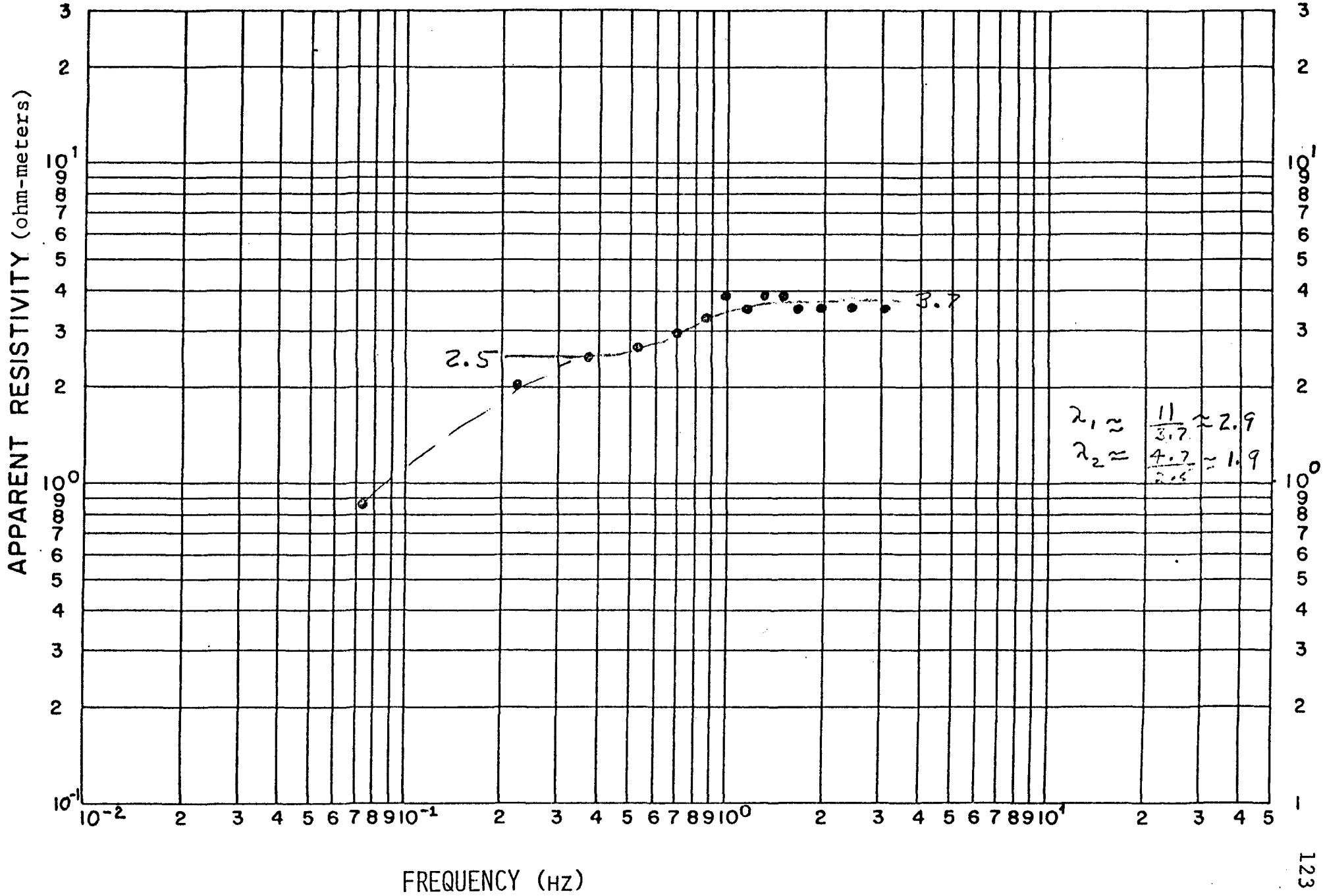

Figure VII-33. TDEM Hz Sounding 12.04